Energy Research and Development Division
FINAL PROJECT REPORT

DEVELOPMENT OF FAULT CURRENT CONTROLLER TECHNOLOGY

Prototyping, Laboratory Testing, and Field Demonstration

Prepared for: California Energy Commission
Prepared by: University of California, Irvine

JUNE 2011
CEC-500-2013-134

PREPARED BY:

Primary Author(s):
Keyue Smedley
Alexander Abramovitz

University of California, Irvine

Contract Number: UC MR-064

Prepared for:

California Energy Commission

Jamie Patterson
Contract Manager

Fernando Pina
Office Manager
Energy Systems Research Office

Laurie ten Hope
Deputy Director
ENERGY RESEARCH AND DEVELOPMENT DIVISION

Robert P. Oglesby
Executive Director

ACKNOWLEDGEMENTS

The University of California, Irvine gratefully acknowledges the financial support from the California Energy Commission, and the administrative support of the California Institute for Energy & Environment (University of California, Berkeley), which made this project possible. We sincerely thank our collaborators at Southern California Edison Co., Zenergy Power plc, the Electric Power Research Institute (EPRI) and Silicon Power Corporation for their technical expertise, teamwork and support which made this project successful. We also express our sincere appreciation to our knowledgeable and supportive Project Advisory Group for their valuable advice, which has been of critical importance in every phase of the project.

Contributing Authors:

Franco Moriconi, Francisco De La Rosa, Alonso Rodriguez, Bert Nelson, Amandeep Singh, Nick Koshnick – Zenergy Power plc
Ram Adapa – Electric Power Research Institute
Christopher R. Clarke, Ed Kamiab, Syed Ahmed – Southern California Edison Co.
Mahesh Gandhi, Swapna Bhat, Simon Bird – Silicon Power Corporation

Project Advisory Group:

Jamie Patterson – California Energy Commission
Lloyd Cibulka – California Institute for Energy and Environment
Bert Nelson, Alonso Rodriguez – Zenergy Power plc
Ram Adapa – Electric Power Research Institute
Alfonso Orozco, Katie Speirs – San Diego Gas & Electric Co.
Bob Yinger, Christopher R. Clarke, Russ Neal, Anthony Johnson, Raj Vora, Ed Kamiab – Southern California Edison Co.
Ron Sharp – Pacific Gas & Electric Co.
Ed Muljadi – National Renewable Energy Laboratory
Jim McHan – California Independent System Operator
Ken Edwards – Bonneville Power Administration
Ron Meyer – Santa Margarita Water District

UC–Irvine Technical Contributors:

Jun Wen
Franco Maddaleno
Liang Zhou
In Wha Jeong
Marco Tedde
Sadigh Khoshkbar Arash
Chaitanya Vartak
Wensheng Song
Pengju Sun
ZhengSheng Wu
Wenchao Xi
Zhuo Zhao
Fei Gu

PREFACE

The California Energy Commission Energy Research and Development Division supports public interest energy research and development that will help improve the quality of life in California by bringing environmentally safe, affordable, and reliable energy services and products to the marketplace.

The Energy Research and Development Division conducts public interest research, development, and demonstration (RD&D) projects to benefit California.

The Energy Research and Development Division strives to conduct the most promising public interest energy research by partnering with RD&D entities, including individuals, businesses, utilities, and public or private research institutions.

Energy Research and Development Division funding efforts are focused on the following RD&D program areas:

- Buildings End-Use Energy Efficiency
- Energy Innovations Small Grants
- Energy-Related Environmental Research
- Energy Systems Integration
- Environmentally Preferred Advanced Generation
- Industrial/Agricultural/Water End-Use Energy Efficiency
- Renewable Energy Technologies
- Transportation

Development of Fault Current Controller Technology is the final report for the Development of Fault Current Controller Technology project (contract number UC MR-064) conducted by University of California, Irvine. The information from this project contributes to Energy Research and Development Energy Systems Integration Program.

For more information about the Energy Research and Development Division, please visit the Energy Commission's website at www.energy.ca.gov/research/ or contact the Energy Commission at 916-327-1551.

ABSTRACT

Fault current controller technology, also frequently referred to as fault current limiter technology, has been identified as a potentially viable solution for expanding the capacity of the transmission system and its service life to meet the growing demand for electricity by addressing the impacts of the resulting higher fault currents. This report discusses the development and field demonstration of distribution-class fault current controller technology. The project focused on prototyping, test plan development, laboratory testing, and field testing and demonstration, with a view toward potential further technical development and application of the technology in transmission-level systems.

A full-size three-phase distribution-level high-temperature superconducting fault current controller prototype was designed, built, and field-tested. The prototype fault current controller went through several iterations of extensive testing prior to field installation. It was then installed for field demonstration from March 2009 through October 2010.

The research team completed an initial design for a fault current controller based on solid-state (power electronics) technology. Initial analysis indicated that design changes to the prototype were necessary to improve its thermal management, the immunity of the control circuits to noise and interference and to address mechanical issues. The additional cost for these items was beyond the scope and budget of this project so this prototype design did not advance to the laboratory and field test stages during the project period.

This report provided a survey of fault current controller technology development status, including both the saturable-core and solid-state types represented by this project, followed by detailed design considerations, laboratory test procedures and results, field test installation and metering, and field demonstration outcomes. The report concluded with a summary of the lessons learned and recommendations for future fault current controller research efforts and commercial industry applications.

Keywords: Fault Current, Fault Current Controller, FCC, Fault Current Limiter, FCL, Short Circuit Current, Power System Protection, Saturable-core Reactor FCL, Solid-State FCL, High Temperature Superconductivity, HTS

Please use the following citation for this report:

Smedley, Keyue; Alexander Abramovitz. (University of California, Irvine). 2011. ***Development of Fault Current Controller Technology.*** California Energy Commission. Publication number: CEC-500-2013-134.

TABLE OF CONTENTS

LIST OF FIGURES

LIST OF TABLES

EXECUTIVE SUMMARY

Introduction

Overall electric current loading on the transmission system has been rapidly increasing to meet the growth in electricity demand. The resulting higher electrical energy levels have increased the potential fault current magnitudes at locations throughout the transmission system. Fault currents in many instances may exceed the capability of existing protection systems such as circuit breakers to interrupt the faults safely and reliably, and represent an imminent threat to electrical equipment and the safety of utility workers and the public. Consequently, a utility must either upgrade breakers and equipment or reconfigure its system to reduce the potential fault current. Both solutions are costly and frequently reduce system reliability and power transfer capability. Application of fault current controller (FCC) technology, also frequently referred to as fault current limiter (FCL) technology has been identified as a potentially viable solution for managing fault currents to keep them within the existing short circuit capacity ratings of the system in order to expand and extend the transmission system's capacity and service life while minimizing capital costs. This approach allows utilities to continue to meet the growing demand for electricity reliably and cost-effectively.

Project Purpose

The California Energy Commission (CEC) funded this project to develop and evaluate reliable, cost-effective, and environmentally acceptable technologies for the control of high fault currents. The goals of the proposed research, directed by Principal Investigator the University of California at Irvine were to establish the desired criteria for FCC performance and to test two different leading FCC technologies against those criteria in controlled laboratory testing and field demonstration in a commercially operating Southern California Edison Company (SCE) distribution system. The overall objective of this project was to facilitate the improved, safe and reliable operation of the power system by advancing FCC technology as a cost-effective and environmentally-preferred option to breaker upgrades or system reconfiguration, and to evaluate the realistic potential of this technology to mitigate fault current levels at higher voltages in the electric system through real-world utility testing. The ultimate program goal was to enable the commercialization of FCC technology for the benefit of California and the United States.

The objectives of the proposed research were to:

1. Establish an FCC test plan including test criteria, test protocol, test site selection, test scheduling, data collection plans, and interface requirements for both the laboratory testing and field demonstration.

2. Prototype two FCCs, one saturable-core type developed by Zenergy Power plc, and one solid-state type developed by the Electric Power Research Institute (EPRI) and Silicon Power Corporation team.

3. Conduct laboratory testing of the two FCCs against the criteria, including pre-connection high-voltage insulation tests, normal operation tests and fault current limiting tests.

4. Install the FCCs on the SCE distribution system and perform field demonstration for a minimum of six months.

5. Complete the evaluation of the technologies on the basis of performance, respective strengths and weaknesses, costs, reliability, installation, operation and maintenance issues and potential for development to high-voltage design.

Project Results

The project started in September 2007. This was not the first attempt in the United States (U.S.) to develop a distribution-level FCC and demonstrate it on an operating power system. However, none of the earlier efforts had led to a successful field demonstration in the U.S. The obstacles to overcome were challenging. There were no industry standards for such a device, complicating the development of testing protocols. There were also significant engineering challenges in developing the prototypes to withstand the currents and voltages in the field. In addition, the prototype FCCs had to meet SCE's specifications for field demonstration on their system. Finally, the FCCs had to demonstrate the ability to withstand live circuit events and severe environmental conditions.

An important step taken in the early stages of the project was a focused effort to develop a test plan that was acceptable to SCE and workable for the teams. This test plan needed to incorporate to the extent possible the relevant engineering standards that apply to electrical apparatus. Zenergy Power worked closely with the Georgia Institute of Technology's (Georgia Tech) National Electric Energy Testing, Research and Applications Center (NEETRAC) and several of its member utilities, including SCE to implement a detailed FCC test program based on selected Institute of Electrical and Electronics Engineers (IEEE) and the Council on Large Electric Systems (CIGRE) standards and protocols for transformers and reactors. The EPRI/Silicon Power team created their plan based on American National Standards Institute (ANSI) C39.09-1999 and ANSI C37.06-2000, covering the entire spectrum of possible tests that needed to be carried out on their FCC, including component level factory tests, system level factory tests, acceptance tests and system field tests. Many technical issues related to laboratory test and field demonstration interfacing were resolved via a series of meetings with knowledgeable SCE engineers. Both teams completed their test plans, which provided valuable design and testing guidelines.

Zenergy Power completed the design, construction, and testing of an FCC based on a saturable-core concept. This type of FCC is basically a coil wound on an iron core and connected in series with the power line. In the normal state the core is biased into magnetic saturation by a dedicated direct current (DC) electromagnet so that the inductance of the magnetically saturated coil and the corresponding voltage drop across the coil terminals are negligible and the coil has no deleterious effect on the system during normal operation. The magnetic core is driven out of saturation by the fault current in the event of a fault. Consequently, the coil

becomes highly inductive, effectively inserting a large impedance into the power circuit and limiting the fault current without any need for active sensing or switching. A key enabling feature of the Zenergy Power high-temperature superconducting (HTS) FCL was the use of a HTS winding for the DC bias circuit, which reduced bias circuit power loss while increasing the intensity of the bias field. The Zenergy Power device is referred to as an HTS FCL. As previously noted, while fault current controller (FCC) is the preferred terminology for the class of technologies that address the management of fault currents, fault current limiter (FCL) is also commonly used. Both Zenergy Power and EPRI/Silicon Power Corporation (Silicon Power) used the term FCL when referring to their devices and their terminology was used in this report in such references.

A full-scale three-phase 12 kilovolt (kV) distribution level HTS FCL prototype was built for a rated load current of 1200 amps (A) (three phase), less than one percent normal voltage drop at maximum load, and 20 percent fault current clipping capability. Zenergy also developed a comprehensive test plan for laboratory testing of their HTS FCL.

The prototype HTS FCL went through a series of rigorous laboratory tests in BC Hydro's Powertech Laboratory in Surrey, British Columbia, Canada. A total of 65 separate tests were conducted, including 32 full-power fault tests with first peak fault current levels up to 59 kilowamps (kA) at the rated voltage. Fault tests included individual fault events of 20-30 cycles duration, as well as multiple fault events in rapid sequence to simulate automatic re-closer operation and extended fault events of up to 82 cycles duration simulating primary protection failure scenarios. The HTS FCL passed the test criteria in all cases. Only minor modifications to the high-voltage isolation layout were needed. The unit was then transferred to the SCE Westminster High-Voltage Test Facility for acceptance tests by SCE per IEEE Standard C57-12.01-2005.

The HTS FCL was installed in SCE's Avanti Circuit of the Future and operated from March 2009 through October 2010 after the successful completion of the acceptance tests. The unit was integrated into SCE's *supervisory control and data acquisition* (SCADA) system and operated in real time to provide protection to the distribution circuit during its field demonstration. A monitoring and data acquisition system was installed to archive performance data of the HTS FCL throughout the field testing period.

Several deficiencies in the original design and construction were revealed during the course of the field demonstration: a programmable logic controller (PLC) random-access memory (RAM) overflow programming issue; a heating, ventilation, and air conditioning (HVAC) shutdown due to excessive ambient temperature; helium leaks in the cryogenic coolers; nitrogen pressure instabilities associated with the liquid nitrogen cooling system; and a terminal block short. These events provided valuable learning experiences for the research team to identify design weaknesses and make necessary corrections along the way, resulting in significant design and implementation enhancements. The FCL also experienced an in-service multiple-fault event during the live grid demonstration and it was able to limit the fault current throughout the individual faults.

The FCL survived and thrived during its 19-month field service demonstration, which included nine months on line and 10 months in standby model. The standby period was due to a back-ordered bypass switch required before the unit could be put back on line after a maintenance outage. The immediate research benefit obtained from the Zenergy Power HTS FCL's operational experience was validating the importance of a more compact, more reliable, and easier to maintain non-HTS design for the FCL, and one which was scalable to transmission voltages.

The field demonstration was instrumental in furthering the development of FCL technology and contributing to Zenergy Power's first commercial sale of a medium-voltage device. Zenergy Power extended the research results to prototype development and applications at the transmission voltage level.

The EPRI and Silicon Power team completed an initial design for an FCL based on solid-state circuit technology employing Super Gate Turn-Off (SGTO) thyristor switches. The FCL design consisted of a set of standard building blocks (SBB), each containing an SGTO-based circuit designed for 5 kV voltage blocking and 2000 A continuous current ratings. The SBBs were used in multiples to form standard power stack (SPS) assemblies rated for 50 kV voltage blocking and 2000 A continuous current ratings. One SPS per phase was required for the 15 kV-class system. Three SPSs were then housed in an oil-filled tank to form a complete three-phase FCL, referred to as the Solid State FCL (SSFCL) unit. In the normal state the SGTO switches were turned on, which allowed continuous rated current to flow through the circuit. The control circuits opened the SGTO switches to insert a current limiting reactor (CLR) into the circuit to limit the fault current when a fault was detected.

The 15kV, 1200 A SSFCL was designed for outdoor use according to the C57.12.00-2010 IEEE Standard for General Requirements for Liquid-Immersed Distribution, Power, and Regulating Transformers. The overall SSFCL package was physically similar to a typical substation transformer tank with an external radiator bank for the cooling system. A comprehensive test plan was also developed for the SSFCL.

Less than optimal thermal performance was predicted during initial simulation of the thermal performance of the SSFCL design, which could have led to undesirable effects on the stability and reliability of the final, manufactured SSFCL. The designs of the thermal management system and the control boards were therefore modified during the course of the project to provide a more efficient thermal management system and to improve the noise immunity of the controls. An unfortunate result of this necessary re-design was a much higher projected construction cost than allowed by the available project budget; therefore, this part of the project was terminated at the conclusion of the design stage. EPRI was able to incorporate this and other lessons learned into a newer, separately-funded SSFCL design, which they intended to develop and offer for demonstration in the future.

The research in this project led to the successful field demonstration of the Zenergy Power HTS FCL, marking a milestone event in the history of FCL development in the U.S. The experience gained from the research contributed to a more reliable controller, a dramatic reduction of the

FCL's size (with a slight increase in weight), and the replacement of liquid nitrogen cryogenic refrigeration by a low-maintenance, dry (non-HTS) cooling system for increased reliability and reduced maintenance requirements.

The Zenergy Power HTS FCL was first laboratory tested successfully against FCL specifications and test criteria developed by U.S. utilities, including the host utility SCE. The HTS FCL was then successfully demonstrated in actual field operation for an extended period, during which it experienced several system events and performed as designed. The HTS FCL unit was rated at 15 kV, 1200 A, 110 kV (Basic Insulation Level), steady-state insertion impedance of less than one percent and a fault current reduction capability of 20 percent at 23 kA maximum fault current.

The first-generation "Spider-core" HTS FCL design had a dry-type transformer (air dielectric) structure, total overall dimensions of 19 feet by 19 feet by seven feet, and weighed approximately 50,000 pounds. The second-generation "Compact" HTS FCL that followed from this demonstration employed innovative core architecture and oil dielectric transformer construction techniques that led to a much more compact size of approximately eight feet by 10 feet by 11 feet and a somewhat increased weight of approximately 67,000 pounds. The Compact FCL had a power rating similar to the Spider-core FCL, but with a much higher fault current limiting performance. The new Compact FCL design was an improved option for applications where real estate was limited, albeit with somewhat increased weight.

The first-generation device had a relatively low power rating on the order of 25 megavolt-amperes (MVA) so the present manufacturing cost may not represent a high value proposition. This issue was being addressed on two fronts: HTS FCL technology was being improved to reduce basic device manufacturing cost, and it was being scaled up for higher voltages and currents. The latter may be more important in terms of cost-effectiveness and value proposition considering the fact that higher voltage substations can often be more crowded and have fewer options for expansion and that higher voltage components such as switchgear, insulators, transformers and bus-work were exponentially more expensive than their low-voltage counterparts. Furthermore, the larger renewable power generators will most likely desire to connect to the transmission system and high-voltage tie-lines have become increasingly more common as more power is wheeled from long distances and as grid interconnections occur to improve reliability and better control power flows. All of these factors were projected to continue to increase energy levels within the grid, leading to potentially unsafe fault current levels. In some cases higher-rated components cannot be retrofitted in the available space, leading to lengthy and costly major upgrades of grid infrastructure. Economic studies and performance models showed that FCC technologies can be very cost-effective compared to major upgrade projects at high voltages at current performance levels and price points.

The HTS FCL demonstration project also brought to light a reliability issue. While the HTS FCL was maintained in good operating condition and performed satisfactorily as a demonstration unit, an improvement is needed for a commercial product. An FCL ideally needs to target "five-nines" reliability (0.99999 availability) with only a single, scheduled, short-duration annual maintenance outage. Even better would be extending the maintenance interval to two years or longer, but an annual outage of a day or less would be acceptable if the FCL were otherwise

reliable and required no additional maintenance periods. Bypassing the FCL from service temporarily for maintenance could be a risk for the circuit if the FCL was to be relied on for protection. Possible temporary solutions for a scheduled bypass could be accomplished by installing an air-core reactor, splitting buses, or otherwise re-configuring the system for short durations, but these methods might not be feasible or acceptable for long-term operation. An FCL should be designed to the maximum extent possible to allow essential routine maintenance, such as cryogenic system maintenance to be performed while the unit is energized. Zenergy Power was aggressively modifying their HTS FCL technologies for reduced maintenance requirements, higher mean time between failure (MTBF) and lower mean time to repair (MTTR).

A key area for improvement identified during the field testing was the liquid nitrogen cooling system, which required periodic maintenance of the cryostat including drying, establishing vacuum and refilling the liquid nitrogen. This may not be practical since the unit would typically be installed in a high-voltage substation area. However, this issue was resolved in the second-generation FCL design by replacing the liquid nitrogen HTS system with a cryogen-free, "dry-type" conductive cooling system, available as a commercial off-the-shelf unit, resulting in a more reliable and robust system requiring less maintenance.

Overall, the Zenergy Power HTS FCL project was considered to have been an important success and it has already led to a scaled-up design for a transmission-level 138 kV FCL application.

The EPRI/Silicon Power SSFCL represented another potentially cost-effective solution to the rapidly increasing fault current levels in utility systems. One advantage of this type of FCL was the flexibility to be configured as either interruptive (i.e., to act as a "solid-state circuit breaker") or simply limiting the fault current (and leaving the fault interruption to existing protective devices), with only minor design differences. Also, a solid-state FCL may be used to limit the current of superconducting cables to enable the use of smaller cable sizes. The solid state FCL also had a unique capability to limit inrush currents, even for capacitive loads.

EPRI/Silicon Power identified some potential thermal management issues in their initial design. An improved system design was completed and the major technical design challenges such as the thermal management system and the control circuit architecture and timing issues were resolved. However, the resulting cost increase to actually construct the device was constrained by the project budget. Thus, this FCL was not able to advance to the laboratory test and field demonstration stages under this project.

According to the design predictions, the system size and weight would be 6.5 feet by 12 feet by 12 feet and the weight would be 62,000 pounds with oil cooling. These size and weight specifications would have been considered acceptable for utility applications.

The SSFCL employed a modular and scalable design. The SSFCL designed for the 12 kV line in this project period was composed of 10 SBBs in series. A future consideration with this design is that voltage sharing to maintain all the SBBs under the blocking voltage under dynamic conditions may be a technical challenge for transmission level applications where the voltage level is above 100 kV.

Overall, the EPRI/Silicon Power team made a substantial first effort in the design, development and improvement of the SSFCL concept. Many engineering challenges were identified and a new design was completed during the project period.

The research team accumulated extensive experience from the development of FCC technology and from the operation and support of the field demonstration at SCE's Avanti Circuit of the Future. Further fast-paced and more advanced development of FCC technology was strongly recommended. Substantial investments in system upgrades would have to be made on a fast-track basis in order to maintain the required levels of electric system availability and reliability as the demand for electrical energy rapidly increases, particularly in response to renewable power and "green technology" initiatives, and in the absence of better alternatives. Significant amounts of these investments may be potentially avoidable if suitable FCC technologies were available to California utilities and if California utilities were given reasonable incentives to deploy the new technologies. The research team recommended that investments be made in an accelerated program of FCC technology focused on reducing the cost, improving the reliability and increasing the voltage and current ratings of FCC.

Project Benefits

Electricity is a vital force in our economy. It is an important goal of the California Institute for Energy and Environment and the California Energy Commission to support the technologies required for providing a reliable, safe and environmentally responsible electrical energy supply. As such, FCC technology is a potentially cost-effective alternative to the capital-intensive upgrades of the power system that would ordinarily be required to meet growth in electrical demand. These demonstration projects have already resulted in two test plans and two full FCC designs, and have contributed to one commercial sale and one migration to a transmission-level application. The recommended enhancements to FCC technology will help California utilities and ratepayers reap the benefits. New and promising technologies are also important for economic vitality and job creation.

CHAPTER 1:
Introduction

The overall electric current loading on the transmission system has been increasing due to continuing growth in electricity demand. These higher power currents have increased the potential fault current magnitudes at locations throughout the transmission system. The fault currents, in many instances, may exceed the capability of existing protection systems (circuit breakers) to interrupt the faults safely and reliably, as well as threaten the safety of electric equipment and utility personnel. Consequently, a utility must upgrade these breakers and equipment or reconfigure its system to reduce the available fault current. Both solutions are costly, and frequently reduce system reliability and power transfer capability. Fault current controller (FCC) technology has been identified in the research community as a potentially viable solution for managing the fault currents within the rated short circuit capacity constraints, in order to meet the growing demand for electricity without the costly capital upgrades that would otherwise be required.

1.1 The Short Circuit Problem in Power Systems

Among the numerous faults occurring in power distribution systems, the short circuit fault is, probably, the most destructive one [1]. The short circuit fault can generate fault current more than 20 times the rated current. Fault currents are normally interrupted by the protection circuits, but serious consequences can still result, such as loss of service to customers, under-voltage or over-voltage transients, and/or loss of system synchronization. In extreme cases, fault currents can melt conductors, destroy insulation, cause fires, or induce strong mechanical forces, all of which can damage equipment. Serious safety, reliability and economic consequences will result from such incidents.

Distribution protection systems mainly rely on two customary and proven protection devices. The first, a fuse, is a simple, rugged, small and reliable protective device that can be used to interrupt fault currents as high as 200 kA. It is a self-triggering device and requires neither sensors nor actuators. A fuse can open in less than half a cycle at current levels that are well under the peak fault current [2], [3]. The major disadvantage of a fuse is that it is a single-use device, which must be manually replaced in order to restore electric service.

The second device is a circuit breaker (CB), a more sophisticated but still proven and reliable protection device [4]. A CB can be “tripped” by monitoring and instrumentation systems and then reset either automatically or remotely. However, CBs with high current interrupting capabilities are typically bulky and expensive. Furthermore, it is recognized that CBs require periodic maintenance and calibration and have a limited number of cycles of operation before teardown and rebuilding is required.

World economic growth poses a fast increasing demand for electrical power. Higher electrical loads, new consumers, and new distributed generation plants are constantly being added to the power grid. Higher fault current is a logical result of the growing capacity of the power grid; there is an increasing possibility that the expected fault current levels will exceed the

interrupting capability of the existing protection systems in the near future, with the problem only getting more urgent as time goes on. Failure of protection equipment to interrupt the fault current may cause extensive damage and put at risk the integrity and stability of the power system. Replacement or upgrading of a great number of CBs is a possible, but costly, solution to cope with the rising fault current levels.

However, the problem extends beyond the potential costs of new CBs. An upgraded CB allows higher fault current to flow through the rest of the now-underrated electrical equipment, which would be subjected to a much higher stress than originally designed for. The high stresses may incur damages even in the case that the CB interrupts the higher fault currents as designed. Furthermore, upgrading the CB to higher currents allows higher energy to the fault. Thus, in the event of the fault, the hazards to electrical installations may become increasingly higher. High fault current can also induce higher voltage in the grounding conductors and reduce the effectiveness of the substation grounding grid protective function. Thus, safety to utility personnel as well as the general public becomes an issue to consider. An additional concern is that, in certain cases, mechanical supports may need to be reinforced to withstand higher stresses from the intense magnetic fields induced by the fault currents. Perhaps even the clearances between the conductors will need to be increased. Therefore, along with upgrading the CBs there may be a need to upgrade some other parts of the system as well. However, limited capital budgets may not allow such a massive upgrade of the existing installations.

There are several traditional approaches to suppress the fault current in electrical systems [5]. System reconfiguration and bus splitting might be preferred for the fast growing areas. However, this approach comes at the cost of added grid complexity as well as additional switchgear. Other methods frequently used include the use of high-impedance transformers, a reactive impedance inserted between transformers and the electrical ground, or air-core reactors. All of these approaches, unfortunately, tend to reduce system efficiency and/or degrade system voltage regulation.

An alternative solution to the problem, which has gained much attention lately, is the application of a Fault Current Controller (FCC) [6]-[10], also known as a Fault Current Limiter (FCL). These terms usually refer to more recent or advanced technologies to control fault currents without the drawbacks of previous approaches. Funded by both government and private companies, research and development activities of various types of FCCs have been reported by many research institutions and private companies in many countries around the world [11], [12]. The recent trends of deregulation, competition and restructuring of the power grid have invoked a renewed interest in innovative FCC technologies for implementation of reliable and economically feasible commercial devices for the grid.

1.2 The FCC Solution

1.2.1 FCC Features and Benefits

Application of FCCs has been identified as one potentially viable approach for limiting the fault currents in power systems to safe levels. An FCC is typically installed in series with the

equipment to be protected. Under normal operating conditions, the FCC should display negligible impedance so that the power flow is unobstructed. In the event of a fault, however, the FCC's impedance should rapidly increase, acting to limit the fault current to an appropriate level.

Insight into FCC concepts and technologies can be found in several excellent references [13]-[15]. In general, FCCs may be classified by their principle of operation and key technological components used. As reported, FCCs can be implemented with passive non-linear elements, inductive devices, vacuum switches, semiconductor switches, superconductors, as well as combinations of these devices. FCCs may also be classified as either an interrupting type or a non-interrupting type. Interrupting FCCs are designed to interrupt the entire fault current, thereby acting as a circuit breaker. The task of a non-interrupting FCC is to limit the fault current magnitude to an acceptable level by absorbing or diverting a portion of the current; the limited current can then be safely interrupted by the existing protection systems. Technical feasibility of various types of FCCs has been already demonstrated with full power prototypes or scaled models.

From review of the literature and discussions with utilities and FCC developers, it becomes apparent that for an FCC to be commercially successful, it should have the following desired features.

In the normal (non-faulted) system condition, the FCC is expected to:

a) have a low insertion impedance;

b) be able to withstand distribution and transmission level voltages and currents (continuous rating);

c) have a low voltage drop;

d) have a low power loss;

e) have a low distortion and provide high downstream power quality; and

f) have low electromagnetic emissions.

In case of a fault, the FCC is required to:

a) be capable of limiting the first fault current peak;

b) display a large increase of impedance;

c) have a sufficient fault-condition impedance;

d) have an acceptable power loss;

e) tolerate the mechanical stresses;

f) endure the temperature rise;

g) withstand the fault condition for a sufficient time;

h) endure a sequence of recurring faults; and

i) be capable of fast transition from normal to faulted state and vice-versa.

On a system level, the FCC is desired to:

a) be a fully autonomous system;

b) be remotely accessible;

c) operate with minimum down time;

d) require no special current sensors or actuators;

e) at minimum, present no interference with existing protection schemes, and ideally have the ability to coordinate with them for improved system protection;

f) have a high level of reliability; and

g) exhibit "fail-safe" operation in case of malfunction.

For wide-scale commercialization, the following attributes of an FCC would be desirable:

a) acceptable size, weight and cost;

b) simple installation procedures;

c) low maintenance requirements;

d) long service life;

e) tolerance for harsh field conditions and weather extremes; and

f) compliance with the basic insulation level (BIL) standards, lightning tests, and other appropriate standards and specifications.

1.2.2 FCCs in the Power Distribution System

An FCC can serve different purposes in the power system, depending on where and how it is installed. Figure 1 illustrates three possible configurations appropriate for FCC installation [16]. The FCCs in positions marked A in Figure 1 can help reduce generator infeed fault currents, prevent transformers from damage, and help reduce the voltage sag on the upstream high-voltage bus during a fault on the medium-voltage bus. Also, transformers with low impedance can be used to maintain voltage regulation at a higher power level and to meet increased demand on a bus without upgrades to circuit breakers or other equipment. Alternatively, an FCC could be installed in the bus tie position B as shown in Figure 1. In the event of a fault on one of the buses, the FCC can help maintain the voltage level on the un-faulted bus. High capacity is available to both buses resulting in better transformer rating utilization. Smaller and less expensive FCCs can be installed in the feeder position, as shown in position C, to provide protection to overstressed equipment that is difficult to replace, such as underground cables or transformers in vaults.

Figure 1: Possible FCC Locations in the Power Grid

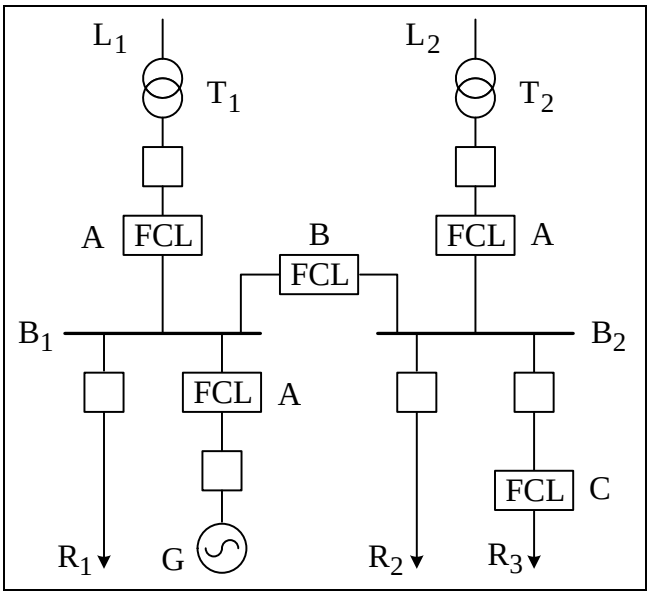

Source: Larbalestier, et. al. [16]

1.2.3 FCC Applications – Simulation Example

Many California and US substations are experiencing a steady increase in electrical loading due to economic growth, introduction of electric vehicles, and proliferation of renewable and distributed generation. In many cases, the substation fault current is approaching or exceeding the capabilities of the existing protective equipment, especially circuit breakers (CBs) with ratings of 63 kA. Although CBs with ratings up to 83 kA are also available, they are much larger, more expensive and sometimes difficult to obtain. Changing the power flow by splitting substation buses or reconfiguring circuits is possible, but can negatively impact system capacity and reliability. FCC technology offers a potentially cost-effective solution without degrading system capacity and reliability.

A PSCAD model of a hypothetical 230kV substation is shown in Figure 2. An FCC, modeled after the Zenergy Power HTS FCL, is installed in the feeder position with a bypass switch. PSCAD simulation was performed with the following parameters: line voltage 230 kV, I_{peak} = 173 kA, I_{symm} = 63 kA, K=173/63 = 2.75 and X/R = 55.06. The simulation results are given in Figure 3. According to the simulation study, the prospective fault current, with FCC bypassed, has 100 kA first peak and 63 kA (rms) fault levels. Figure 3 shows the effect of an FCC that trims about 18 percent of the fault current. With such a device the fault current is controlled to a safer 55 kA level.

This simulation example provides insight into the required specifications of a transmission level FCC. It is shown that a high-voltage FCC, i.e., 66 kV and up to 230 kV, with 10-15 percent reduction of prospective fault current, is a feasible solution to the problem of excessive fault current. If an FCC proves to be commercially successful, the lifetime of a range of substations

with the 63 kA existing CB limit can be extended. Keeping these substations operational for another decade or two has significant economic implications.

Figure 2: PSCAD Model of Hypothetical 230 kV Substation with FCC Protection

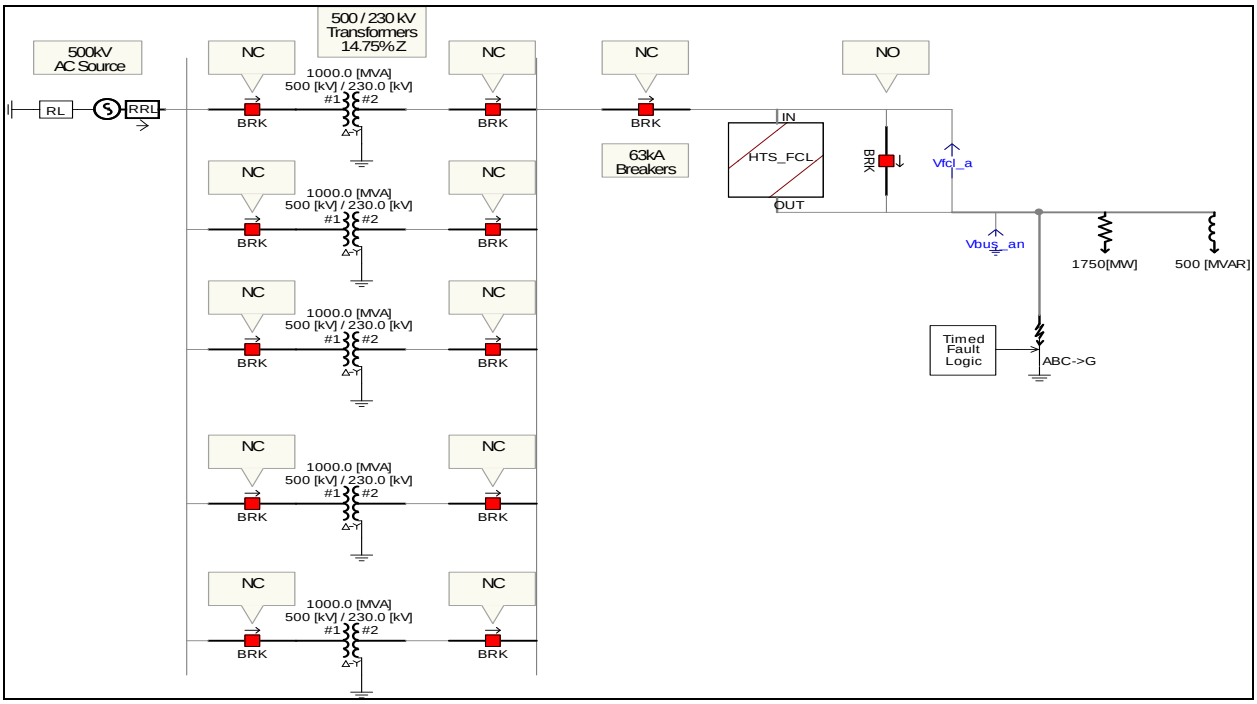

Source: Zenergy Power plc

Figure 3: Comparison of PSCAD Simulation Waveforms of the Fault Current of a Hypothetical 230 kV Substation, with: No Protection Devices; Air Core Inductor; FCL.

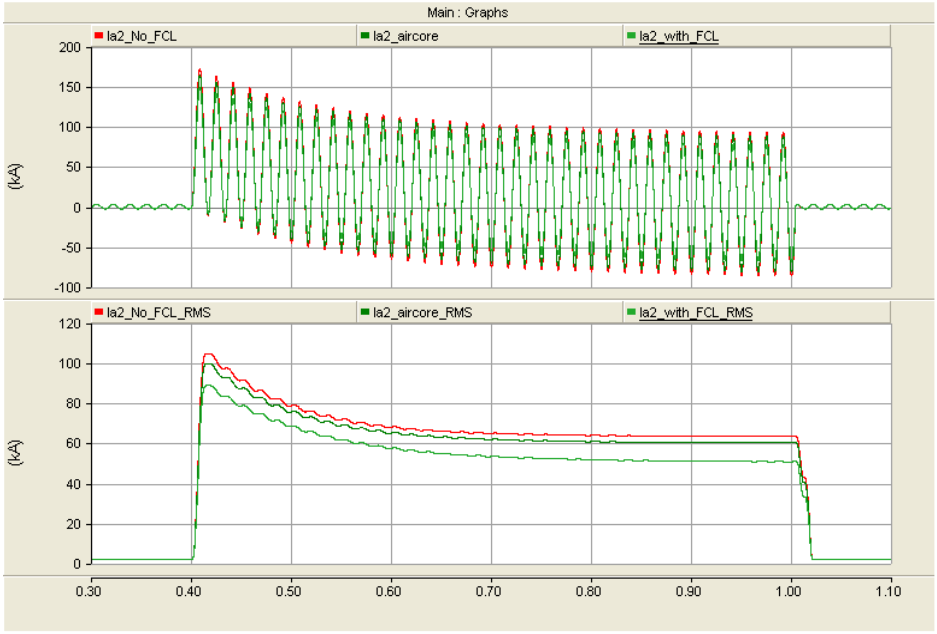

(a) Top graph: instantaneous line currents. Bottom graph: rms currents.

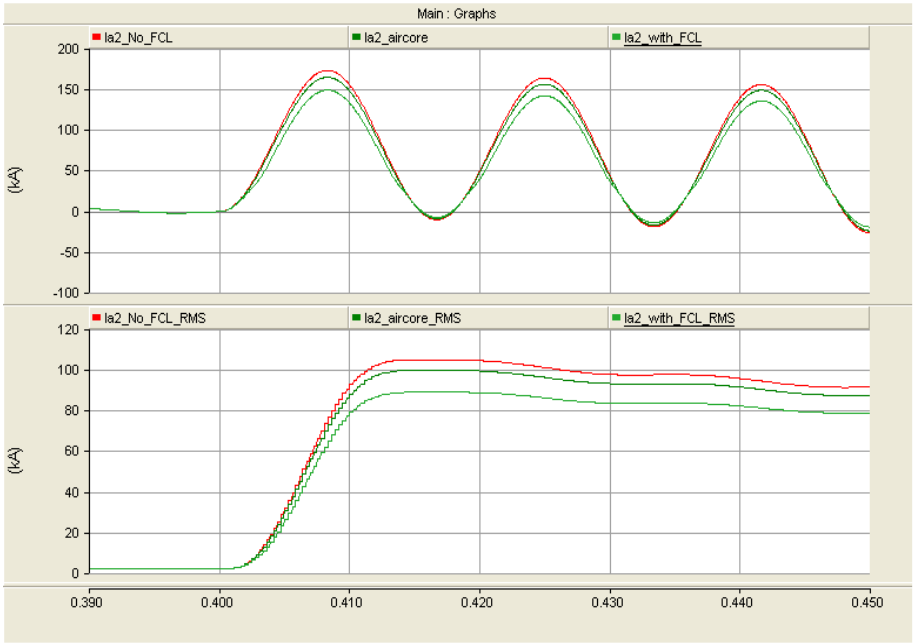

(b) Expanded view of fault onset. Top Graph: Instantaneous line currents. Bottom Graph: rms currents.

Source: Zenergy Power plc

1.3 FCC Development Objectives

The objectives of this project were to develop and demonstrate reliable, cost-effective, and environmentally acceptable technologies to equip the transmission grid to handle higher fault currents. The goals of the research were to establish the desired criteria for fault current controller performance and to test two different leading technologies against the criteria via controlled laboratory testing and field demonstration in an SCE distribution circuit. The research tasks were as follows:

1. Establish an FCC test plan including test criteria, test protocol, test site selection, test scheduling, data collection plans, and interface requirements for both the laboratory testing and field demonstration.
2. Develop two prototype FCCs, a saturable-core type developed by Zenergy Power plc, and a solid-state type developed by the Electric Power Research Institute (EPRI) and Silicon Power Corp. team.
3. Conduct laboratory testing of the two FCCs against the criteria, including pre-connection high-voltage insulation tests, normal operation tests, and fault current limiting tests.
4. Install the FCCs on the SCE distribution system and perform field demonstration for a minimum of six months.
5. Evaluate the technologies on the basis of performance, respective strengths and weaknesses, costs, reliability, installation, operation, and maintenance issues, and potential for development to high-voltage design.

The intended outcome of this project is to facilitate improved, safe and reliable operation of the power system by advancing FCC technology as a cost-effective and environmentally-preferred option to circuit breaker upgrades or system reconfiguration, and by evaluating the potential of this technology to mitigate fault current levels at higher voltages in the electric system through real-world utility testing. The ultimate program goal is to enable the commercialization of FCC technology for the benefit of California and the United States.

CHAPTER 2:
Fault Current Controller Technology Survey

This chapter presents an overview of past research activities, recent advances, and emerging technologies of FCCs, and provides brief discussions about the operating principles and main features of several representative FCCs based on solid-state and saturable-core concepts.

2.1 Solid-State Fault Current Controller Technologies

The advancement in high-power semiconductor technologies such as new thyristors, high-power IGBTs and IGCTs, and emerging SiC devices, makes it possible to implement a commercially viable FCC using solid-state electronic designs. In the following discussion, the solid-state FCC topologies are classified into three major groups: the Series Switch, the Bridge and the Resonant types.

2.1.1 Series Switch-type FCCs

The Series Switch-type FCC, illustrated in Figure 4, is composed of a bidirectional controlled semiconductor switch, S_{ss}, and a bypass network. The bidirectional switch may be implemented with various semiconductor devices, whereas the bypass network can be a combination of several parallel branches: the normal-state bypass, S_{bp}; fault current bypass, Z_f; a zinc oxide (ZnO) overvoltage protection bypass device; and a snubber network. Depending on the FCC's fault response algorithm, the bypass network can be a simple one or sophisticated one.

The normal-state bypass is usually implemented by means of an electromechanical switch, the purpose of which is to provide a low-resistance conduction path in order to avoid the semiconductor conduction losses and waveform distortion in the normal state.

Figure 4: Basic Topology of the Series Switch-type FCC

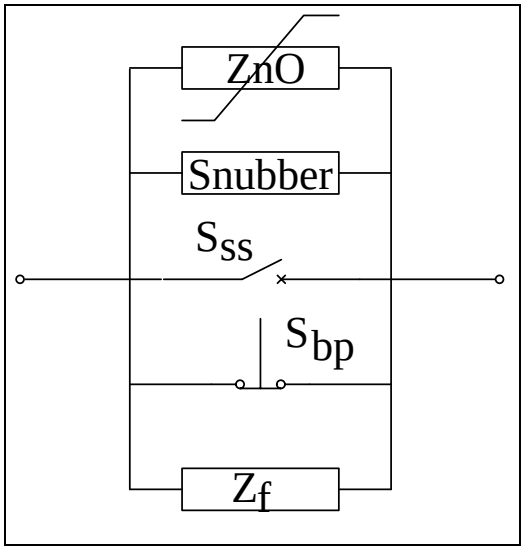

Source: University of California – Irvine

The fault current bypass is employed by the non-interruptive types of FCCs to restrict the fault current flowing in the power circuit and to allow existing protection schemes to take appropriate action during a fault. The fault current bypass can be implemented with either resistive or inductive components. The inductive bypass is the preferred solution due to its reduced thermal management requirement. The interrupting FCCs do not need fault current bypass. Some schemes simply turn off the switches to interrupt the current, while other designs control the semiconductor switches to modulate the fault current and keep it within the acceptable limits.

While the fault current bypass is optional, the overvoltage protection bypass is a must, which is usually implemented by a high-voltage, high-power ZnO varistor (variable resistor), also called an arrester. As the semiconductor switch is commanded to turn off, the varistor provides an alternate current path, while limiting the voltage across the semiconductor switch and absorbing some of the energy stored in the line inductance. In the case where the semiconductor switch is a composite one, the varistors can also be placed across each individual semiconductor device to limit the voltage across the series-connected devices and prevent overvoltage breakdown due to turn-off or turn-on delays.

The snubber network is an important part of the solid-state FCC. The task of the snubber is to limit the voltage rise across the switch at the turn-off instant and keep the dv/dt (rate of change of voltage) below the maximum allowed value according to the manufacturer specifications.

The semiconductor switch in Figure 4 can be implemented by a number of solid-state technologies, e.g., SCR [17], ETO [18], GTO [19], or IGBT [20], [21], [22].

2.1.2 Bridge-type FCCs

Bridge-type FCCs are implemented using a current-fed full bridge arrangement as shown by the basic schematic in Figure 5(a). This topology is inherently well-suited to using diodes as well as advanced thyristors as line-commutated switches. Bridge-type FCCs do not have a normal state bypass, and may or may not have a fault current bypass, but they do need an overvoltage protection bypass.

In the normal state all the bridge elements are "on," providing an unrestricted conduction path for the AC current, as shown in Figure 5(b). The bridge-type FCC relies on the insertion of a DC current source in series with the line to limit the AC fault current, as illustrated in Figure 5(c). In practice, a bridge-type FCC would likely use reactors to emulate the current source action. If the bridge is implemented by thyristors or semiconductor-controlled switches, AC current interruption or diversion to a fault current bypass is possible, as shown in Figure 5(d).

Figure 6(a) shows the schematic of an interesting rectifier bridge-type FCC, proposed by Boenig and Paice [23] and patented in the early 1980s; this circuit has evolved into many derivatives over the years.

Prior to start-up, the DC bias supply connected in series with L_1 charges the inductor to a DC current level that is higher than the expected AC peak current. All bridge diodes are in full conduction and free-wheel the reactor current. Hence, the AC terminals of the bridge appear

"short circuited" and present a low insertion impedance. The AC line current splits equally between the bridge legs. Depending on the line current polarity, one diode pair carries the summation current ½(I_{dc}+|i_{ac}|), and the other diode pair carries the differential current ½(I_{dc}–|i_{ac}|).

The equivalent circuits for the normal state and the fault condition state are illustrated in Figures 6(b) and 6(c), respectively. When a downstream short-circuit fault occurs, the rising AC fault current exceeds the DC current level. Consequently, the diode pair for the differential current turns off when its current reaches zero. The diode pair for the summation current remains on and steers the line current through reactor L_1. Consequently, the fault current is limited by L_1 allowing the circuit breaker to take a protective action. Upon interruption, the current in the DC reactor freewheels through the bridge and the energy absorbed during the fault is then dissipated in the diodes and wiring resistance.

Figure 5: Bridge-Type FCC

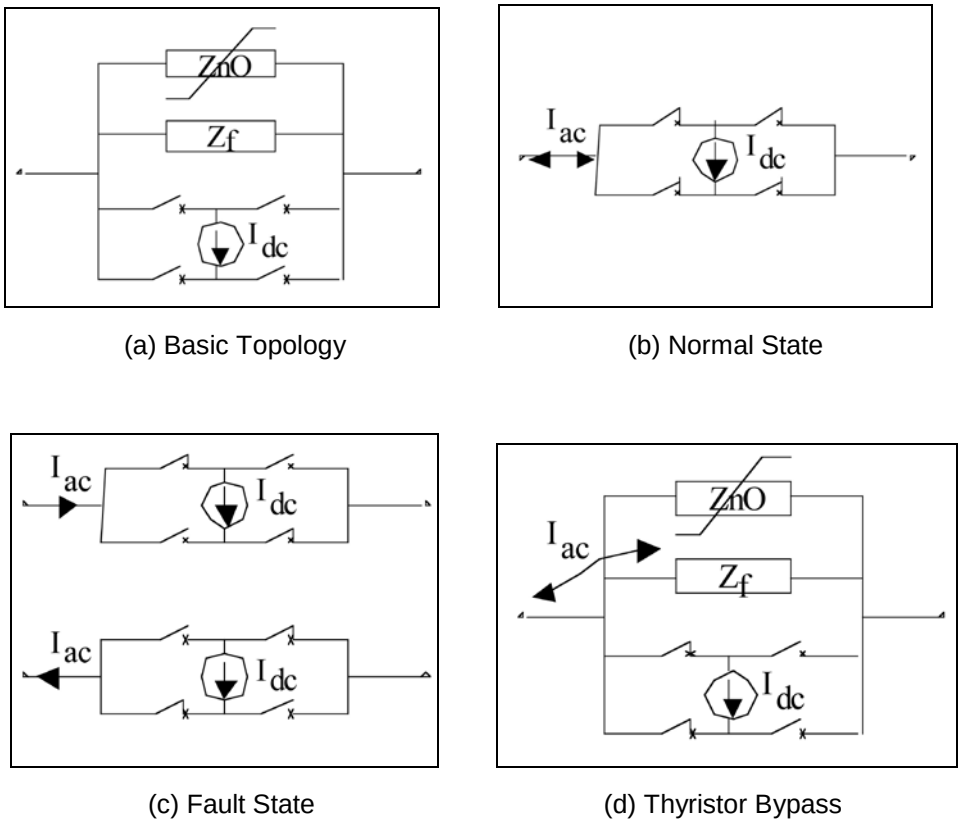

(a) Basic Topology (b) Normal State

(c) Fault State (d) Thyristor Bypass

Source: University of California – Irvine

The advantage of this type of FCC is that neither controlled devices nor a control circuit are needed. Available power diodes have rather high blocking voltage and current ratings. The current rating of the diodes and limiting reactor L_1 is dictated by the peak fault current. Since the current limiting reactor L_1 is on the DC side of the rectifier, during a fault condition the inductor is subject to high DC voltage, which causes inductor current build-up and eventually

saturates the inductor. Once the inductor is saturated, the current increases sharply and the FCC may lose its current-limiting capability. Therefore, this type of FCC cannot sustain the fault condition indefinitely; rather, it limits the fault current build-up rate, helps to safely ride through faults of short durations and, in the event of a major fault, it buys just enough time for the circuit breaker to take action. Also, the diodes should be rated to withstand the full fault current magnitude. A clear disadvantage of this FCC is the rather significant conduction losses in normal state operation caused by the constantly flowing high DC current. To alleviate the conduction losses Boenig and Paice [23] used a superconducting coil as a DC reactor. For this reason the rectifier bridge FCC is sometimes referred to as a "superconducting" type; however, the superconducting reactor is not a necessary feature in terms of the basic operating principle.

Figure 6: Single-reactor Rectifier Bridge FCC

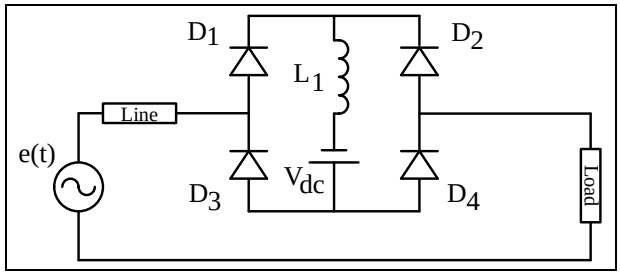

(a) Circuit schematic

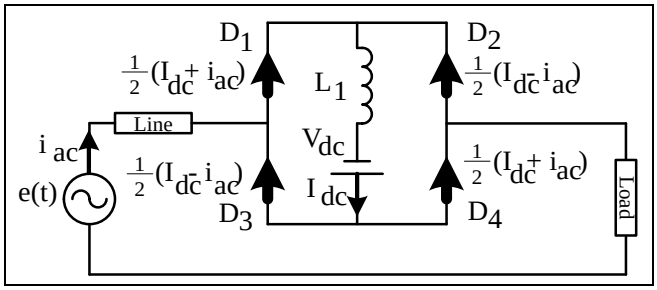

(b) Equivalent circuit for the normal state

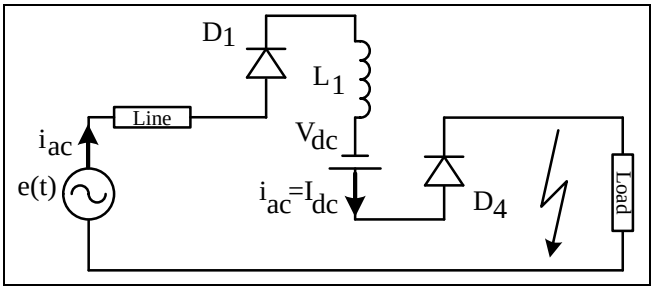

(c) Equivalent circuit for the faulted state

Source: Boenig and Paice [23]

Another example of a three-phase rectifier-type FCC is described by Nomura et al. [25] and shown in Figure 7. This FCC uses a full-bridge three-phase diode rectifier with a

superconducting coil acting as a DC reactor at the secondary winding of the isolating transformer. The transformer's primary three-phase coils are inserted in series with the line to provide the FCC function. The distinct feature of this FCC is the absence of a DC bias supply; it relies on the rectified grid voltage of the secondary to charge the DC reactor. Otherwise, the FCC operating principles are similar to that of the FCC previously described. The transformer isolation makes this FCC suitable for higher voltage applications. Alternatively, diodes with lower voltage ratings can be used.

Figure 7: Transformer-isolated Three-phase Rectifier Bridge FCC

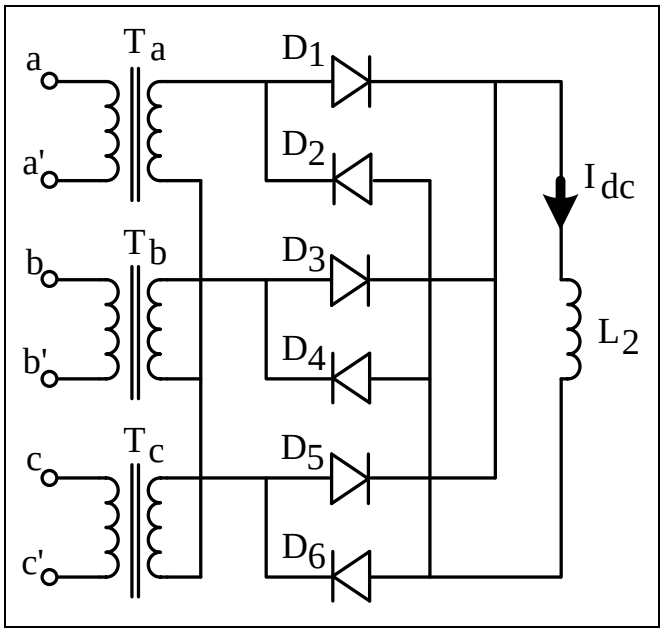

Source: Nomura et al. [25]

A single-phase SCR bridge-type FCC is shown in Figure 8 (Liu, Jiang and Wu [26]). At start-up the SCRs are gated to charge the L_1 reactor with a DC current equal to or higher than a pre-set peak line current. Alternatively, the charging may be accomplished by an auxiliary DC supply connected across L_1. All the SCRs are then gated to remain in full conduction. When a downstream short-circuit fault occurs, the rising AC fault current reaches the DC current level. Consequently, the SCR pair, which is carrying the differential current, turns off at zero current, whereas the SCR pair carrying the summation current remains on and steers the line current through L_1 in order to limit the fault current. Meanwhile, the gate signals to SCRs T_1 and T_2 are removed so that the conducting SCRs extinguish at the zero crossing of the fault current. The gating of T_3 and T_4 remain on to provide a freewheeling path for the L_1 current. In the next half cycle, the fault current flows through the fault current bypass reactor L_2.

Due to the fact that the fault bypass inductor is subject to an AC voltage, there is no current build-up in the L_2 reactor. Consequently, this type of FCC can endure rather long faults. The fault current bypass reactor L_2 should have a greater current rating than the DC reactor L_1. The latter should be designed to withstand only a half cycle of the line voltage. In practice the

current in the AC reactor L_2 only lasts for a few cycles until the circuit breaker trips; therefore L_2 can be relatively small. Also, since the fault current is diverted to the fault current bypass, the switch current stress is lower. Thus, this kind of FCC generally exhibits high reliability. In addition, since no cryogenics systems are required, both the initial cost and the maintenance cost of this FCC are expected to be low.

The zinc oxide (ZnO) arrestor prevents over-voltages from developing across the bridge and also provides a discharge path for the L_2 reactor at the instant of circuit breaker opening.

Figure 8: Two-Reactor SCR Bridge-type FCC

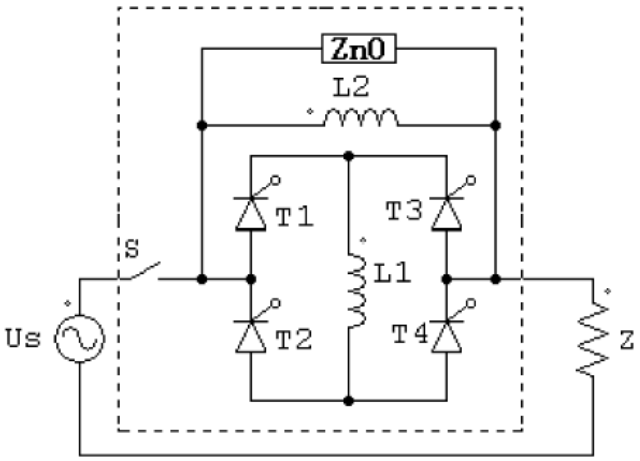

Source: Lu, Jiang and Wu [26]

Many other approaches are reported with half-controlled IGCT switches [27], [28]; single switch IGCT bridge [29], [30]; transformer isolated GTO bridge [31]; saturable DC reactor bridge [32]; GTO bridge with emergency power source function [33]; superconducting magnetic energy storage (SMES) system [34]; and switched-resistance bridge [35], among others.

2.1.3 Some Practical Difficulties of the Bridge-type FCCs

In each of the circuits described above, there exist equivalent resistances R_{dc} and R_{ac} representing the losses of the AC and DC circuits, respectively. These are always present and help dissipate the fault energy. The resistance R_{ac} incurs a power loss only during the fault period, whereas the resistance R_{dc} incurs the loss during the normal state operation as well as during the fault period. Due to the high DC reactor current the DC power loss can be very significant. This lowers the FCC normal-state efficiency and poses an additional thermal management problem. By adopting a superconducting DC reactor, the DC losses can be significantly reduced, but at the cost of a cryogenic system which requires periodic maintenance.

Furthermore, for proper operation of the Bridge-type FCC, the DC inductor current has to be maintained above a preset peak AC current. Thus, in practice, the inductor has to be recharged in order to compensate for the current decay. Because of this, a self-charging approach is

preferred to one using an external DC supply. In this approach, as the differential current ceases, one pair of devices turns off and the inductor is inserted into the line for recharging. Since this happens near the peak of the line voltage, the instantaneous voltage drop across the inductor "shaves the peak" of the line voltage and causes voltage distortion; the larger the DC inductor, the greater the distortion. Moreover, with a large DC inductor, the Bridge type FCC will have difficulty in accommodating a rapid load increase [35]. Figure 9 shows a simulation of the line current, I_{ac}, and the DC reactor current, I_{dc}, during the transient and the steady state conditions. The simulation was performed with the PSIM software package (by Powersim, www.powersimtech.com) for the circuit shown in Figure 19 for the improved saturable-core FCC with magnetic decoupling (Cvoric, de Haan and Ferreira [48]; see section 2.2.4) for 12 kV line voltage and 1 kA load, summing DC reactor of 20 mH with 0.1 Ω stray resistance. Recharging of the DC reactor introduces a clearly noticeable distortion. The design tradeoff between the power quality in the normal state and fault current limiting performance can be alleviated by introducing an AC by-pass inductor in addition to the DC reactor but with a smaller value.

Better power quality can be obtained by using a DC bias supply, which pumps the DC reactor current above the peak AC line current. This bias supply has to provide a rather significant DC current at low voltage. Several proposals can be found in the literature for DC bias supply implementation, e.g. [26], [36], [38].

Figure 9: AC Line and DC Reactor Currents for a Bridge-type FCC

Source: University of California – Irvine

2.1.4 Resonant-type FCCs

Instead of having distinct normal-state and fault current bypass elements, the resonant types of FCCs use switches to reconfigure their networks either into the normal state (NS) or into the fault condition (FC) sub-topologies (see Figure 10). These FCCs employ a series resonant circuit (also called a resonant tank) as their normal-state bypass. To achieve near-zero series

impedance, the resonant circuit is fine-tuned to the line frequency. Under fault conditions, the circuit is switched to the fault state sub-topology and is then out of resonance. Therefore, a much higher impedance is presented to the line. Accordingly, resonant FCCs can reduce the fault current but do not have interruption capability.

In practice, a bypass switch should be included in the installation in order to maintain service in case of FCC malfunction, by allowing the device to be taken off-line for maintenance.

Several interesting FCCs based on resonant circuits and thyristor switches have been proposed, as in [38]-[41]. The FCC topologies shown in Figure 11 are generally representative of the circuits found in the literature sources. In the normal state the resonant circuit is tuned to the line frequency, presenting negligible impedance to the line. In an event of a fault, the thyristors are turned on either to introduce a short circuit or to connect an additional component to the resonant circuit, which takes the circuit out of resonance. Subsequently, the fault current is suppressed by the high impedance of the mistuned resonant circuit.

Figure 10: Topology of the Resonant-type FCC

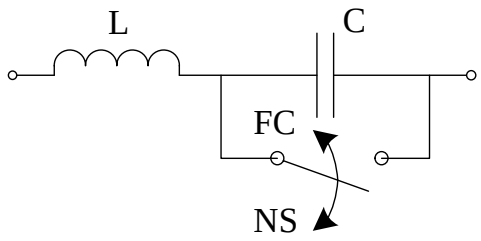

Source: University of California – Irvine

Figure 11: Types of Resonant-circuit FCCs

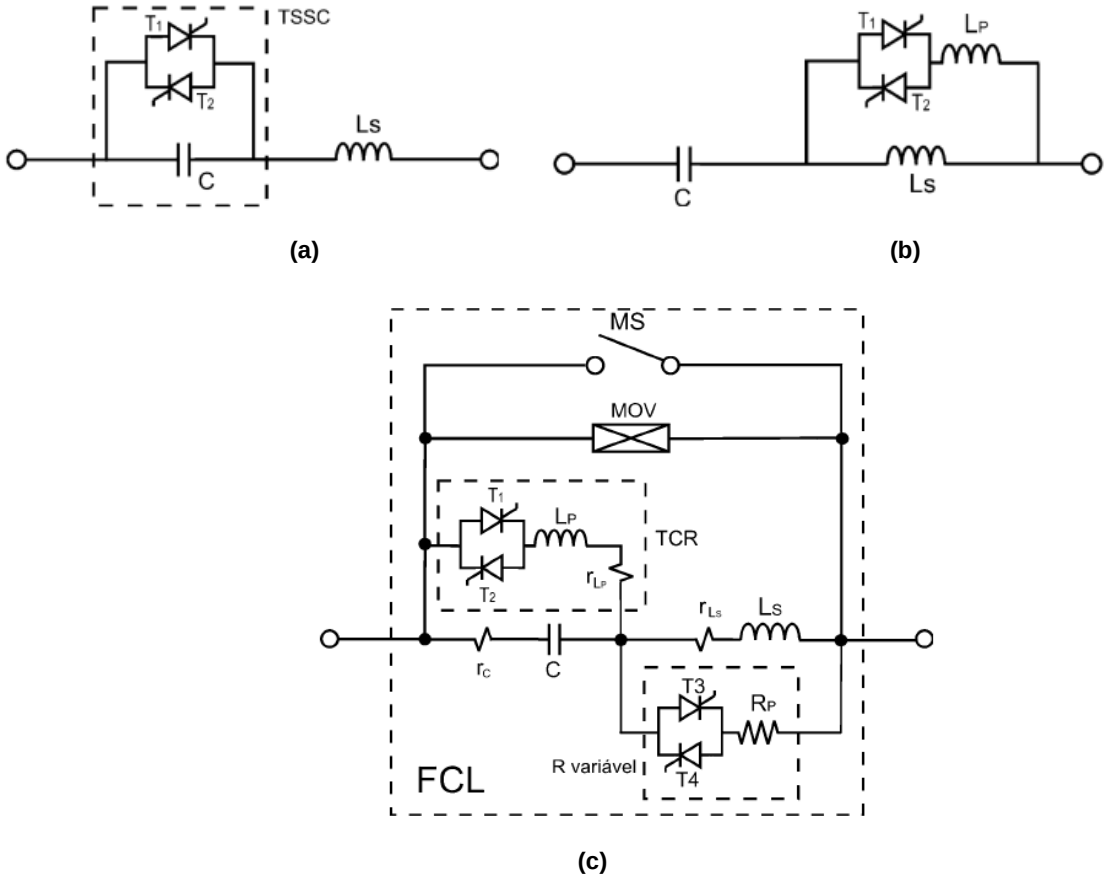

Source: Lanes et al. [38]

The key advantages of a resonant FCC include better power quality and a desirable zero-voltage or zero-current switching operation. Another advantage is that the switches are activated in fault condition only and remain off in the normal state. This contributes to better efficiency and reliability and reduces thermal management requirements. However, the resonant circuit may impose higher peak voltages or current stresses on the semiconductor devices. Fault transients also create over-voltages or voltage sags. Moreover, the inductor and capacitor size and cost may be considerable, and require precise tuning.

Another example of FCC, proposed by Hojo et al. [42] (see Figure 12), consists of a series inductor and a self-commutated voltage source inverter connected in series with the line by an isolating transformer. (It should be noted that this FCC may also be classified as a resonant type.) In the normal state, the inverter is operated in a capacitive mode to compensate for the voltage drop across the series inductor. During a fault, the inverter is commanded to operate in inductive mode in order to impede the fault current.

Figure 12: Inverter-based FCC

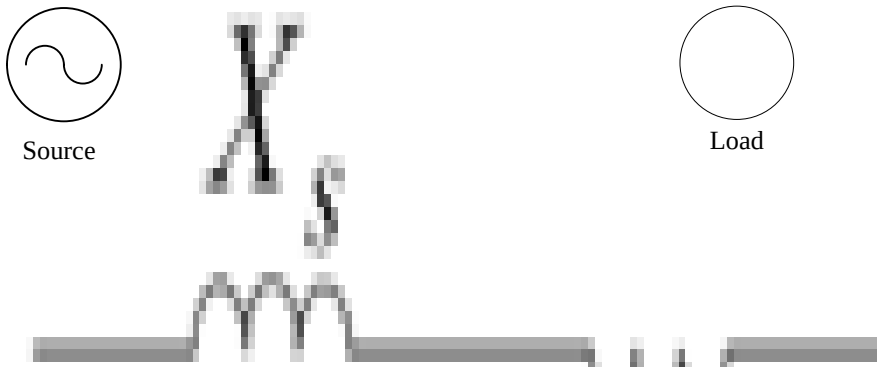

Source: Hojo et al. [42]

Such FCCs can also be beneficially used in the normal state to improve the power quality of downstream voltage by compensating for line voltage distortion and voltage sags [43], [44].

The disadvantage of this approach is that the inverter has to process high currents and must operate at a relatively high frequency using pulse-width modulation (PWM) control. Also, conduction and switching losses are considerable, and the inverter's DC link capacitors have to be of a relatively large value to handle the large amplitude currents while maintaining a moderate DC bus voltage swing.

2.2 Saturable-core Fault Current Controller Technologies

Saturable-core FCCs exploit the nonlinear characteristics of ferromagnetic materials in order to achieve a variable inductance. In essence, such an FCC is simply a coil of copper wire wound around an iron core and connected in series with the electric circuit to be protected. In the normal state, the iron core is saturated by a dedicated bias circuit, and the inductance of the saturated coil and the resultant voltage drop across the coil terminals are both negligible. Thus, the coil has no obvious effect on the electric circuit. However, in the event of a fault, the high AC fault current drives the magnetic core out of saturation, and the resulting high inductance of the coil limits the fault current. This basic principle of "passive" inductive switching can be employed in a variety of ways to implement a saturable-core FCC. The various designs mainly differ in terms of the core shape, magnetic circuit configuration, and core bias arrangement.

Many saturable-core FCCs also incorporate superconducting technologies and are frequently referred to as superconducting devices. However, the key physical principle of a saturable-core FCC is the inherent mechanism of impedance change due to magnetic core properties, whereas the superconducting part is the assisting technology which aims to enhance performance, such as higher current limiting capability, higher magnetic field intensity, reduced power loss, more compact design, etc. Saturable-core FCCs can also be successfully designed using non-superconducting components.

Saturable-core FCC technologies tend to exhibit physical and electrical characteristics that are similar to other distribution equipment, such as transformers and power reactors. Particular mention should be made of their ruggedness and inherent ability to quickly react to a fault without any detection circuitry. Furthermore, a saturable-core FCC presents an inductive impedance to the line during the faulted state. The absorbed energy is stored in the magnetic field and mostly recycled back to the system, which reduces the power dissipation and can help to alleviate thermal management issues.

Several feasible ideas for implementation of saturable-core FCCs have been proposed. According to the literature, the major contributors to the cost of saturable-core FCCs are the superconducting wire, the cryostat and the associated cooling system, and the materials costs of the iron core and copper wire. It is a significant engineering challenge to minimize the cost of the components in the design such that the FCC is an affordable and commercially viable device for distribution and transmission systems. Another engineering challenge is to minimize the voltage surge induced in the DC bias circuit during the fault.

In the following sections, several concepts of saturable-core FCCs are reviewed, considering the aforementioned characteristics.

2.2.1 Basic Saturable-core FCC

A basic single-phase saturable-core FCC device was patented in the early 1980s as described by Raju, Parton and Bartram [45]. The fundamental structure of this type of FCC is illustrated in Figure 13.

Figure 13: Conceptual Structure of a Saturable-core FCC

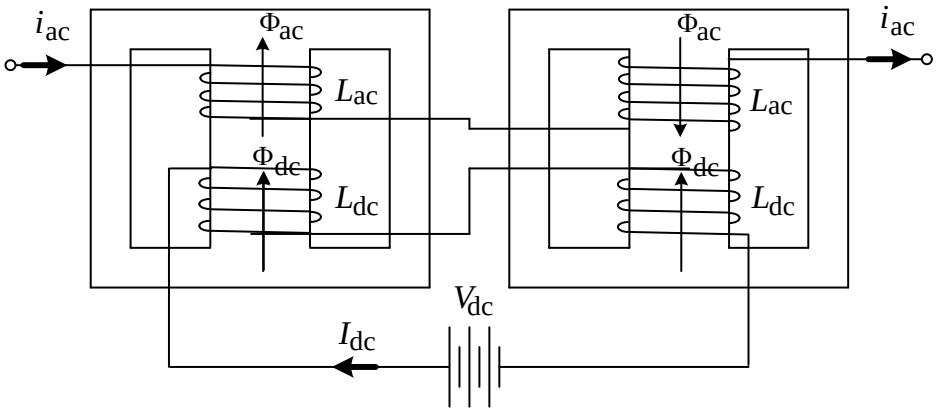

Source: Raju et al. [45]

This type of FCC is constructed around two iron cores, each core designed in what is termed an "EE" shape, and with AC and DC coils wound around the center limbs. The AC coils are conventional copper coils connected in series differentially and inserted into the AC line in series with the protected load, as shown in Figure 14. The DC coils comprise the bias circuit, wound on top of the AC coils and fed by a low-voltage, high-current DC power supply. With superconducting (SC) wires, the DC coils impose zero resistance to the bias circuit. Hence, the bias current is limited only by the internal resistance of the power supply. This allows

attainment of high DC current, generation of a strong magnetic field and efficient saturation of both cores.

Figure 14: Connection of a Saturable-Core FCC

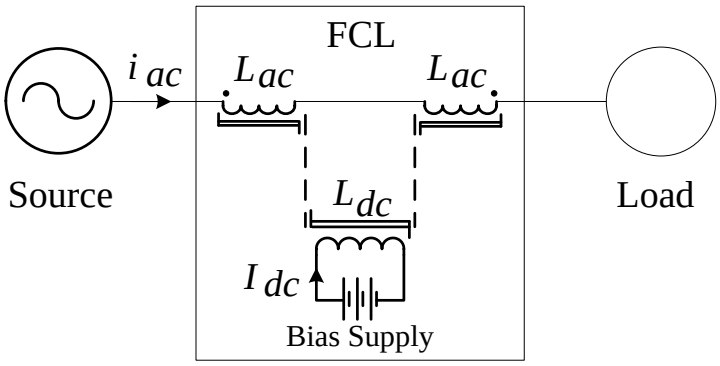

Source: Raju et al. [45]

The principle of operation of this device is described by considering the magnetomotive force (mmf)-flux relationships. By regulating the DC coil current, the mmf-flux operating point of both cores is established in the vicinity of point B (see Figure 15). As the AC line current flows through the AC coils, the core operating point is shifted. Due to the differential connection of the AC coils, the AC-induced mmf in one core reinforces the DC mmf, whereas in the other core the AC mmf weakens the DC mmf. Therefore, the operating point of one core shifts into a deeper saturation (point A), while the operating point of the other core moves toward a shallow saturation (point C), closer to the hysteresis knee point. In the normal state both cores remain in saturation so that their combined inductance is low. When a fault occurs, the abnormal amplitude of the fault current is capable of driving the core with the counteracting mmf out of saturation into region C-D of the hysteresis curve. Here, the permeance (ability to conduct magnetic flux) of the desaturated core sharply increases, resulting in a considerable increase in coil inductance and, consequently, higher impedance, which limits the fault current. Depending on the AC line current polarity, the coils alternate in and out of saturation to limit the current in each half cycle.

The FCC inductance may be characterized as a function of the AC current amplitude, as shown in Figure 16. The current threshold value, I_{knee}, corresponds to the operating point C, whereas the value I_{max} corresponds to the operating point D. As the current amplitude is increased above I_{max} the core enters the reverse saturation region to the left of D. As a result, at current levels above I_{max}, FCC inductance falls back to the low value. Therefore, I_{knee} defines the highest normal current amplitude above which the FCC current limiting commences, whereas I_{max} defines the current level above which the current-limiting effect is lost.

Figure 15: Saturable-core FCC Operating Points

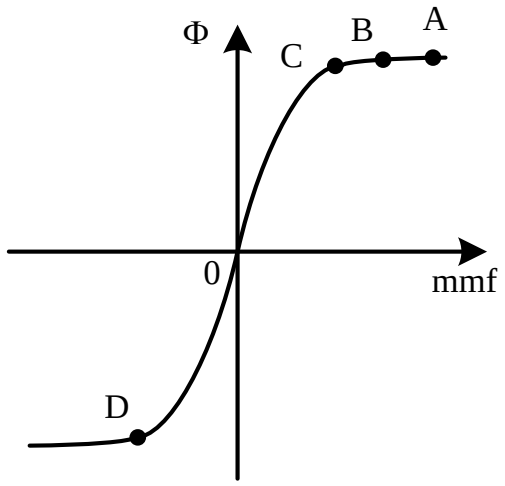

Source: University of California – Irvine

Figure 16: Saturable-Core FCC Inductance as a Function of AC Current

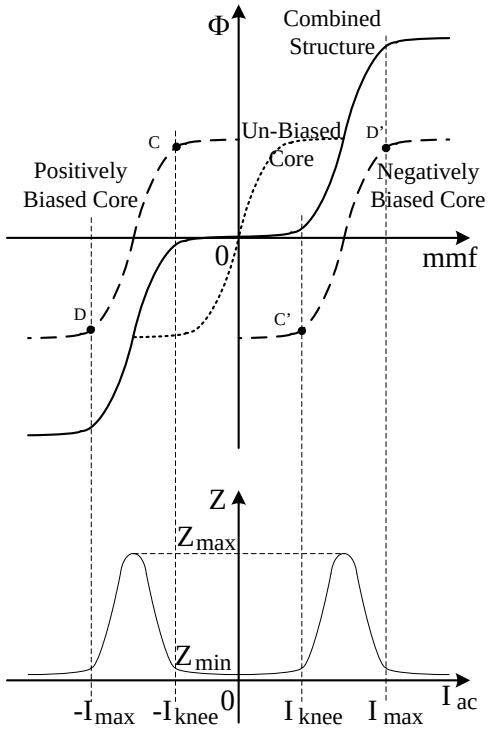

Source: Raju et al. [45]

The advantages of this approach include a simple and symmetrical core design, ruggedness and fail-safe operation. However, the designer's choice of two "E" cores per phase, each with coils wound on the center limb, makes it difficult to implement a compact distribution-level three-

phase FCC, since it requires a battery of six cores, positioned sufficiently far apart from each other to provide safe clearances. In addition to the drawback of the resultant bulky size, the design of the cryogenics system is challenging. The original design used a quite bulky liquid nitrogen cryostat to chill the superconducting DC coils. FCCs of higher power rating may have larger dimensions so that each core may have to be provided with a dedicated cryostat and superconducting DC coil. Another problem with this magnetic design is the transformer coupling between the AC and DC coils in the faulted condition. The high voltage across the AC coil may induce a large voltage in the DC coil and cause possible damage to the DC power supply. As a protective measure, a resistor in series with the DC coil was used, at the cost of higher losses in the bias circuit.

2.2.2 Saturable Reactor Limiter for Current

A "saturable reactor limiter (SRL) for current" as proposed by Oberbeck, Stanton and Stewart [46] actually preceded that of Raju et al. [45]. The structure of a bipolar, single-phase SRL is shown in Figure 17, constructed using a core with four limbs, the first of which has an air gap. The DC bias coil is wound on the second limb. The AC coils are wound on the third and fourth limbs and are connected in electrical opposition in series with the protective load. The current in the DC bias coil induces a DC flux that drives the core into saturation. In the normal state, the AC current is insufficient to desaturate the core so the AC coil inductance is low. In the fault condition, the high fault current generates mmf of sufficient intensity to overcome the DC bias mmf and desaturate the AC limb carrying counteracting mmf. The increased AC coil inductance during the fault condition limits the fault current.

Figure 17: Structure of a Saturable Reactor Limiter (SLR)

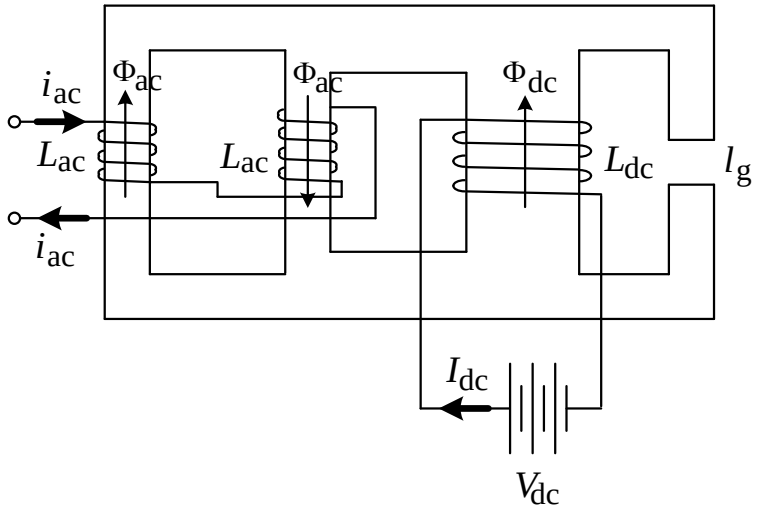

Source: Oberbeck et al. [46]

The idea behind this magnetic structure approach is that in the faulted state the AC flux desaturates one limb and then flows through the gapped limb rather than through the strongly saturated DC coil limb. In consequence, the AC flux is diverted from the DC coil. This results in

significant reduction of the magnetic coupling of the AC coil to the DC coil. Therefore, this type of SRL may have a reduced voltage surge in the DC winding under fault conditions.

The major disadvantage, however, is the significant power loss of the bias circuit, since an ordinary DC coil was used. The resulting DC coil temperature rise restricts the bias current level and, accordingly, the attainable mmf. Furthermore, assuming that the AC coil limbs and the gapped limb are of the same cross-section, in order to keep the AC limbs in deep saturation with the same flux density, the cross-section of the horizontal segments, between the DC limb and the AC limb, is required to be twice the cross-section of the AC limb; but the cross-section of the DC limb must be about 2-3 times the cross-section of the AC limb. As a result, this design of FCC has a complicated core structure that is difficult to build, and the achieved DC-AC coil decoupling comes at the cost of additional core volume and weight as well as production complexity and cost.

No suggestion was made by Oberbeck et al. [46] regarding how to construct a three-phase SRL. One possible solution is simply to arrange three single-phase units together. Another solution might be to extend the magnetic core so that two additional pairs of AC limbs could be fitted for each phase; in this case, only a single DC bias coil is needed, but the core structure becomes even more complicated.

Another disadvantage that can result from the asymmetry of the core is unequal I_{knee}, I_{max} and Z_{max} values for the positive and negative current paths.

2.2.3 Magnetic-controlled Switcher-type Fault Current Controller

A single-phase FCC as shown in Figure 18 was proposed by Pan and Jiang [47]. This FCC was constructed with EE cores with the AC coils wound on the outer limbs, which have a smaller cross section than the rest of the core. The DC bias coil was wound on the central limb. Another added feature is the inductor L_{dc} in series with the DC bias supply. Owing to these two features the operating principle is somewhat different from the aforementioned FCCs.

Figure 18: Magnetic-controlled Switcher-type FCL

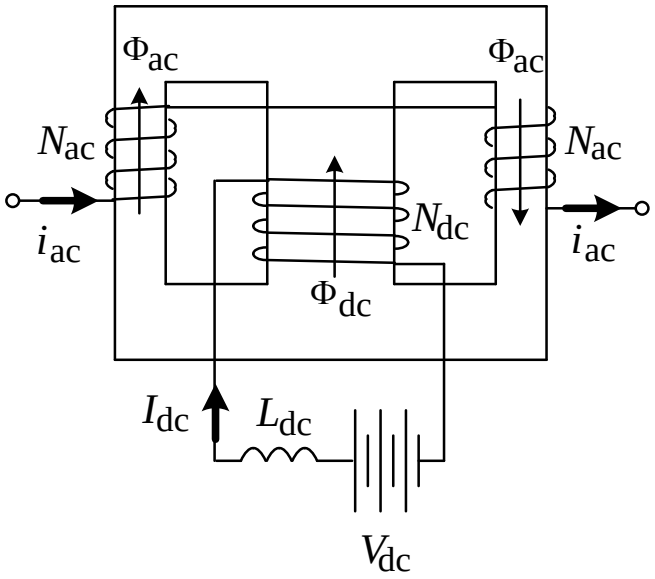

Source: Pan and Jiang [47]

The FCC is connected to the line in the manner previously illustrated by Figure 14. In the normal state, the outer limbs are biased to saturation, while the rest of the core remains in the linear region. This takes place due to the lesser cross-section of the outer limbs. As a result of the saturation of the outer limbs, the inductance of the AC coils and their resulting impedance is very low so that the normal power flow is unobstructed.

In the faulted state, the large amplitude of the fault current drives one outer limb into deeper saturation, while the other limb is desaturated. Consequently, a closed magnetic path with a high permeance is established providing high magnetic coupling between the desaturated AC coil and the DC coil. The operation of the magnetic structure therefore resembles that of a linear transformer: the desaturated AC coil exhibits high inductance and starts acting as a transformer primary, and, by virtue of the transformer action, the impedance of the DC circuit is reflected to the line.

The advantage of selective saturation of the core segments is that the inductance of the DC coil remains relatively large and requires lower bias current to keep the AC limbs saturated. This feature allows an ordinary, i.e., non-superconducting, DC bias coil to be used. Thus, the production and maintenance cost of the auxiliary support systems can be reduced. This advantage is offset by the added volume, weight and cost of the core and the DC-side inductor L_{dc}.

The fault impedance of this FCC design is determined by the impedance of the inductor L_{dc}, reflected according to the turns-ratio of the AC and DC coils, in parallel with the inductance of the desaturated AC coil. The high impedance introduced into the line helps limit the fault current. However, since the reflected and magnetizing impedances appear in parallel, their

equivalent impedance is lowered. Therefore, the effectiveness of the method is somewhat reduced, requiring a higher number of turns of the AC and DC coils. This results in a structure with larger window area, larger core, and higher copper weight. In addition, the normal-state impedance is higher and therefore causes a higher voltage drop across the FCC terminals.

Saturation of the FCC core requires high mmf, which is achieved by a sizeable number of turns of the non-superconducting DC coil. Therefore, the turns ratio between the DC and AC coils is high, and a very high voltage is induced in the DC coil under the fault condition. Proper isolation is necessary for the DC coil, which further increases the thickness and volume of the DC coil and consequently the window area of the core and the overall core size. Additional concerns are related to L_{dc}: though the power supply current is limited by the DC inductor, L_{dc}, a high voltage at the DC bias circuit poses a safety issue. Moreover, the DC bias supply has to carry the sum of DC plus the reflected AC fault currents. The bottom line is that an effective design for this type of FCC poses numerous engineering challenges.

2.2.4 Improved Saturable-core FCC with Magnetic Decoupling

The SRL proposed by Oberbeck et al. [46] was further improved by Cvoric, de Haan and Ferreira [48] to achieve a better decoupling between the DC and AC coils. The key idea is to interchange the positions of the DC and AC coils, as shown in Figure 19. The bias coil is wound on an outer limb, whereas the AC coil is wound on a central limb. Otherwise the principle of operation is identical to [46].

The advantage of this magnetic structure is that in the faulted state the AC magnetic flux flows through the desaturated gapped limb, positioned further away from the DC coil. Thus, the coupling between the AC and DC coils is weaker than that in the original structure of [46], resulting in a greatly reduced voltage surge induced in the DC coil. Note that in the faulted state, the permeance of the AC coil magnetic path is determined mainly by the air gap: the shorter the air gap, the higher the permeance. The AC coil can then be constructed with a lower number of turns, resulting in lower copper weight, lower normal state inductance, lower voltage drop and reduced conduction losses.

Figure 19: Saturable-Core FCL with Magnetic Decoupling

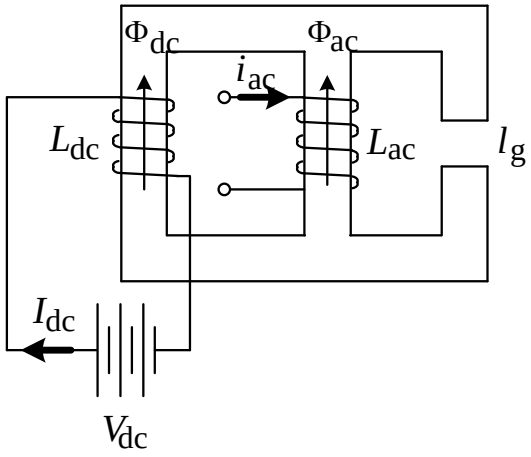

Source: Cvoric et al. [48]

However, the need for an additional core limb, the asymmetric core structure, the additional iron volume, and the overall cost remain the main disadvantages.

Another idea for implementing an FCC with reduced core volume was presented by Cvoric et al. [49]. This single-phase FCC was constructed on a pair of EE cores having a deeply gapped middle limb.

2.2.5 Saturable-core FCC with Parallel Permanent Magnet Bias

The FCC bias circuit as reported by Raju et al. [45] utilized a superconducting DC coil to allow higher bias current and reduced DC bias losses. However, superconducting wire is a major factor contributing to the overall FCC cost. The cryostat and DC bias supply both require extensive maintenance and may adversely affect overall system reliability.

A permanent magnet (PM) bias circuit as proposed by Iwdiara et al. [50] and Liu et al. [51] can potentially alleviate these problems. Several other derivatives of this idea have also been reported in the literature. A proof-of-concept laboratory prototype was reported in [51] to verify the idea. The PM biasing structure was installed as the center limb of the core structure, as shown in Figure 20. Since the PM flux is split between two parallel branches, this bias arrangement is referred to as "parallel PM bias." The advantages of this approach include lower cost, lower volume of the device, ruggedness, and higher reliability. The disadvantages of parallel PM bias are the lower field intensity and PM demagnetization.

2.2.6 A Series-biased Permanent Magnet FCC

A single-phase 400V/63kA FCC using a permanent magnet (PM) for series biasing was experimentally demonstrated by Rasolonjanahary et al. [53]. The basic structure of this type of FCC is shown in Figure 21(a). In this design the PMs were inserted as segments of a "C" iron core.

Figure 20: A Parallel-Biased Permanent Magnet FCC

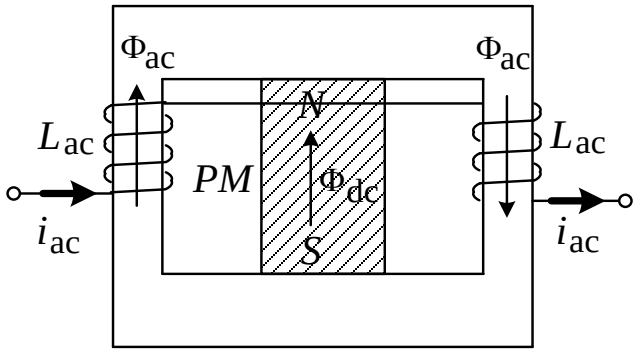

Source: Liu et al. [51]

The principles of operation of such a device exploit the hysteresis property of the PM material. In the normal state, due to the lower current amplitude, the magnetic field strength is decreased before the flux density reaches B_s, so the operation follows the minor B-H loop within the saturation region (see Figure 21(b), upper right quadrant). Therefore, in the normal state the inductance of the saturated coil, L_{ac}, is low. Regardless of the polarity, a high fault current in the AC windings will cause large variations in magnetic field, following the major B-H loop. Normal operation (following the minor B-H loop) therefore incurs low flux density variations and low losses, whereas during faulted conditions greater flux variations occur and much energy is dissipated when following the major loop. Thus, in the faulted state, the FCC's inductance and the equivalent series resistance increase considerably. The design challenge of such an FCC is to minimize the losses and voltage drop across the FCC terminals in the normal state, while attaining a large voltage drop under the fault condition.

Figure 21: A Series-Biased Permanent Magnet FCC

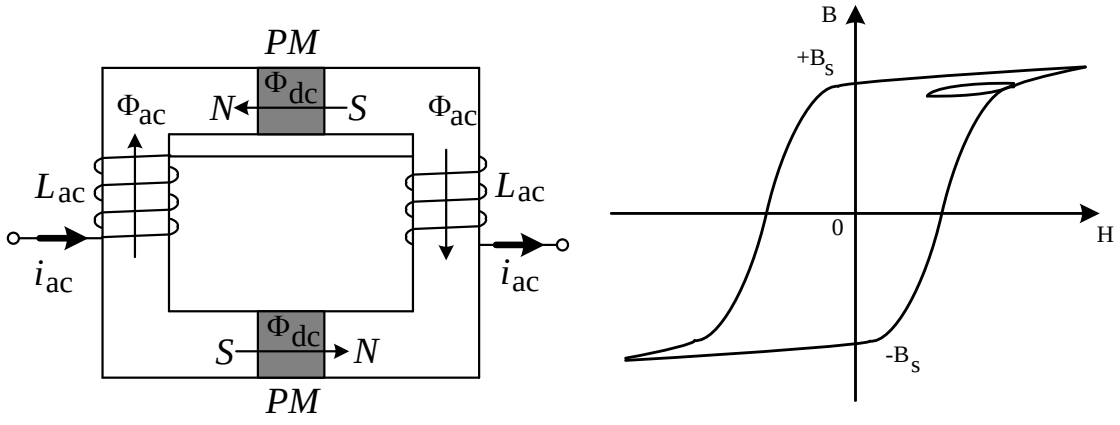

(a) Physical Structure **(b) B-H Operating Curve**

Source: Rasolonjanahary et al. [53]

The main advantages of a series-biased PM FCC are the relative simplicity of construction and a bias circuit that does not require a DC power source. The result is a more compact, lower weight, all passive, and more reliable FCC that, potentially, can operate in harsh weather conditions with minimum or no maintenance.

The disadvantages of the approach include higher normal-state voltage drop and power dissipation due to the PM's core hysteresis and eddy current losses. To minimize the eddy currents the PM was constructed by stacking several insulated disks [53]. Another disadvantage of this FCC is that it cannot limit the first peak fault current. This is because the initial fault current surge may take the PM material from a point of normal saturation along the minor loop towards the deepest saturation point of the major loop lying in the same quadrant of the B-H curve (see Figure 21(b)). Along such a trajectory the relative permeability is low. As a result, the FCC's AC coil inductance remains low, and may not clip the first peak of the fault current. Also, after a relatively long fault event, the PM may need some time to cool down before resuming a normal state function.

Additional handling and mechanical construction problems will arise due to the natural tendency of the PMs to repel each other and attract other metal objects.

2.2.7 A Three-Material Passive dI/dt Limiter

Another concept for a PM-biased FCC was proposed by Young, Dawson and Konrad [54], in which only some parts of the core segments are saturated, as shown in Figure 22.

The core of the device consists of four AC coils connected in series. Each coil is wound on a low-saturation-density core material segment and biased by a PM. Both high permeability and high saturation flux density core segments are placed at the corners so as to provide a closed magnetic path.

Figure 22: A Three-Material Passive dI/dt Limiter

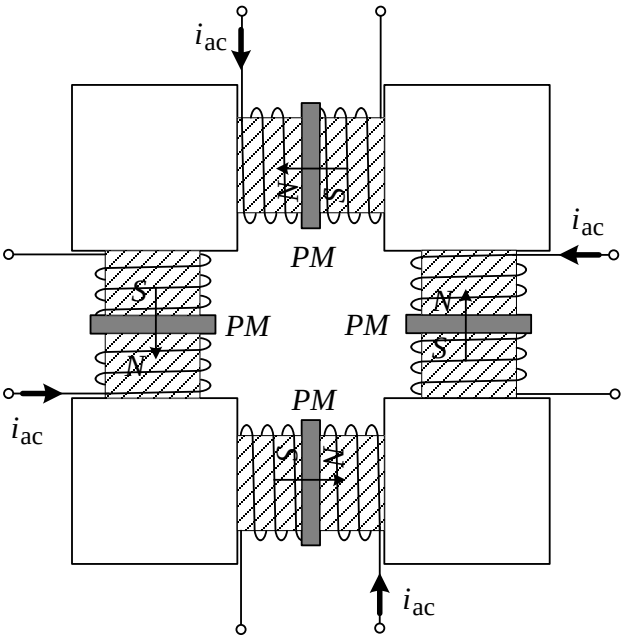

Source: Young et al. [54]

In the normal state, the PMs have sufficient intensity to saturate the low saturation density segments. With cores saturated, the inductance of the coils is low. The high saturation flux density material at the corners remains unsaturated, and it allows flux bending. As a result, the flux is confined to the device and the flux leakage is minimized. This results in a more uniform flux distribution in the saturated segments of the core. When a fault occurs, the larger current of an appropriate polarity induces an opposing mmf that reduces the flux density in the core. Consequently, the low saturation flux density segments are desaturated and the coil presents a higher inductance to the electric circuit, limiting the fault current.

However, in view of the previously mentioned drawbacks of PM bias and a relatively large number of components and the complexity of this design, this FCC structure appears as a less attractive option compared to most others of its type.

Another PM-biased FCC exploiting the same concept, but with a simplified design, was proposed by Young, Dawson, Iwahara and Yamada [55], as shown in Figure 23. Its "EE"-shaped magnetic structure has a center limb made of a low saturation density material with a PM inserted in the center of the limb. The rest of the core segments are composed of a high saturation density material. The AC coil is wound on the center limb. With a reduced number of components, this design can be constructed more easily, and is better suited for implementing a practical device than the previously described device. However, it displays the common weakness of the series PM bias FCCs in that the resultant mmf always passes through the PM, causing elevated losses and demagnetization of the PM core.

Figure 23: A Three-material Magnetic Current Limiter

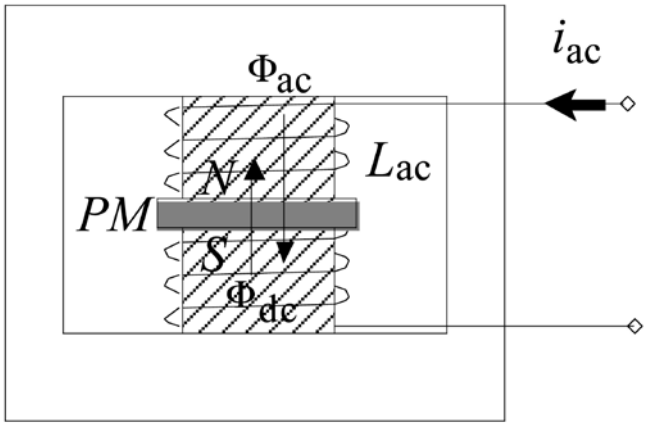

Source: Young et al. [55]

2.2.8 Saturated Open-Core FCC

The structure of a Saturated Open-Core FCC as proposed by Rozenshtein et al. [56] is shown in Figure 24. In this design, the DC bias coil is wound on the narrow segment of a closed, strongly elongated "CC"-shaped magnetic core. The AC coil is wound around the core so as to engulf both elongated segments of the core. Owing to this magnetic design the core provides a closed magnetic path for the DC bias flux; however, to the AC coil it appears as an open core.

The high-permeability closed magnetic path can be easily saturated by moderate-amplitude DC bias current. Notice that the "go" and "return" DC fluxes are flowing in opposing directions through the midst of the AC coil. Regardless of the AC current polarity, the induced AC flux reinforces the DC flux in one segment and counteracts the DC flux in the other segment of the core. In the normal state the AC flux is low, so all the segments of the core remain saturated and the AC coil acts as an air core inductor with low inductance. In the event of a fault, the large AC fault current desaturates the core segment carrying the counteracting flux. Thus, the AC coil appears as having a high permeability open core and, consequently, presents a larger inductance to the fault current.

A clear advantage of this FCC is that only one magnetic core and one AC coil per phase are required. A three-phase FCC requires a bank of three cores, roughly half the size of the previously mentioned FCCs. A single DC coil may serve all three cores. Furthermore, making the DC coil superconducting helps improve the bias circuit performance and reduce losses. Such an approach enables decreasing the volume, weight and cost of the FCC and allows for a compact design with tunable limiting factors. Another important advantage of this FCC design is the decreased coupling between AC and the DC coils, resulting from the orthogonal arrangement of the AC and DC coils.

Figure 24: A Saturated Open-core FCC

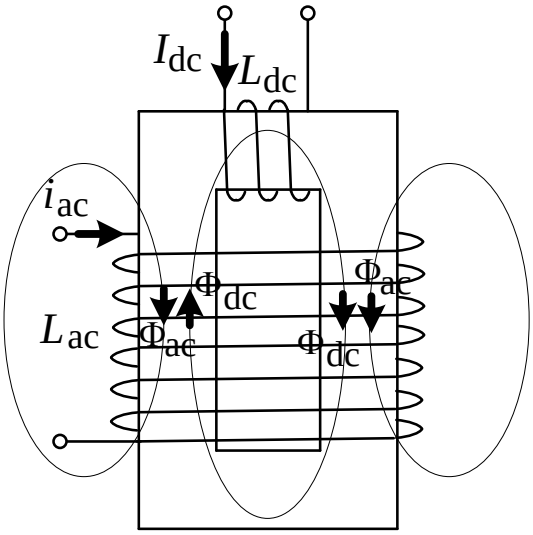

Source: Rozenshtein et al. [56]

2.2.9 Bias Power Supply Issues

Low-voltage, high-current DC bias supply is required by most of the Saturated Core FCCs, the exception being the PM-biased FCCs. The bias circuit can be either a simple unregulated or phase-controlled rectifier bridge, or a switched-mode power supply. A clear advantage of the regulated supplies is the option to preset for the anticipated fault current magnitude by adjusting the bias current accordingly.

A switched-mode power supply is the preferred solution due to its much higher efficiency compared to other approaches. An example of the switched-mode bias circuit is shown in Figure 25. The circuit can be recognized as an inverted Buck chopper fed by a three-phase rectifier, as proposed by Hong et al. [57]. Here, the superconducting DC coil is employed as the buck inductor. The large DC coil inductance helps in attaining low bias current ripples. The chopper is duty-cycle-controlled to provide precise regulation of the average DC coil current.

A serious concern, common to DC-biased saturated-core FCCs, is the voltage surge across the DC bias coil (He et al. [58]). The surge may occur as the AC coil comes out of saturation and establishes a linear operating regime in the core, thereby inducing a very high voltage surge in the DC coil. Since the number of turns of the DC coil is greater than that of the AC coil, the problem is quite serious and may result in damaging the electrical insulation of the DC coil, damaging the bias supply itself, burning out the superconducting wire, or destroying the cryostat.

One possible solution to the problem was proposed by Raju et al. [45] using an ordinary series resistor. This, however, incurs a large DC power loss. A ZnO resistor installed in series with the DC coil was proposed by Hong et al. [57], as shown in Figure 25. In the normal state the energy released by the ZnO resistor is bypassed by a switch to help improve the efficiency of the bias

circuit. When a fault occurs, the bypass is opened and the DC coil current is diverted to the ZnO arrestor, which absorbs the energy while keeping a constant voltage across the DC coil terminals. This helps to protect the coil and bias supply circuitry from the induced voltage. The disadvantage of this approach is that fast active control of the bypass switch is required.

Figure 25: DC Magnetization System for a 35 kV, 90 MVA Superconducting Saturated Iron-Core FCL

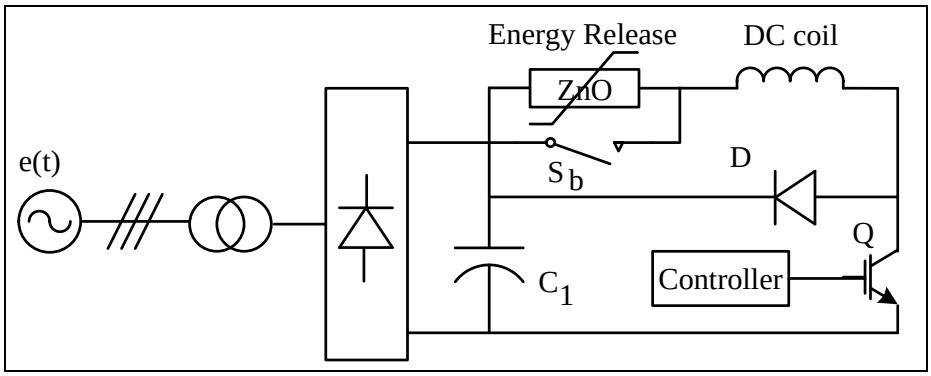

Source: Hong et al. [57]

Another approach was proposed by Yin, Zhang and Gong [59], in which a low-turns, non-superconducting suppressive winding, L_{aux}, was wound on the DC bias limb and electrically connected in parallel with the superconducting bias winding, L_{dc}, as shown in Figure 26(a). In the normal state the DC bias current flows mainly through the superconducting winding due to its zero resistance. Under fault conditions, however, the terminal voltage of the two parallel windings is determined by the low-turn number suppressive winding so that the surge voltage across the coil terminals is effectively reduced. The disadvantage of this approach is that though the resulting terminal voltage is low, still, through the transformer-like action, the AC induced voltage contributes to elevated current in the bias circuit to some degree.

Another interesting idea was proposed by Oberbeck et al. [46]. In order to protect the DC coil from the induced AC flux, a shorted winding was added on the DC bias limb (see Figure 26(b)). The shorted winding has no effect on DC operation; however, it reacts on the AC flux. A current is established in the shorted winding which, by Lenz's Law, creates a counteracting flux and reduces the undesirable AC flux in the DC limb. This appears to be a good solution to the problem. However, Oberbeck et al. [46] provide no report of experimental verification of the effectiveness or limitations of the proposed method.

Figure 26: Parallel Overvoltage Suppression Winding Configurations

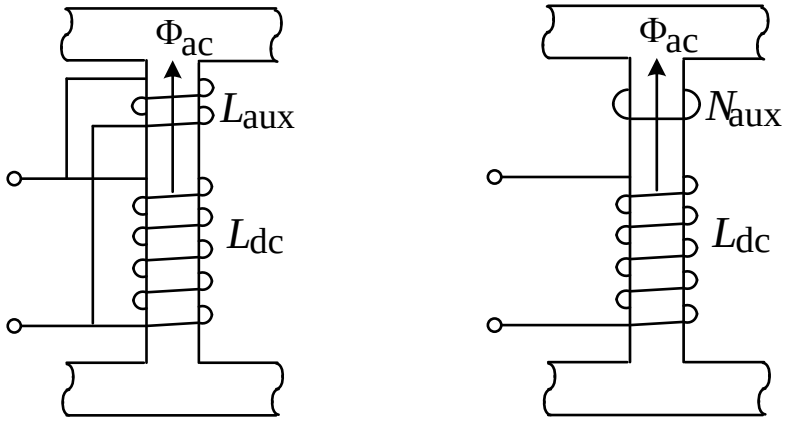

(a) Parallel

Source: Hong et al. [57]

(b) Shorted

Source: Oberbeck et al. [46]

2.3 Summary

This chapter surveyed solid-state and saturable-core Fault Current Controller technologies for AC power systems and reported on recent research work done in this area. Notwithstanding the fact that the research and development of FCCs has been going on for many years, diversity of FCC concepts is still rather limited. Seemingly, much of the effort has been dedicated to optimization of components, improving the efficiency and reducing the cost of a limited number of basic ideas.

Experimental FCC systems described in this survey indicate continuing progress in this field. However, a practical, efficient, reliable and economically feasible device, suited to utility needs, has remained elusive.

The main challenge for Solid-State FCCs is related to the insufficient voltage and current ratings of existing semiconductor devices, which are much lower than needed for operation in transmission and distribution power systems. Thus, stacking of a number of solid-state modules is typically required, which gives rise to voltage and current sharing issues.

The difficulties with the Saturable-Core FCCs are related to the magnetic coupling and, more importantly, to the typically large size and high weight of the devices, which pose difficult challenges to the commercial viability of these FCCs.

Nevertheless, innovation in FCC technologies is continuing. Two promising technologies, a saturable-core, passive-switching type of FCC by Zenergy Power and a solid-state, active-switching type by EPRI/Silicon Power, were the focus of this project and intensively investigated for further development. The following chapters provide a detailed report on the results of these investigations.

CHAPTER 3:
EPRI/Silicon Power Solid-State Current Limiter Development

3.1 EPRI/Silicon Power Solid-State Current Limiter Concept

EPRI/Silicon Power based their FCC concept on a Solid-State Current Limiter (SSCL) design using the Super GTO (SGTO) thyristor technology with a modular approach [60], [61]. A Standard Building Block (SBB) was developed that can be stacked in series and in parallel to attain the desired voltage and current ratings. The power train of a single SBB is illustrated in Figure 27. SBB includes a main SGTO switch, auxiliary commutation circuit, fault bypass current-limiting inductor, and an overvoltage bypass varistor/arrestor. The main SGTO switch is composed of anti-parallel connected SGTOs. The commutation circuit consists of an auxiliary SGTO switch and a series resonant commutation network.

Figure 27: SSCL Schematic

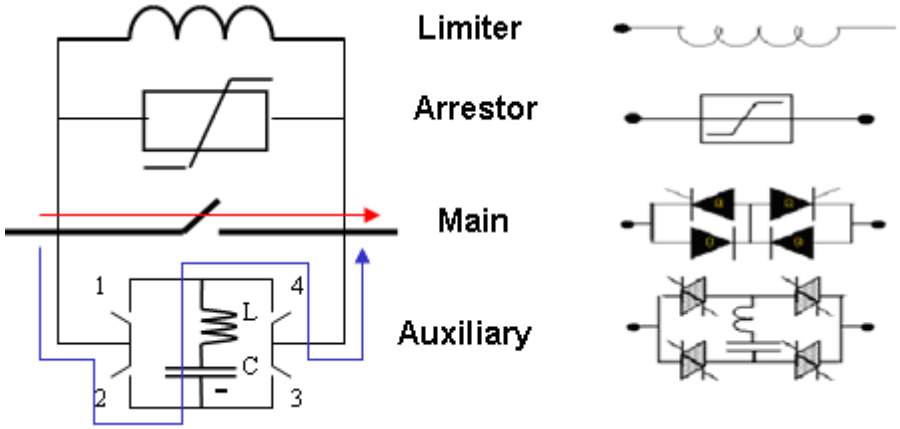

Source: Electric Power Research Institute

In the normal state the main GTO switches are gated "on" to carry the line current with only a negligible voltage drop across the switches. In the event of a fault, the auxiliary circuit is activated in order to provide low-stress turn-off of the main switches. The high switching speed and superior di/dt capability of the auxiliary SGTO allows the commutation circuit to apply a high-amplitude, short-duration resonant current pulse to the conducting main switch in order to reduce the current of the main switch to zero at the turn-off instant. Thus, a reliable turn-off of the main GTO switches is obtained which significantly reduces the switching losses of the main switches. After the main switches turn off, the commutation capacitor resonates with the line inductance and provides a soft dv/dt transient across the main switches. The switch voltage is allowed to rise until it is clamped by the varistor at 4 kV. The varistor then sees the full fault current. However, with 4 kV across the current-limiting inductor, only a few tenths of a millisecond is sufficient for the inductor to take over the current, and the varistor becomes

inactive. Henceforth, the fault current is limited by the inserted inductor. PSCAD software was used to simulate the SSCL. Principal waveforms of the simulated circuit are shown in Figure 28.

Figure 28: Simulated Waveforms of the SSCL Circuit

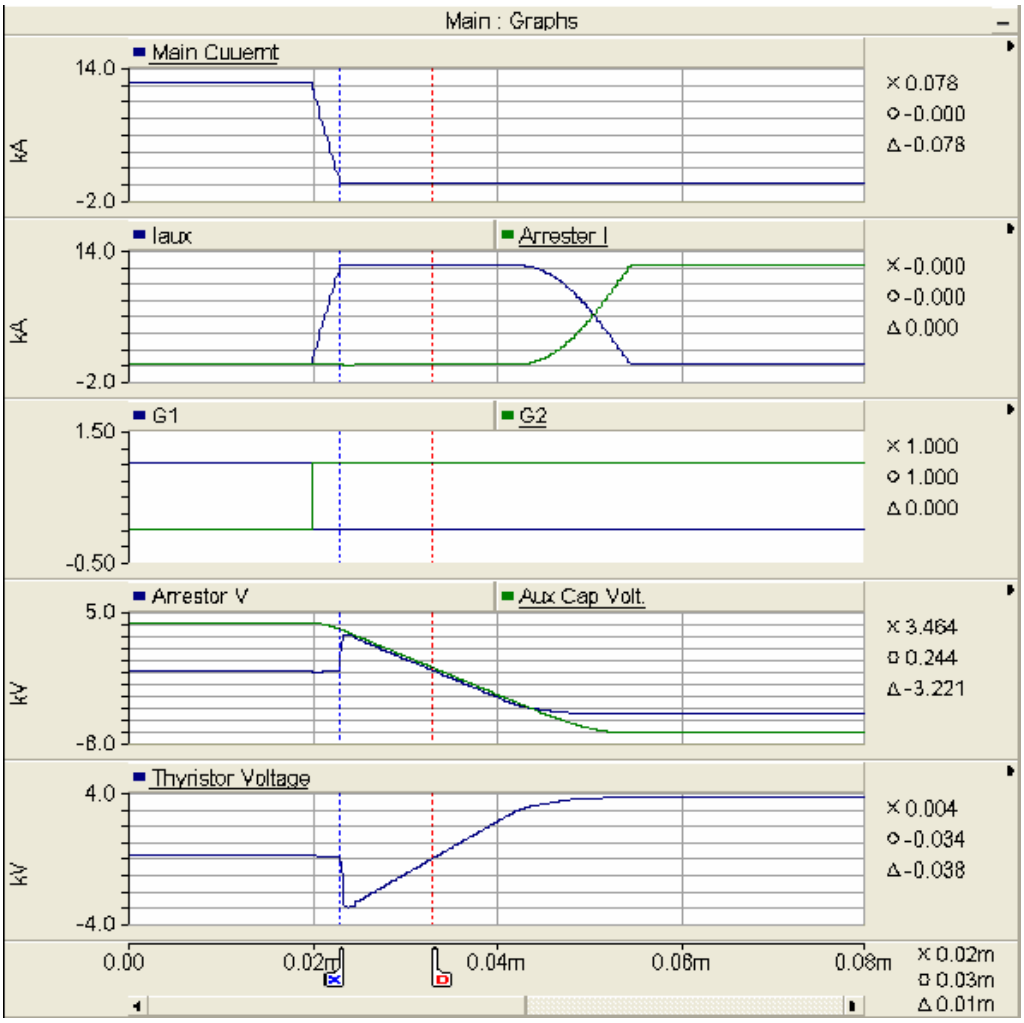

Source: Electric Power Research Institute

3.2 SSCL Design

3.2.1 Standard Building Block and Standard Power Stack

In order to facilitate manufacturing and to reduce the maintenance and ownership costs of the unit, a modular approach with standard building blocks (SBB) is used. Figure 29 shows the SBB design. One SBB contains the complete circuitry represented in Figure 27, including the main switches, auxiliary switches, varistors and the current-limiting inductor, in addition to the control boards. Each of these building blocks is a complete SSCL switch rated up to 2 kA and about 5 kV blocking, resembling a fully functional SSCL. The number of series SBBs required is determined by the breakdown voltage of the main switch modules and the arrestor voltage. The current-limiting inductor is chosen based on the fault current requirement of a particular unit.

Ten SBBs will be connected in series to form a standard power stack (SPS) for a complete single-phase unit rated for 15 kV and 1200 A. A conceptual view of an SPS with 10 SBBs in series is shown in Figure 29. The inductor size chosen for the required 9 kA let-through current rating is 142 μH.

Figure 29: Modular Structure of the SSCL

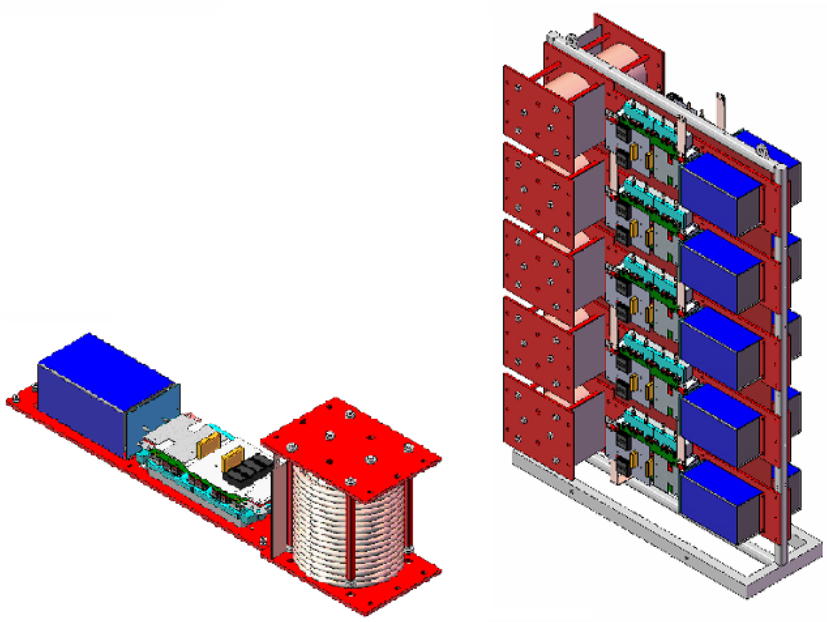

(a) Standard Building Block **(b) Standard Power Stack**

Source: Electric Power Research Institute/Silicon Power Corp.

3.2.2 Final Assembly

The final design for manufacture of a complete distribution-level SSCL is as follows: Multiple Standard Power Stacks are packaged into a three-phase unit as shown in Figure 30. The housing encloses the power modules, current limiting reactors, bus bars and manifolds, assembled in a tank that has cover-mounted primary and secondary bushings and a provision to connect directly to the overhead utility power lines. The tank is made of 3/8" steel and will have sufficient mechanical strength to withstand environmental conditions for the expected service duration. The tank also includes accessories such as a liquid level gauge, liquid temperature gauge, pressure vacuum gauges, pressure-relief device, control cabinet mounting, and cooling radiators.

3.2.3 Thermal Design

The 15 kV, 1200 A SSCL is designed for outdoor substation use and follows the IEEE Standard for General Requirements for Liquid-Immersed Distribution, Power, and Regulating Transformers, C57.12.00-2006[1]. The overall package is similar to a standard substation transformer tank with an external radiator bank. Immersing the system in a mineral oil

[1] Since superseded by C57.12.00-2010.

dielectric fluid provides a high degree of electrical insulation. The radiator bank is connected to a series of cold plates that are located directly underneath the power electronics devices. The cold plates provide highly efficient, directional cooling with a relatively low coolant flow rate and small pump size. The coolant chosen for the system is the same mineral oil as for the bulk tank. This reduces the chance of incompatible fluids mixing. The tank design is such that all of the power electronics will be immersed in Crosstrans 206 mineral oil as a dielectric. The radiator bank provides cooling of the tank by use of forced-air cooling from external fans.

Figure 30: The SSCL Assembly and Its Components

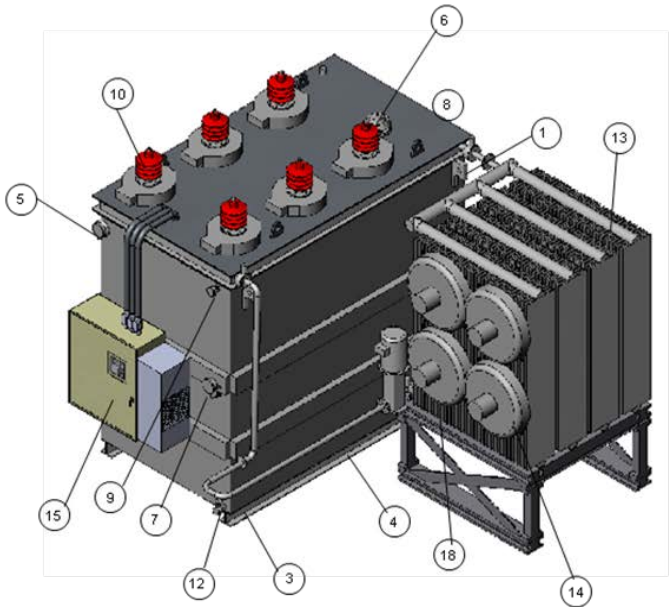

1. Lifting Hooks for Complete Unit
2. Lifting Hooks for Tank Cover
3. Tank Grounding Provisions
4. Transformer Base
5. Liquid Level Gauge
6. Pressure Relief Device
7. Dial Type Thermometer
8. Gas Relay
9. Pressure Gauge with Bleed Valve
10. Bushing
11. Drain Valve
12. Filler Valve
13. Radiator/Heat Exchanger Assembly
14. Cooling Fans
15. Control Cabinet
16. Inert Gas Cabinet (Nitrogen)
17. Current Transformer
18. Oil Circulation Pump
19. Shut-off/Isolation (valves)

Source: Electric Power Research Institute/Silicon Power Corp.

3.2.4 Controls Design

The SSCL is designed to operate primarily from a remote operator interface. It also has the ability to be operated locally. The controls can provide ON/OFF switching, equipment protection, display and monitoring of operating parameters, a fault log, access protection, e-Tagout, and safety padlocking, among others. The SSCL controls will also provide a trip-free feature such that any "close" signal will not inhibit the SSCL from opening upon command.

The control hardware is divided into two groups as shown in Figure 31. First is the device level, incorporating all device level controls like gate drives, sensing and device protection. Above that is the system level master controller, consisting of all system level controls like display, data acquisition, Local Operator Interface or human-machine interface (HMI), supervisory controls, data storage and retrieval. The communication between the two tiers is via fiber optic cables, which provide galvanic isolation and noise immunity; both are critical for proper functioning of the controls. The system controller is built around a Schweitzer Engineering Laboratories (SEL) controller. The selection of this particular controller technology is based on the performance requirements, complexity, reliability, and cost.

The Schweitzer system controller is an off-the-shelf controller (see Figure 32), which provides manual ON/OFF controls, equipment protection, display and monitoring of operating parameters, local and remote interface and access protection. It also facilitates the IEC-61850 standard protocol communication. The monitoring functions are performed by using the inputs from the standard CT and PT instrumentation in the substation.

3.2.5 SSCL Design Changes

The design of the SSCL evolved over the course of the project. Some of the design changes were required for proper operation of the system. Others were to accommodate a particular mode of operation or to use a specific mechanism to fulfill a given role. The main areas affected by these design changes were the thermal management system and the control boards. These design changes, and other material cost changes, led to an overrun in the estimated material budget for construction of the SSCL. Details of these design changes are provided below.

Figure 31: SSCL Control Architecture

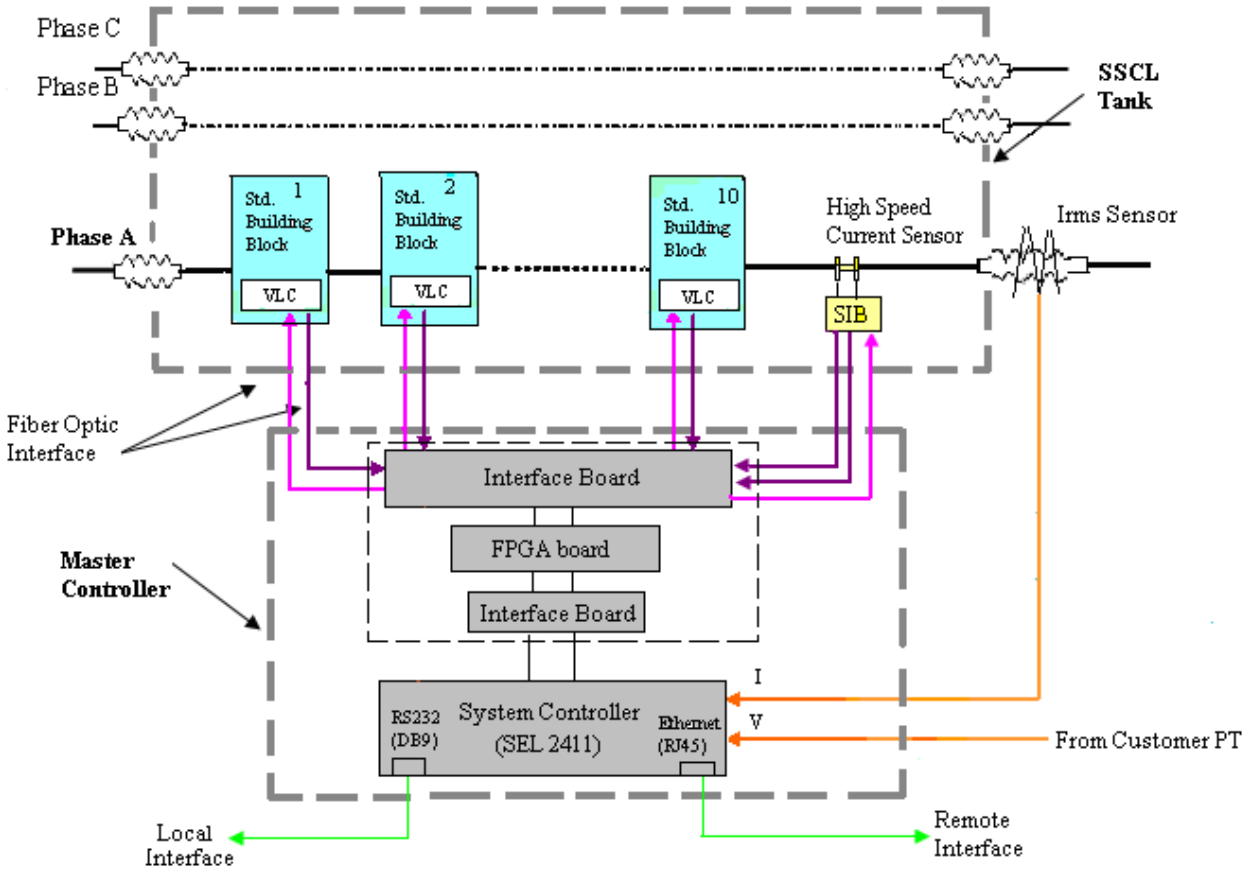

Source: Electric Power Research Institute/Silicon Power Corp.

3.2.5.1 Thermal Management System

The original design for the SSCL envisioned the SGTO modules being mounted on heat sinks with dielectric oil being forced over the fins of the heat sinks before returning to an external radiator system to exchange heat with the ambient air. Simulation studies showed that in this design the SGTO modules would have been operating at different temperatures and would

have experienced different thermal stresses at the two ends of the stack, a less than optimal situation that could increase the probability of unforeseen failure modes.

The design was therefore adjusted to locate the SGTO modules on cold plates containing internal serpentine paths for oil flow. Oil can be pumped into the individual cold plates to remove the heat generated by the SGTO modules. With the new design the SGTO modules all see the same temperature differential and each SGTO module experiences the same stress, improving the reliability of the system.

Figure 32: SEL Industrial Panel-mount Controller

- Utility Grade
- Schweitzer (SEL) make, Model #2411
- Microprocessor based
- LCD Display
- Touch Pad
- **IEC 61850 Protocol Compliant**
- Designed for Indoor/ Outdoor use
- Type tested to sections of C37.90, IEC 60255, IEC 60068 and IEC 61000 standards

Source: Schweitzer Engineering Laboratories

The change to a cold-plate cooling system also reduces the volume of oil required for the closed circuit cooling system and allows for the ability to direct cooling fluid from the manifold to the current limiting inductors if desired.

3.2.5.2 Electrical and Control System

The original design concept used a single control board for the standard building block, combining both power and controls. As the project progressed, the decision was made to place the control and power functions on separate boards to provide better noise immunity. This in turn led to custom designs for the microcontroller-based visual logic controller (VLC) board, the floating power supply board and the capacitor trickle charge board. This separation allows a less complex design for the individual boards. The floating power supply board components now include EMCO™ high voltage power supplies, which are rare and expensive components. The EMCO™ power supplies are required in order to maintain the charge on the commutation capacitor. The VLC board communicates with the upstream FPGA (field-programmable gate array) board via fiber optics, which also helps to improve noise immunity.

The high-speed current sensor design also underwent some modifications. The initial design performed well in a certain subset of the measurement range, but the response exhibited an undesirable non-linear behavior over other parts of the range. The design was modified to improve the response across the entire measurement range.

The control cabinet design also evolved to accommodate the new control components. The control cabinet now includes the FPGA board, the master SEL controller, the required control power circuits and relays, fan and pump starters and fiber-optics interface board.

3.2.5.3 SGTO Modules

The SGTO modules required for the SSCL have overcome some manufacturing issues during the course of the project. During the initial manufacturing stages, an unacceptably high number of the SGTO wafers were becoming cracked or chipped. The problem was found to be the result of the sawing process used to dice the silicon wafers and produce the individual SGTO die. The saw was hitting small pieces of nickel on the top and bottom of the wafers. A layer of protective material has been added to stop the nickel buildup; the cracks have been virtually eliminated, and the wafer yield has improved to acceptable levels. The protective layer also had the unexpected benefit of improving the voltage capability of the SGTOs.

The final design of the auxiliary module includes two diodes in series, to handle the expected current and voltage conditions. There is the possibility of removing the second diode in the future but this cannot be verified without further testing.

3.2.5.4 Material Cost Changes

The estimated cost to construct the new and improved SSCL design has significantly increased, more than double over the original design. The principal reasons are changes to the functional requirements of the unit for improved performance, and also increases in materials costs since the original estimate was developed.

3.3 SBB Testing

Testing of the critical building block components such as the current limiting inductor has been undertaken. The control boards and auxiliary power supply components have been tested in the laboratory. The standard building block tests have verified the ability of the SGTO modules to turn off in the required time and to block the necessary voltage. A series of tests was conducted to demonstrate the maximum current that a single SGTO module could interrupt (Figure 33). It was found that a single SGTO module was capable of interrupting over 6.5 kA in a matter of microseconds. Exact time taken is a function of the auxiliary circuit, not the SGTO module itself. It should be noted that the 6.5 kA per module is well in excess of the value required for operation of the SSCL in the proposed design. A second series of tests measured the current sharing between modules in the same standard building block. The current sharing was observed to agree to within 5 percent.

3.4 Summary

The Solid-State Current Limiter (SSCL) design presented here is the result of pioneering work in the high-power electronics equipment industry. The SSCL employs a modular and scalable design, applicable to a range of voltage classes. Such an SSCL can provide a solution to the rapidly rising available fault currents seen in utility systems. The advantages of the emerging EPRI/Silicon Power SSCL approach are immediate recovery after a fault, no voltage or current

distortion, no cryogenics, low losses and reduced size and weight. In addition, this type of FCC can be designed for interruptive capability as well as management of excess fault current.

Some major technical issues have been resolved and the detailed design of the system has been completed. The design of the standard building block, control system, power stack and tank were all finalized.

The main technical issues encountered have been related to the thermal management system and the SGTO modules. The thermal management system design now features a forced oil system, with oil passing through cold plates under the SGTO devices and cooled via an external radiator system. This thermal management design has been verified by simulations performed at the Novatherm Lab of Villanova University.

The results of the hardware design and elemental testing are promising and warrant further research. The SGTO module and standard building block testing has demonstrated several important functional requirements, including current interruption and module-to-module current sharing. Control board testing has demonstrated the key algorithm functional requirements.

Figure 33: Current Interruption Simulation Results for the Standard Building Block (SBB) Module

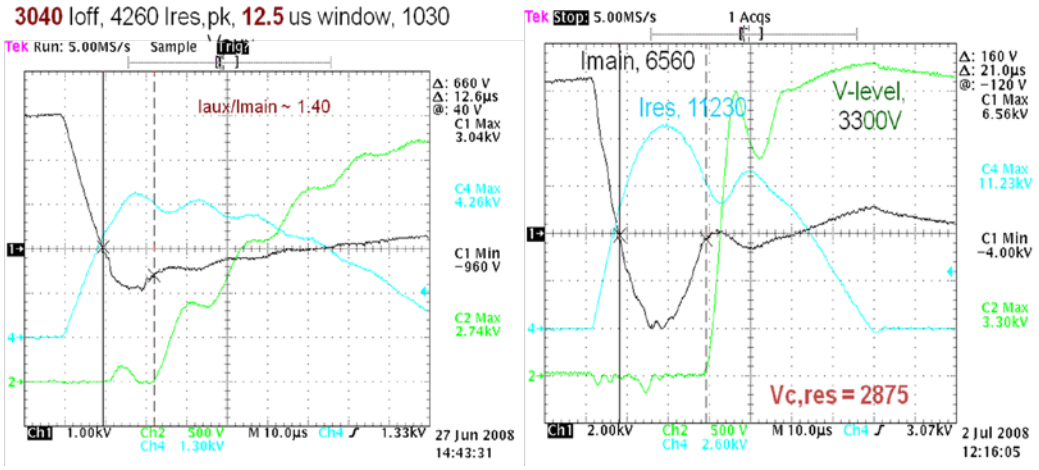

(a) Fastest Time **(b) Largest Current**

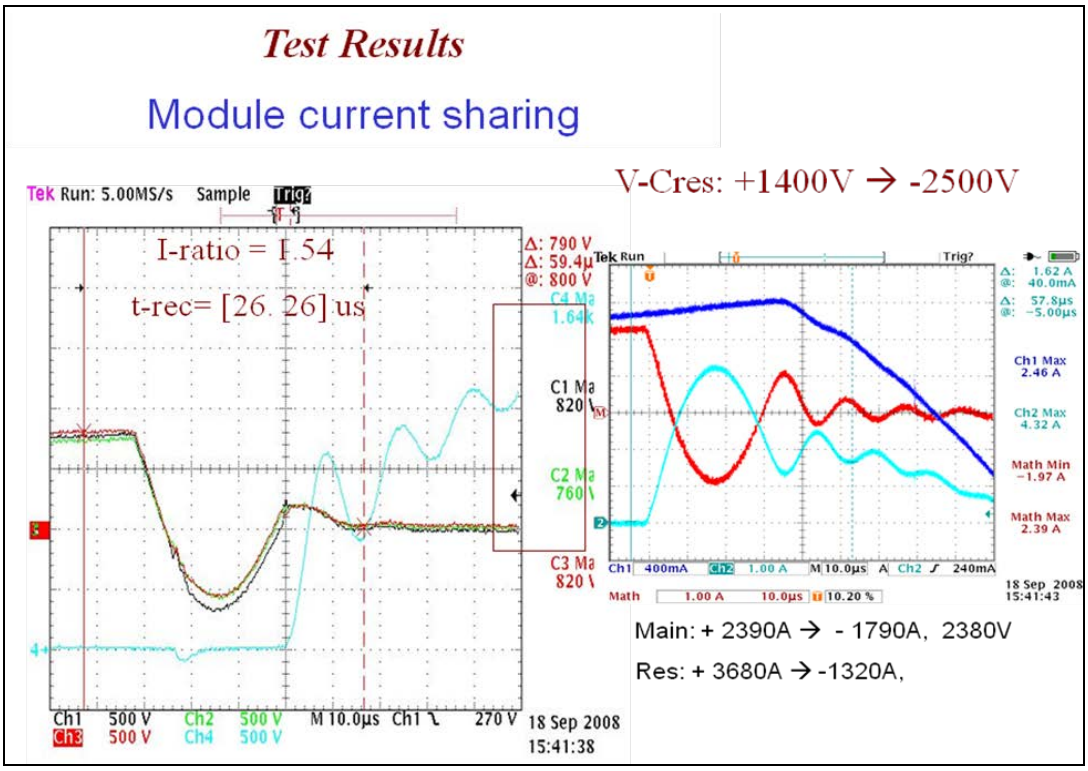

(c) Current sharing during fault operation.

Source: Electric Power Research Institute/Silicon Power Corp.

A summary of the tests that have been completed so far is as follows: SGTO module current interruption test; Standard Building Block topology demonstration; Standard Building Block control boards and gate drive functionality test; Standard Building Block power supply test; auxiliary power supply inverter and transformer test; and current-limiting inductor testing. The tests have contributed to increased robustness of the design and have provided valuable feedback to the improved performance of the system.

The scope of work for a continuation of this development effort would include the construction of the Standard Building Blocks and the manufacture and testing of the SSCL. The possible future steps for the 15 kV, 1200 A, three-phase SSCL could include SBB construction and testing at Silicon Power, power stack assembly, assembly of full size SSCL, testing at an independent high voltage lab and field demonstration at a utility site.

CHAPTER 4:
Zenergy Power First-generation HTS FCL Development

4.1 Zenergy Power HTS FCL Concept

The Zenergy Power FCL is based on their High-Temperature Superconducting Fault Current Limiter (HTS FCL) approach using the Saturable-Core Reactor concept, following the ideas proposed by Raju et al. [45], Keilin et al. [62] and Xin [63]. The proposed HTS FCL is a three-phase device. Each phase of the proposed HTS FCL is constructed around a dual iron core with three coils wound around each limb, as shown in Figure 34. The DC bias coil is wound around the combined center limb. A pair of AC coils is wound on the outer legs of the cores. The idea is similar to that of [45], however, in this design, the AC coils are implemented using "CC" cores, rather than "EE" cores. This approach has the advantage of requiring just a single DC bias coil to be shared by the two cores.

Figure 34: Conceptual Structure of Zenergy Power Single-Phase Saturable-Core Reactor FCL

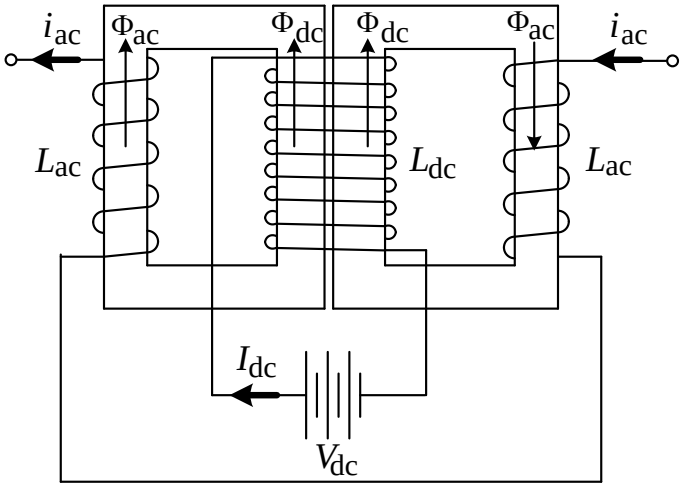

Source: Zenergy Power plc

In similar fashion to the saturable-core reactor FCCs described in the previous chapter, the AC coils are connected in series, differentially, and are inserted into the AC line in series with the load as shown in Figure 14. The mmf-flux operating point of all the cores is established by the DC coil in the vicinity of point B (see Figure 15). As the AC line current flows through the AC coils, the core operating point is shifted. Due to the differential connection of the AC coils, the AC-induced mmf in one core reinforces the DC mmf, whereas in the other core it weakens the bias mmf. Therefore, the operating point of one core shifts into a deeper saturation (point A), whereas the operating point of the other core moves towards shallow saturation, at point C, closer to the hysteresis knee point. In the normal state the cores are designed to remain in saturation so that they impose low impedance to the power system. When a fault occurs, the

high amplitude of the fault current drives one of the cores out of saturation into the steep region of the hysteresis curve. The unsaturated AC coil is capable of supporting a large voltage across its terminals, and thus limits the fault current. Depending on the AC line current polarity, the coils alternate in and out of saturation to reduce the current in each half cycle.

4.2 First-Generation "Spider" HTS FCL Design and Prototyping

The Zenergy Power first generation prototype incorporates three pairs of single-phase FCLs in a spider-like structure featuring a hexagonal iron core with a thick central limb as shown in Figure 35(a). The three pairs of AC coils are wound on the outer legs of the cores using non-superconducting conventional copper coils. Each pair of the AC coils are connected in series, differentially, and inserted into the appropriate phase. The DC coil is made of first generation High Temperature Superconducting (HTS) wire wound around the center limb. The HTS coil forms a strong electromagnet fed by a low-voltage, high-current DC power supply. The HTS coil provides an efficient method of saturating all six cores with minimum DC power losses.

It is worth noting that during normal operation the cores operate almost symmetrically, so that the AC flux in the center leg is mostly canceled out. As a result, there is no AC voltage induced in the DC coil. During the fault, however, the cores operate asymmetrically, with one or more of the cores partially desaturated. Therefore, in a practical device, coupling between the AC and DC coils can be a problem. However, the Zenergy Power design ensures that the coupling is only a few percent and, therefore, of no significant consequence. This reduces the risk of high voltage shock to the DC coil and power supply.

Figure 35: Three-phase Zenergy Power Saturable-core Reactor HTS FCL

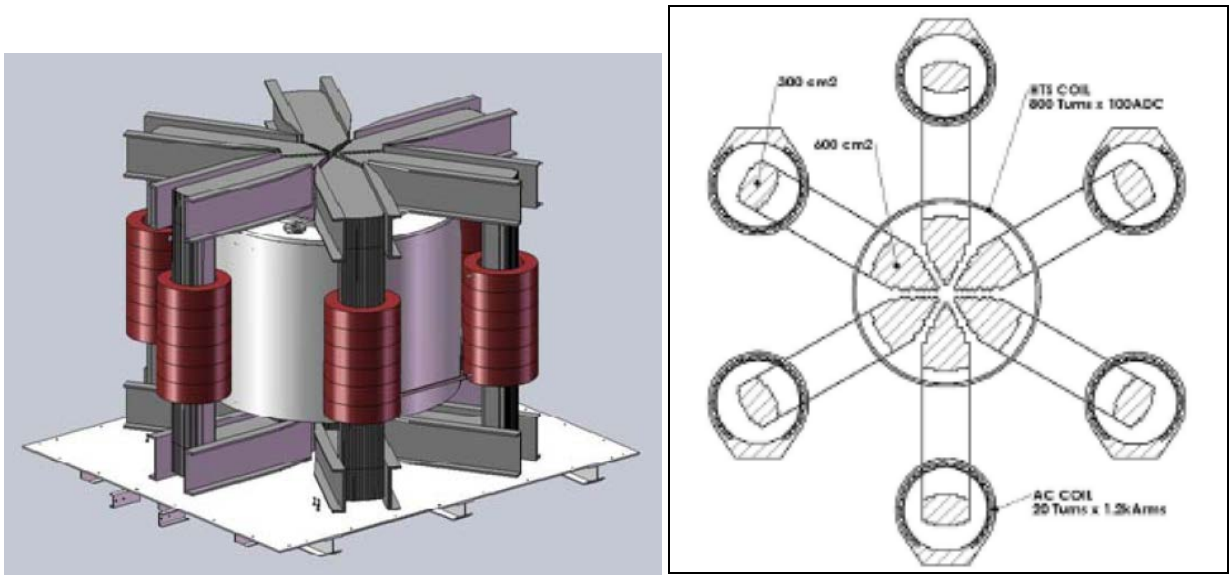

(a) Physical Structure **(b) Vertical View**

Source: Zenergy Power plc

Zenergy constructed a full-size, three-phase, distribution-level FCL prototype. The prototype FCL employs cast-epoxy AC coils and a closed-loop cryogenic cooling system that uses sub-cooled liquid nitrogen at approximately 68º K to increase the working current of the DC HTS bias coil to maximize the DC magnetic bias flux. The basic design parameters of the prototype FCL are shown in Table 1. The cutaway views of the distribution-level three-phase HTS FCL assembly are shown in Figure 36. The view of the internal structure and physical view of the experimental prototype HTS FCL unit are shown in Figure 37.

Figure 36: Cutaway Views of the Distribution-Level Three-Phase HTS FCL Assembly

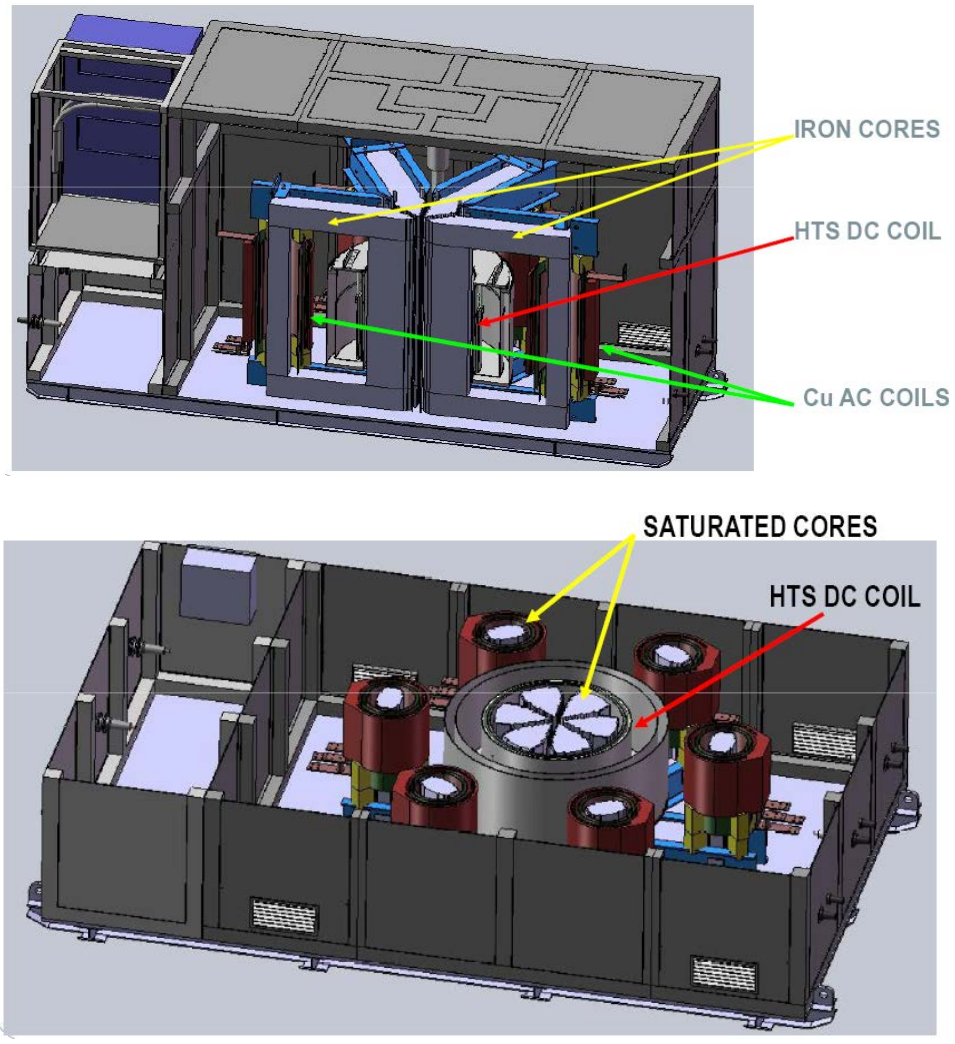

Source: Zenergy Power plc

The prototype FCL was designed for a modest fault current limiting capability and was intended to limit a 23 kA (rms) potential steady-state fault current by 20 percent. During the design, great emphasis was placed on accurately modeling and predicting the performance of the FCL and its associated electrical waveforms, simulation analysis of different line conditions,

and predicting the interaction of the FCL with other power system components. Table 1 provides a list of the key electrical and mechanical characteristics of the prototype HTS FCL.

Figure 37: Experimental Zenergy Power HTS FCL Prototype

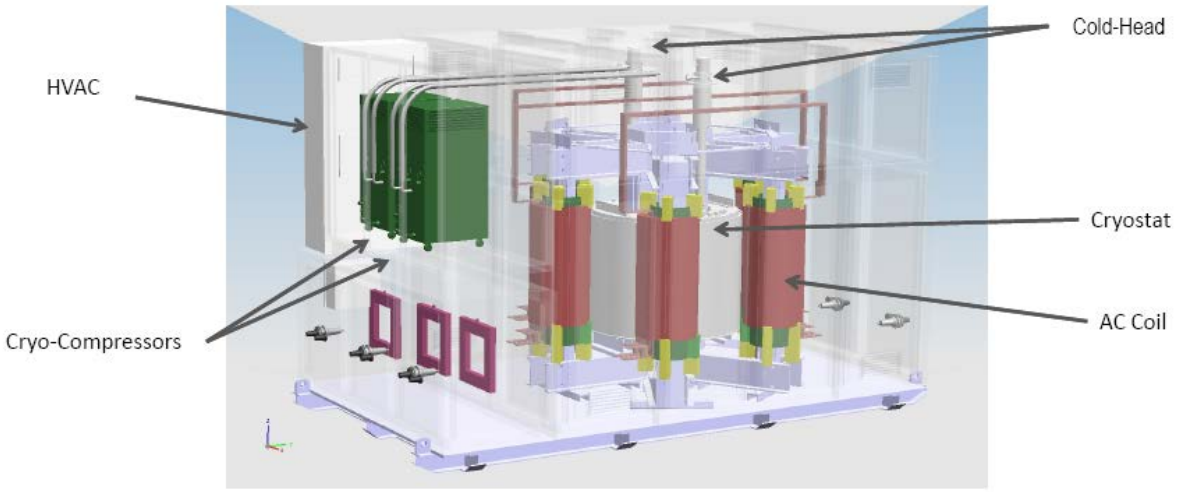

(a) Main Components

(b) Physical View: Outer Panels Temporarily Removed

Source: Zenergy Power plc

Table 1: Design Parameters and Main Features of the Zenergy Power Prototype HTS FCL.

Line voltage	12.47 kV
Maximum load current	800 A (3-phase 60 Hz)
Voltage drop at max. load	<1% (70 V rms)
Prospective fault current	23 kA rms symmetrical
Asymmetry (X/R)	21.6
Fault limiting capability	20%
Fault type	3 phase to ground
Fault duration	30 cycles
Recovery time	Instantaneous
Iron Core Weight (lbs)	52,000
Cost of Iron @ $3.00/lb	$156,000
Size	19' x 19'

Source: Zenergy Power plc

4.3 HTS FCL Modeling

4.3.1 Nonlinear Inductance Model

Saturable-core HTS FCLs consist of a set of coils wound around one or more ferromagnetic cores. A superconducting magnet is coupled to the core region in such a way that the DC magnetization force can saturate the magnetic material. In the Zenergy Power FCL, each AC phase consists of two coils connected in series and wound around two core regions. The windings are oriented such that, in one core, positive AC current counteracts (bucks) the superconducting DC bias, while in the other core, negative AC current assists (boosts) the superconducting DC bias.

The nonlinear model that describes the behavior of the device is based on the physical principle described in a previous chapter and was described by Zenergy in a paper presented at the 2010 IEEE PES Transmission and Distribution Conference and Exposition [64]. The core material has a B-H curve that can be approximated by an inverse tangent function, as follows:

$$B(i_{ac}) = \frac{-2B_{sat}}{1+\tan^{-1}\left(K\pi-\frac{\pi}{2}\right)}\left[1+\tan^{-1}\left(K\frac{\pi}{I_{max}}(I_{max}-i_{ac})-\frac{\pi}{2}\right)\right]+2B_{sat} \qquad (1)$$

Here, i_{ac} is the instantaneous AC line current, and I_{max} is the line current that fully saturates the cores, at which point the average magnetic field is B_{sat}, and parameter K determines the range of

line currents where the magnetic state of the cores are actively changing from saturated to unsaturated. The equation is scaled in such a way that B = 0 at the bias point, i.e., with $i_{ac} = 0$, and the majority of the change in field occurs just before $i_{ac} = I_{max}$. The induced voltage, or back emf, across this section of the FCL is $V = \tilde{L}\, \partial i/\partial t$, where $\tilde{L}$ is the differential inductance defined as:

$$\tilde{L} = n_{ac} A_{core} \frac{\partial B(i_{ac})}{\partial i_{ac}} \qquad (2)$$

Here, n_{ac} is the number of turns in the AC coil, which carries the line current, and A_{core} is the cross-sectional area of the paramagnetic core material. In some cases, this model is improved by imposing two additional conditions. First, $\tilde{L}$ must be greater than or equal to an additional parameter called L_{air}. This value represents the insertion impedance as an equivalent air-core inductance. Furthermore, if i_{ac} is greater than I_{max}, then $\tilde{L}$ is constrained to be L_{air}. This accounts for the fact that, when the line current is very large, the FCL's magnetic core is reverse saturated and the impedance is once again approximately equal to the insertion impedance of an equivalent air-core inductor. The equations above provide a general framework for describing the behavior of an FCL in an electric circuit. This framework requires four input parameters: I_{max}, B_{sat}, K, and L_{air}. As described in the following sections, finite element modeling (FEM) methods were used in simulations to calculate the average magnetic flux for various static values of DC and line currents. A least-squares fitting procedure was used to determine the above parameters. To validate the model, PSCAD electrical simulation software was used to implement the FCL nonlinear inductance model and the simulation results were compared to the experimental results from the extensive tests performed on the 15 kV FCL device.

4.3.2 Finite Element Model and Analysis

4.3.2.1 Finite Element Model

The finite element method was originally developed for structural analysis, and it has since proven to be a versatile method of analysis and adapted to other fields, such as heat transfer analysis and, in this case, magnetic field analysis. The objective of finite element analysis is to find an approximate solution of a given boundary-value problem, by representing a region of calculation by finite subdivisions where a spaced grid of nodes replaces a conduction region. These nodes are the location where the solution is computed. The finite subdivisions are called "finite elements" and they can have arbitrary shapes, resulting in a very versatile analysis method. The collection of finite elements and nodes is called a finite element mesh. Continuous variables, such as mechanical stress, temperature or magnetic flux, can be represented over the finite element by a linear combination of polynomials called interpolation functions [80].

Precise finite element model (FEM) results require a number of inputs, including physical geometry, accurate descriptions of the electromagnetic properties of each material, and the current densities in the superconducting and AC coils. Calculations were performed using the ANSYS FEM code, developed by Ozen Engineering, Inc. The geometric parameters were either input directly from mechanical CAD drawings or by command files. Because the designs have many elements, calculation speed is a significant constraint. In most cases the models make use

of geometric symmetries to improve the calculation speed. The B-H curve for the magnetic material was estimated from measured data shown in Figure 38. All calculations were performed under the static approximation. This assumption is justified by the fact that physical devices do not display significant hysteretic behavior.

Figure 38: Magnetization Curve of M-6 Steel Used in the Finite Element Model

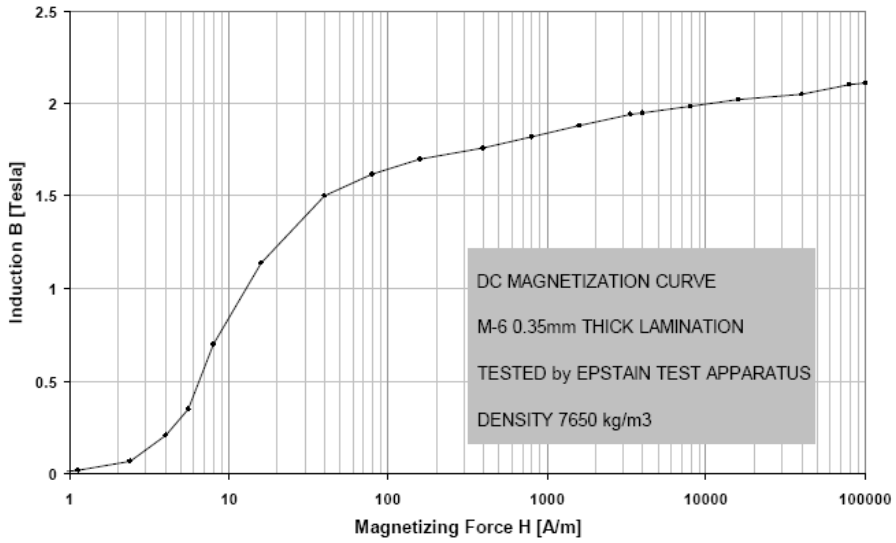

Source: Zenergy Power plc

The LMATRIX subroutine of ANSYS provides the differential inductance matrix for the number of coils present in the model, and the total flux linkage in each coil, under a given set of current density conditions. The FEM program provides graphical outputs that allow easy visualization of geometric properties (see Figure 39). The iron cores (gray) serve as flux links between the superconducting magnet in the center of the device (blue) and the AC coils (orange). This three-phase device has six AC coils in total: one boosting coil and one bucking coil for each phase at any given time.

Graphical outputs also provide insight for future designs, allowing analysis of magnetic field densities in each region (see Figure 40). After using the graphical outputs to verify the model is working well, either the flux or the inductance outputs can be used to calculate the parameters for the nonlinear inductor model.

4.3.2.2 Finite Element Model Analysis

FEM analysis allows modeling of the performance of devices prior to their construction. First, a series of flux or inductance values over a range of AC and DC currents are calculated. The data points shown in Figure 41 were calculated for a superconducting bias current of 100 amps, and 800 turns, resulting in 80,000 amp-turns. The process can be repeated for other superconducting DC bias points if necessary. Figure 41(a) shows the average magnetic field linking the boosting and the bucking coils. The values were calculated from flux values, $\Phi(i_{ac})$, with the equation:

$$B_{ansys} = \Phi(i_{ac})/n_{ac}A_{core} \qquad (3)$$

Figure 39: Finite Element Model of a 15 kV Three-Phase FCL

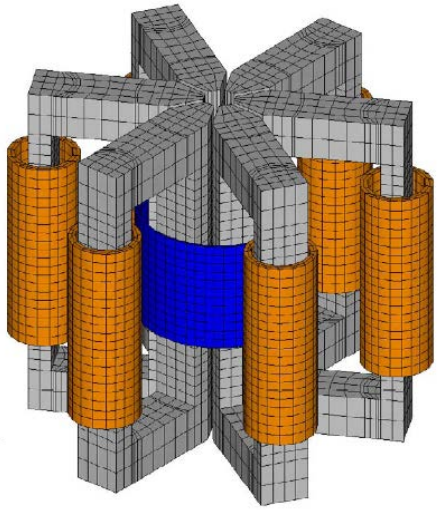

Source: Zenergy Power plc

Figure 40: Total Flux Density Due to DC Magnetization at 80,000 Amp-Turns

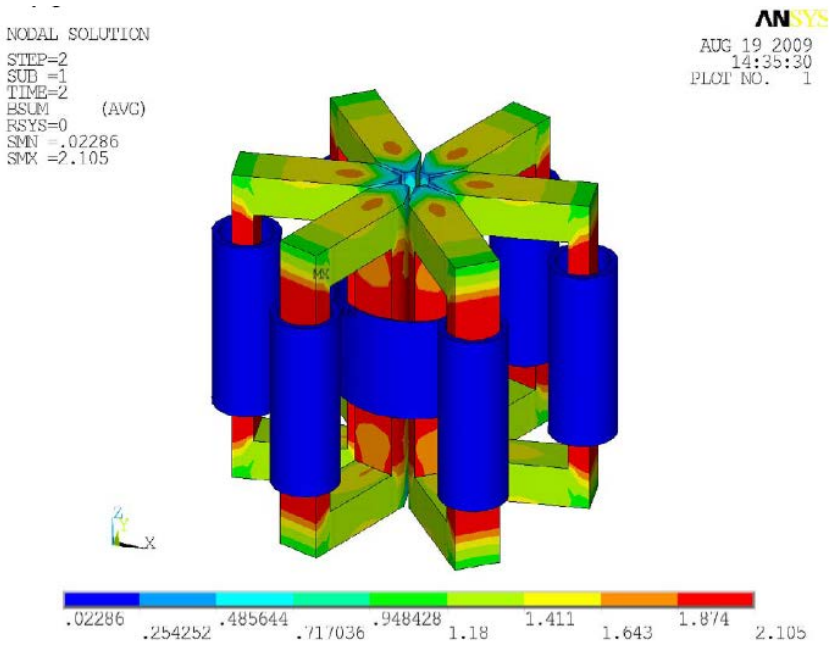

Source: Zenergy Power plc

In this case, n_{ac} = 20 turns and A_{core} = 300 cm^2. Figure 41(b) shows the sum of these magnetic fields. The inductance values shown in Figure 41(c) were calculated from Figure 41(b) with the relation:

$$\tilde{L} = n_{ac}\, A_{core}\, B(i_{ac})/i_{ac} \qquad (4)$$

The dotted red lines in Figure 41(b) show the model described above applied to both the boosting and bucking cores. A similar fit was obtained for the inductance values shown in Figure 41(c). This inductance is related to the differential inductance by:

$$L = \frac{1}{i_{ac}} \int_0^{i_{ac}} \tilde{L}(i)di \qquad (5)$$

and was performed numerically to account for the conditional statements applied to our differentially-defined inductance when $i_{ac} > I_{max}$ and $L \sim< L_{air}$. Next, the best-fit values from the inductance fit were used to compare this model to the measured behavior of the FCL device.

Figure 41: FEM Simulated Results and Model Fitting

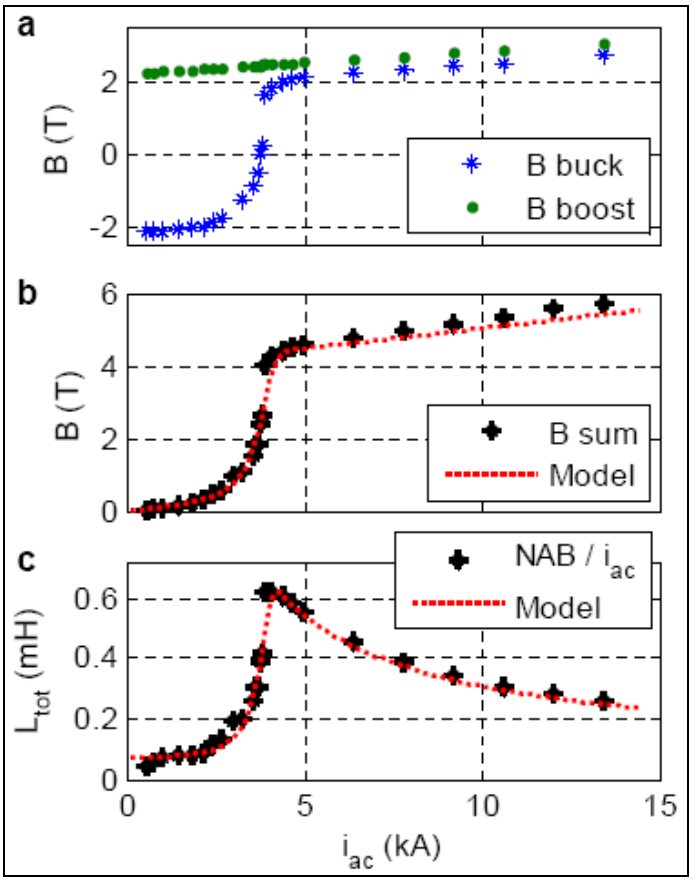

Source: Zenergy Power plc

4.3.3 Experimental Model Validation

Short circuit tests of Zenergy's 15 kV HTS FCL took place at Powertech Laboratories in Surrey, British Columbia, Canada. The three-phase FCL was connected to the test source voltage as shown in Figure 42, and auxiliary breakers (AUX) provided the fault current by closing all three phases to ground. Source resistance and reactance were selected to provide the necessary prospective fault current levels with the required asymmetry factor.

Figure 42: Zenergy HTS FCL High-Power Short-circuit Test Setup

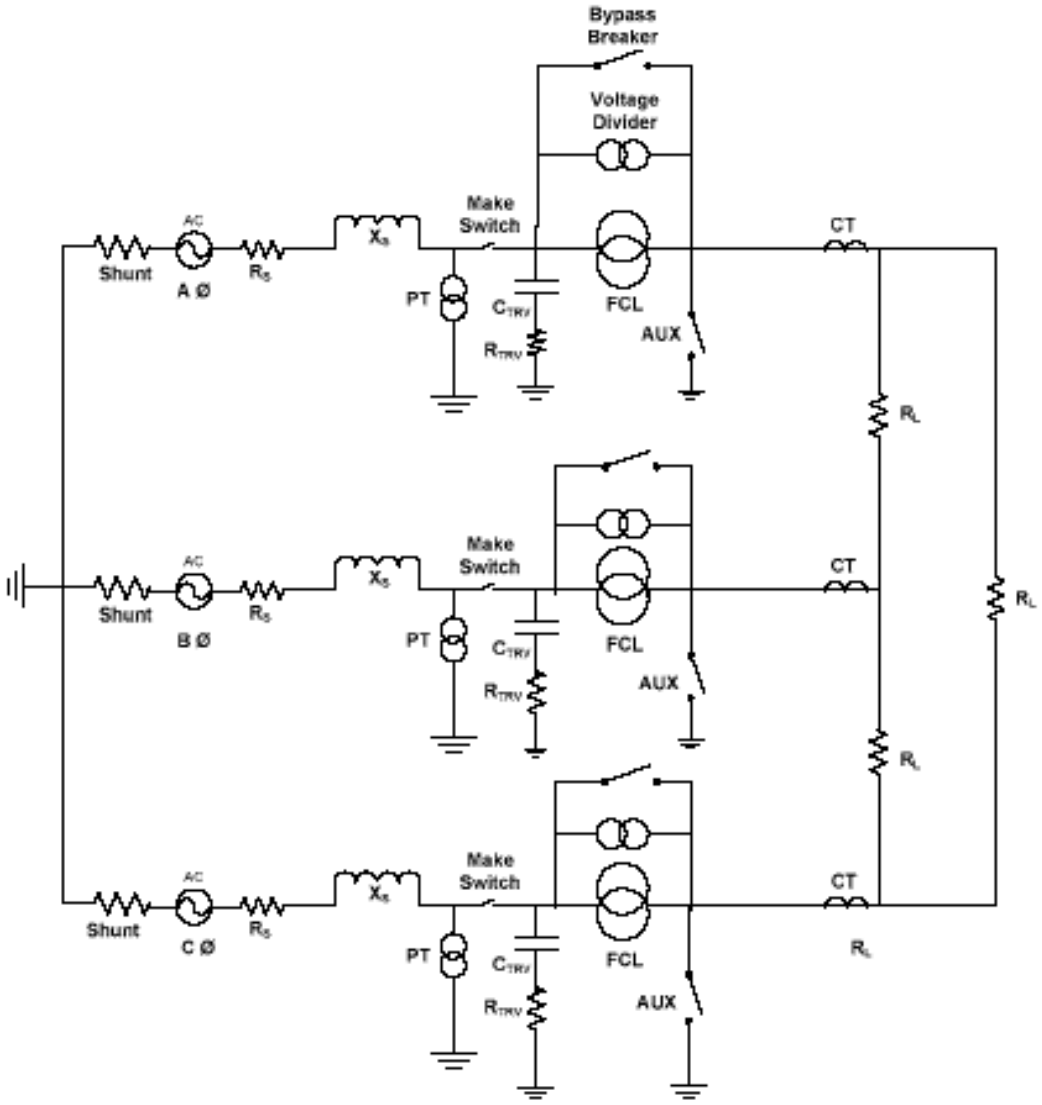

Source: Zenergy Power plc/Powertech Laboratories

Figure 43 shows several tests performed with two cycles of load current followed two cycles under faulted conditions. Figure 43(a) shows a 6.5 kV line-to-line system with two 830 A load cycles followed by a 3kA fault; the symmetrical part of the fault current was limited by 17 percent. Figure 43(b) shows the same 6.5 kV line-to-line system with a 12.5 kA fault; the symmetrical part of the fault current was limited by 30 percent in this case. Figure 43(c) shows a 13.1 kV line-to-ground system with two 780 A load cycles followed by a 20 kA fault; the symmetrical part of the fault current was limited by 20 percent. All tests were performed with an X_s/R_s ratio greater than 20. The symmetrical fault limiting performance of the model is provided in Figures 44 and 45.

The experimental results were analyzed using a simplified lump-sum circuit that consists of a voltage source, the nonlinear voltage FCL model, and a time-dependent load resistor. The

idealized source has the voltages listed above and a source impedance of 0.8 mH and 14 mΩ. The FCL includes the current-dependent inductance described above, along with a resistance of 1 mΩ. The simplified model's load impedance was chosen to generate the correct current during the loading cycles. This impedance was switched to zero during the fault cycles.

Figure 43: Zenergy HTS FCL Short-Circuit Tests: Measured and Modeled Current as a Function of Time

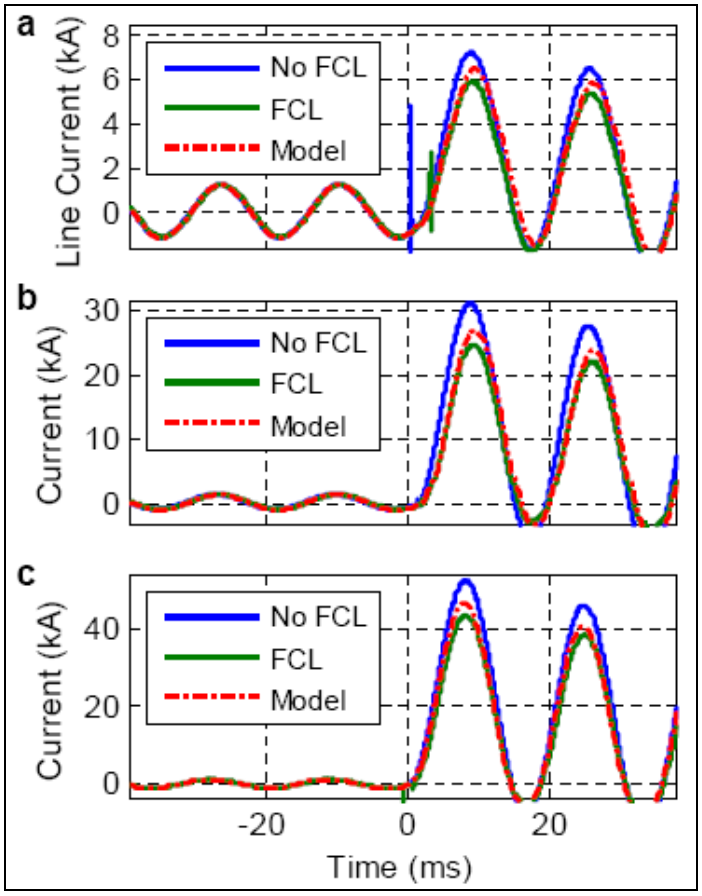

Source: Zenergy Power plc/Powertech Laboratories

It was found that the nonlinear FCL voltage model quantitatively reproduced the measured results. The FEM analysis provides a concrete method for estimating the model parameters for the saturated-core FCL design. The estimated parameters were used for the modeled results shown in Figures 43 and 44. Figure 44(a) shows the 12.5 kA symmetrical fault current after 21 cycles (350 ms) of continuous operation. At this point, the estimated parameters provide excellent predictions for overall fault current reduction. The qualitative features of the FCL voltage response are also estimated well, as shown in Figure 44(b). Figure 44(c) shows the average magnetic field defined by the measured flux change (i.e., the integrated bushing-to-bushing measured voltage with respect to time) divided by $n_{ac}A_{core}$.

While the qualitative features of the magnetic field are reproduced well by the model, the quantitative agreement is not precise. In order to increase the accuracy of the model the input parameters were adjusted to match the measured response. Figure 45 demonstrates the

qualitative agreement that is possible after the model updating, measuring the same parameters as in Figure 44.

Figure 44: Measured vs. Modeled Parameters for the Zenergy HTS FCL

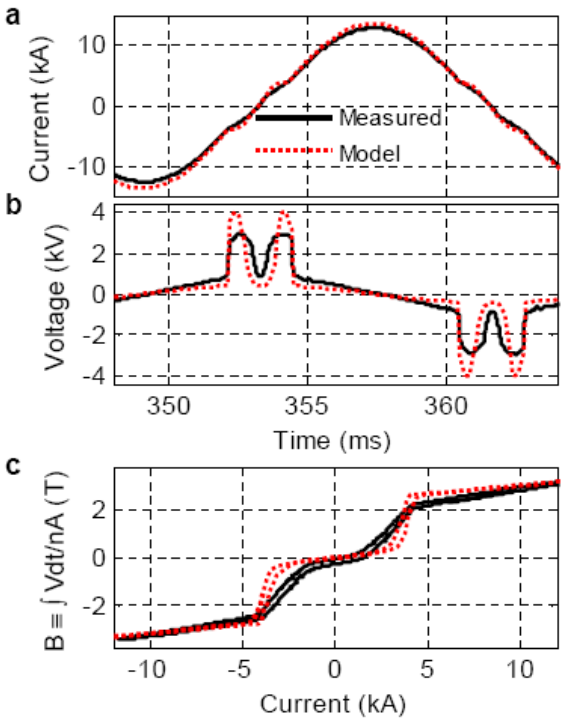

Source: Zenergy Power plc/Powertech Laboratories

Figure 45: Measured vs. Updated Modeling Results for the Zenergy HTS FCL

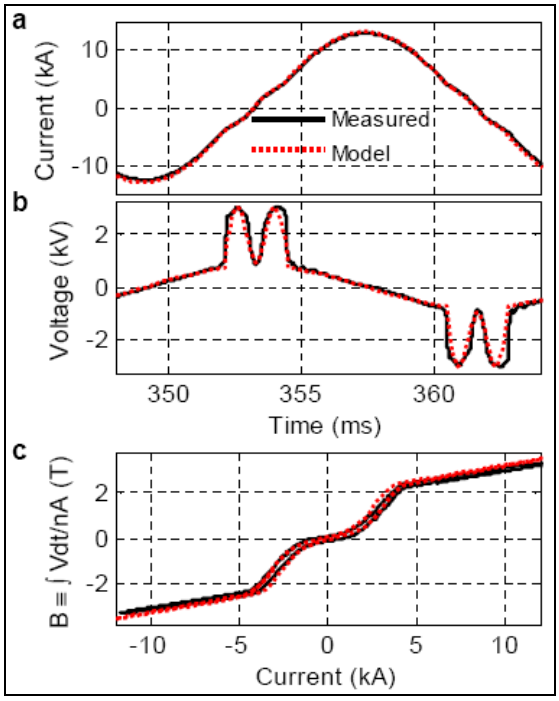

Source: Zenergy Power plc/Powertech Laboratories

4.4 Summary

This chapter reported on the recent development of a Saturable-core FCL by Zenergy Power plc. Successful controlled and field testing of the FCL proved the technological feasibility of the device. The FCL prototype was tested at Powertech Labs, and the revised prototype was tested by the Southern California Edison Co. at their Westminster engineering laboratory, and subsequently was installed in and underwent field testing at SCE's Avanti Circuit of the Future from March 2009 to October 2010. Although the design was still not optimized at this stage, the FCL prototype operated successfully and provided an extensive learning experience for the developer, Zenergy Power, for SCE's engineers and technicians, and for UCI researchers.

This prototype FCL has the advantages of a passive design, the ability of limiting the first peak fault current, automatic recovery under load, and fail-safe operation. Moreover, the DC bias magnet showcased an excellent application of superconducting technology, where the superconductor experienced no quenching during fault events, and thus no recovery time, for control of multiple faults. In addition, the adiabatic operating regime of the HTS coil presents a relatively small heat load to the cryocoolers.

State-of-the-art HTS technologies use liquid nitrogen to achieve high-temperature superconductivity, and provide significant advantages over their low-temperature, liquid-helium counterparts, since the liquid nitrogen systems are less complex compared to the liquid helium systems, and offer significant savings in cryogenic equipment costs and a reduction in operational costs. Furthermore, in the Zenergy design, only one HTS DC coil is needed, albeit a

relatively large-diameter one. An additional advantage of this FCL design is the placement of the HTS coil on the center limb, which gives a sufficient electrostatic clearance to the high-voltage AC coils wound on the outer limbs. The isolated high-voltage and cryogenic systems lead to a simplified high-voltage design.

A systematic approach to modeling of the electrical behavior of the saturated-core HTS FCL was also developed. The empirically-derived model was supported by FEM electromagnetic simulations as well as circuit analysis, and then fine-tuned to match the experimental results. The nonlinear FCL modeling, with the FEM-updated parameters, provided an excellent tool for predicting the overall fault current reduction of a saturated-core HTS fault current limiter. The FCL model was used by Zenergy in designing a superior "second-generation" 15 kV FCL with the objective of developing a transmission-level FCL in the near term.

CHAPTER 5:
Zenergy Power HTS FCL Laboratory Testing

5.1 Standards

At the time of this writing, there were no official certification procedures or standards in place for testing of FCLs. The testing procedure for the prototype FCL was developed under a joint effort of NEETRAC, SCE, Zenergy Power, and the University of California – Irvine (UCI). The procedure was derived from the existing IEEE Standards C57.16-1996 [76] and C57.12.01-2005 [77]. Zenergy Engineering Specification ZP/ES-2008-05 (Attachment I), comprises the test protocol developed for this project; it has been submitted to the appropriate IEEE and CIGRE Working Groups for their consideration in development of new or revised standards and certification procedures covering FCC technologies.

The prototype was shipped to BC Hydro's Powertech Laboratory in Surrey, BC, Canada for laboratory testing, which was performed in three categories: basic pre-connection tests, normal state performance, and fault condition testing. FCL testing criteria are summarized in Table 2.

Table 2: Zenergy FCL Testing Criteria

No.	Test	Reference
1	Winding Resistance	IEEE Std. C57.16-1996
2	Impedance	IEEE Std. C57.16-1996
3	Total Losses	IEEE Std. C57.16-1996
4	Temperature Rise	IEEE Std. C57.16-1996
5	Applied Voltage	IEEE Std. C57.16-1996
6	Insulation Power Factor	IEEE Std. C57.12.01-2005
7	Insulation Resistance Measurement	IEEE Std. C57.12.01-2005
8	Fault Current	Engineering Spec. ZP-ES-08-05
9	Turn-to-Turn	IEEE Std. C57.12.01-2005
10	Lightning Impulse @ 110 KV	IEEE Std. C57.12.01-2005
11	Chopped Wave Impulse	IEEE Std. C57-12.01-2005
12	Audible Sound	Engineering Spec. ZP-ES-08-05
13	Partial Discharge	IEEE Std. C57.16-1996
14	Seismic Verification	IEEE Std. 693-2005

Source: Zenergy Power plc/NEETRAC/SCE/UC–Irvine

5.2 Pre-connection Testing

A series of pre-connection dielectric and high-voltage tests were designed to verify the integrity of insulation of the FCL device, bushings and supporting structures, and also to measure the AC coil resistance.

During the pre-connection testing, the FCL prototype was exposed to a series of high voltage lightning impulse tests. These were meant to ensure that the device could cope with anticipated adverse conditions on the distribution grid, in a manner similar to other existing distribution equipment.

The Partial Discharge test is designed to test the insulation of the device. To conduct the test both terminals of each phase of the FCL were shorted. Then, each phase was connected to 11.3 kV line-to-ground (L-G) for 10 seconds. The voltage was then reduced to 9.5 kV, held for 60 seconds and then the partial discharge was measured. After the first partial discharge test, each phase was energized at the applied potential test level of 34 kV for 60 seconds. The voltage was then reduced to 9.5 kV, held for 60 seconds and then the partial discharge level was measured again. Partial discharge levels at 9.5 kV fell below the recommended 100 pC (picoCoulomb) value in the three phases; the FCL therefore passed the test.

The objective of the Lightning Full Impulse test is to simulate a traveling wave due to lightning strikes. This test is a good indicator of quality of insulation, design and manufacture. With the terminals of each phase under test connected together, each phase was subjected to one reduced full wave and three full waves of positive polarity, with a crest voltage of 110 kV for the full waves. Initially, the FCL had flashovers. Reconfiguration of the connecting cables and added insulation sleeves resolved the problem and all three phases withstood the lightning impulse tests.

The goal of the Chopped Wave Impulse test is to emulate a sudden flashover of line insulation. A chopped wave imposes a high rate of change in voltage and generates oscillations which result in high internal voltage stress. Thus, the Chopped Wave Impulse test is more challenging. To conduct the test both terminals of each phase of the FCL were shorted. Then, high-voltage impulses were applied to each phase of the FCL in the following order: one reduced full wave, one full wave, one reduced chopped wave, two chopped waves, followed by two full waves, with a crest voltage of 110 kV for the full waves and 120 kV for the chopped waves. Initially, phases A and B passed the test, but phase C failed. The FCL passed the repeated testing after reconfiguration of the connectors and additional insulation was added.

The goal of the Turn-to-Turn test is to detect inter-turn insulation breakdown in the copper coils. The turn-to-turn test consisted of a series of high frequency, exponentially decaying ("ringing") voltages between the terminals of each winding, implemented by repeatedly charging a capacitor and discharging it through sphere gaps into each terminal of the FCL, which generated ringing. Other terminals of the FCL were grounded during the tests. One reduced and three full-wave impulses of positive polarity were applied to each terminal of the fault current limiter. The peak of the full waveform was 95 kV. The discharge waveforms were

oscillating at the same frequency and damping, which meant that no inter-turn fault occurred, and the FCL had passed the test.

The purpose of the Applied Voltage test is to ensure that the device can withstand the required power frequency voltage from the bushing to ground. This test also stresses the insulation in between the different windings. During the test a potential test level of 34 kV was applied for 60 seconds on the supporting structure, including insulators. The FCL passed this test.

5.3 Normal State Performance Testing

The sequence of the normal state performance tests was designed to measure the steady-state voltage drop, impedance, and power losses, and to verify the thermal design.

The FCL was connected to a three-phase bus voltage of 12.4 kV and loaded as shown in Figure 42. The test was conducted under a set of predetermined load currents. The load power factor was close to 0.9. The voltage drop across each phase was measured and insertion impedance of the FCL was found. The FCL passed this test with less than a 1 percent drop in the nominal voltage.

In the normal state the voltage drop across the FCL terminals remains low, so the terminal voltage distortion has a negligible effect on line currents and the power quality remains good. As shown in Figure 46, the full load currents appear to be of satisfactory quality.

Figure 46: Experimental Waveform of FCL Full-load Current in the Normal State

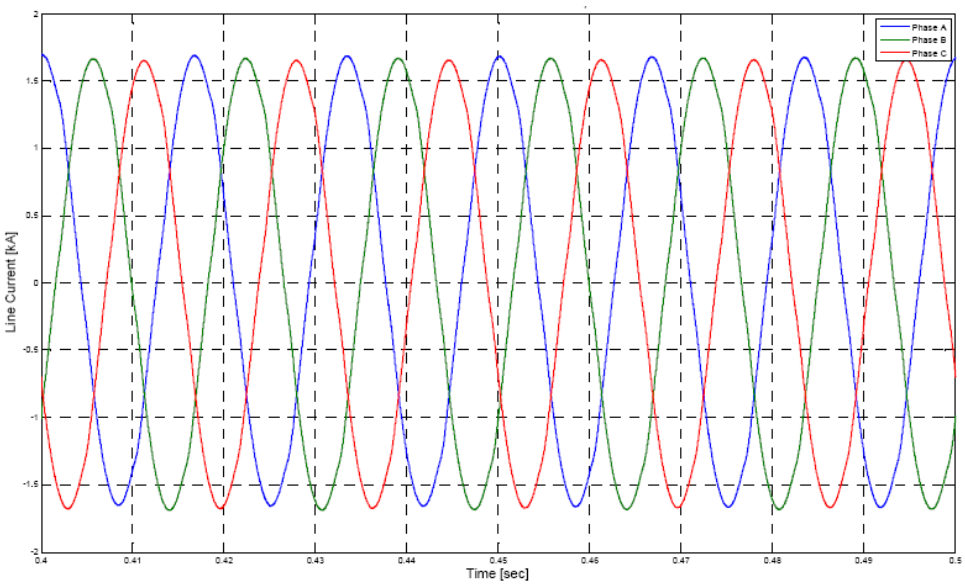

Source: Zenergy Power plc

The FCL insertion impedance and rms voltage drop, across a single phase of the experimental prototype under different load current conditions and DC bias currents, are shown in Figures 47(a) and (b), respectively. Both the FCL insertion impedance and the voltage drop have a nonlinear dependence on the load current and increase as the FCL prepares to assume the current limiting function.

The FCL's power losses are caused primarily by the AC coil resistance. Figure 48 shows the normal state power losses of the FCL measured as a function of the load current.

The temperature rise test was conducted according to the test setup in Figure 42. Temperature was measured on the AC coils with thermocouples on different parts of the AC coils. Load current was increased until the nominal current of 750 A was reached. The test was conducted for nearly 18 hours. The measured temperature of the hottest thermocouple on the AC coil during the temperature rise test was compared to the analytical thermal model in Figure 49. The thermal time constant was found to be equal to 3 hours. A final temperature rise of 35º C above the ambient 22º C was recorded.

Figure 47: Measured FCL Impedance (Ω) and Voltage Drop (%) as a Function of Load Current

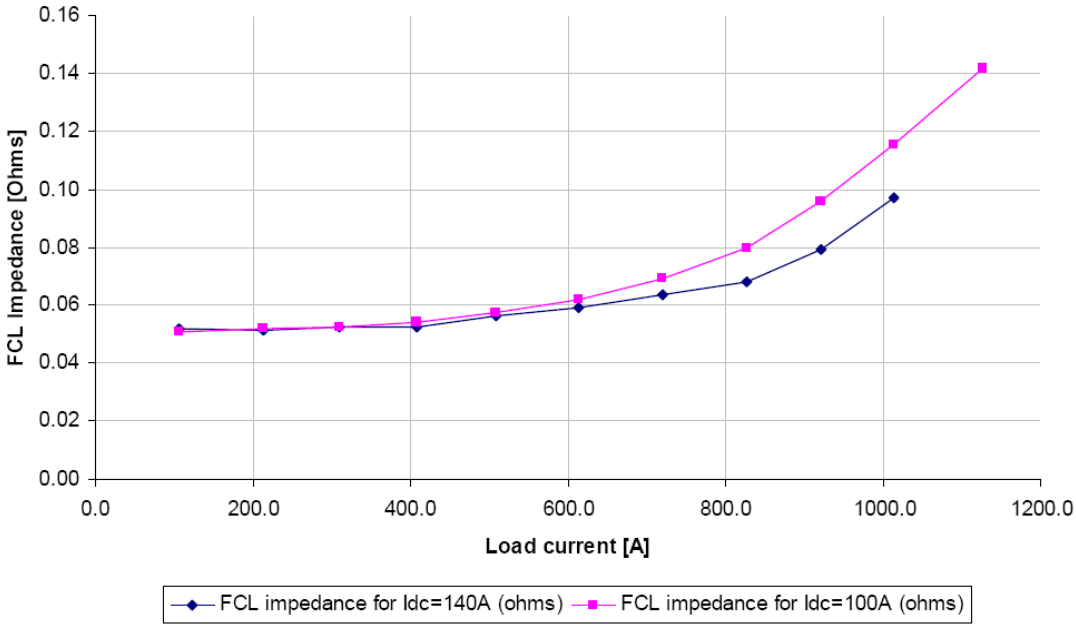

(a) FCL Impedance (Ω)

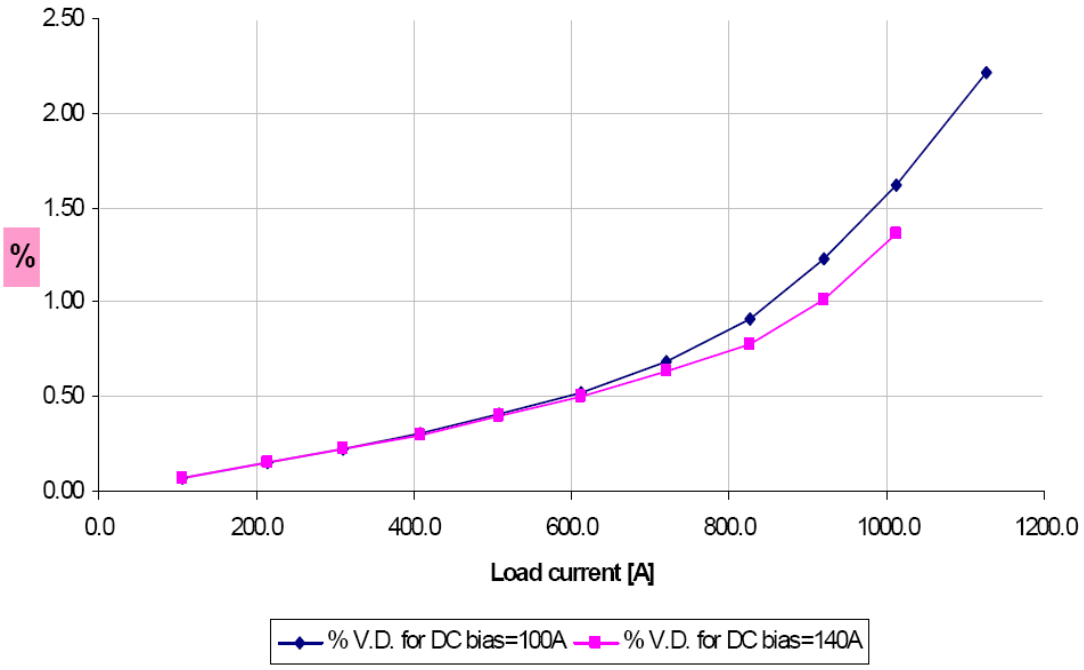

(b) Voltage Drop (%)

Source: Zenergy Power plc

Figure 48: Measured Normal-State FCL Power Loss (%) as a Function of Load Current

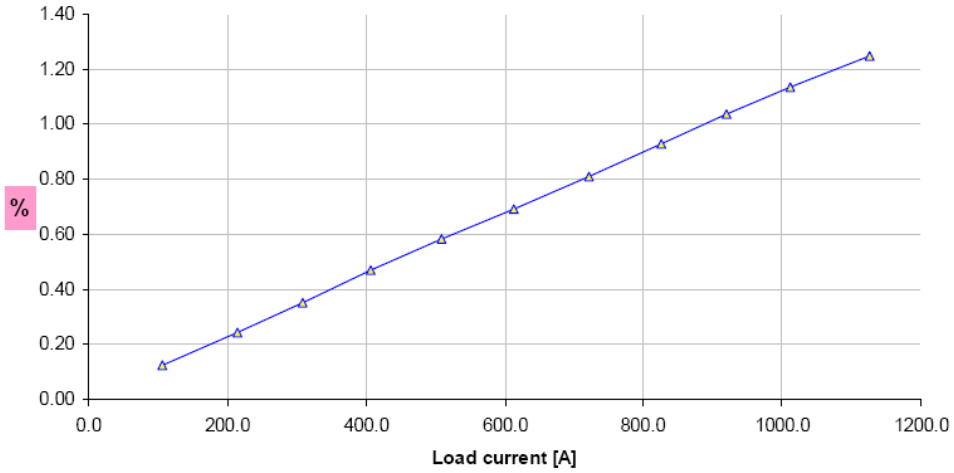

Source: Zenergy Power plc

Figure 49: Measured Temperature on AC Coil During Temperature Rise Test with 750 A (rms) Load Current per Phase

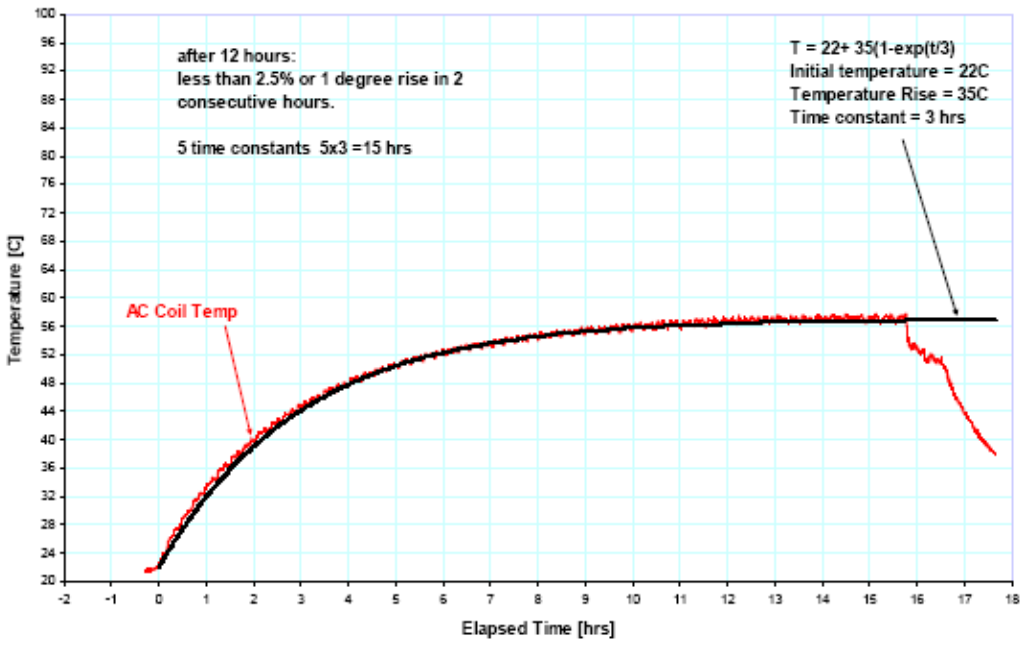

Source: Zenergy Power plc

The non-linear core characteristic makes the FCL a nonlinear device with sharply varying insertion inductance, X_{ins}. The insertion impedance ($Z_{ins} = R_{ins} + X_{ins}$) depends on the core magnetic properties, number of turns in the AC coil, and the DC bias mmf. The experimentally-measured impedance of a single pair of AC coils as a function of DC bias is shown in Figure 50. The measurement was performed at low AC current level. The dashed arrow shows the minimum DC bias mmf required to saturate the core and keep the FCL in the low impedance state.

Figure 50: FCL Insertion Impedance as a Function of DC Bias MMF

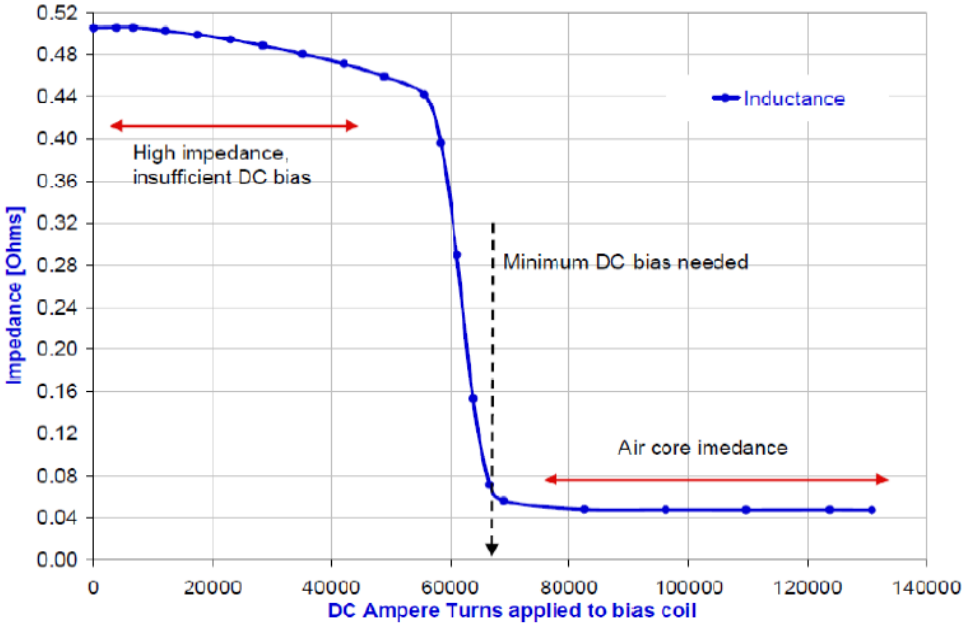

Source: Zenergy Power plc

The FCL insertion impedance Z_{ins} is a function of the AC current magnitude. Generally, the insertion impedance increases with the magnitude of the AC current. Therefore, the DC bias mmf was optimized to attain the largest insertion impedance change in response to the increase in the AC current.

5.4 Fault Condition Testing

The objective of the fault condition testing was to evaluate the fault current limiting capabilities of the FCL under laboratory conditions.

5.4.1 Single-fault Test

The prototype FCL was subjected to a series of faults with different prospective fault current levels. Experimental results of a 23 kA prospective fault current are shown in Figure 51. Figure 51(a) shows the comparison of the prospective current magnitude with no FCL to the clipped (i.e., limited by FCL) AC line currents during the fault experiment. Clearly, the FCL is able to successfully limit the first peak of the fault current in addition to limiting the successive current peaks. Figure 51(b) shows the expanded view of FCL terminal voltage during the fault.

A comparison of the predicted (by the FCL's simulation model) to the measured percent of fault current clipping versus prospective fault current level is shown in Figure 52. The prototype FCL achieved 20 percent clipping of 20kA prospective fault current.

Figure 51: Experimental Results of Zenergy HTS FCL Clipping a 23 kA Fault

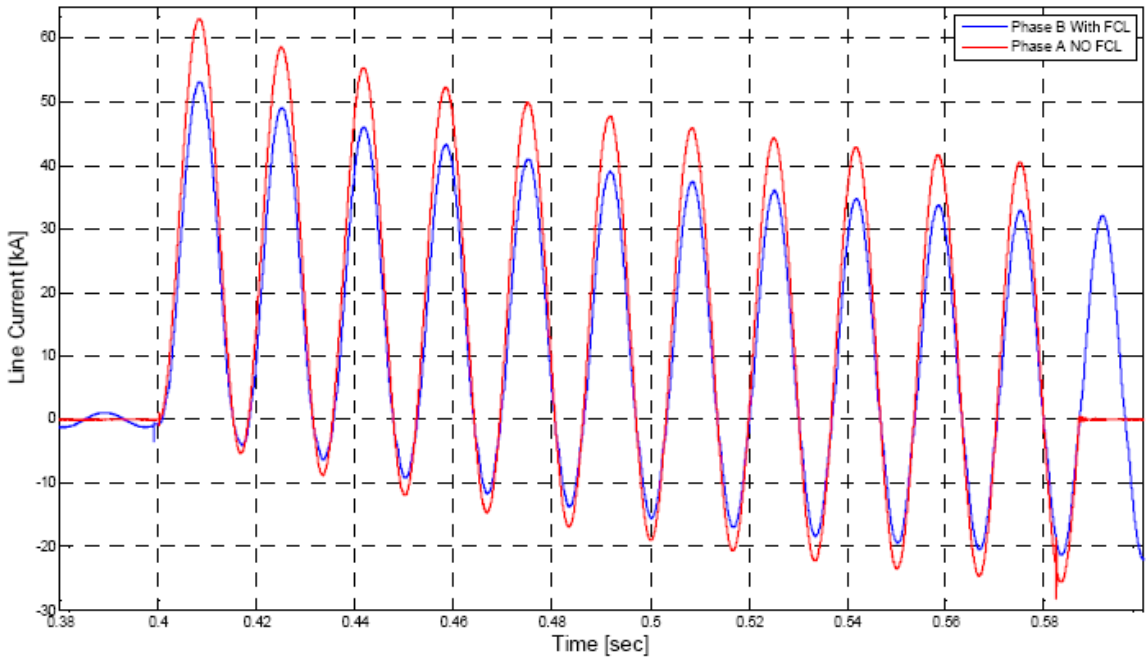

(a) Prospective vs. Clipped Fault Current

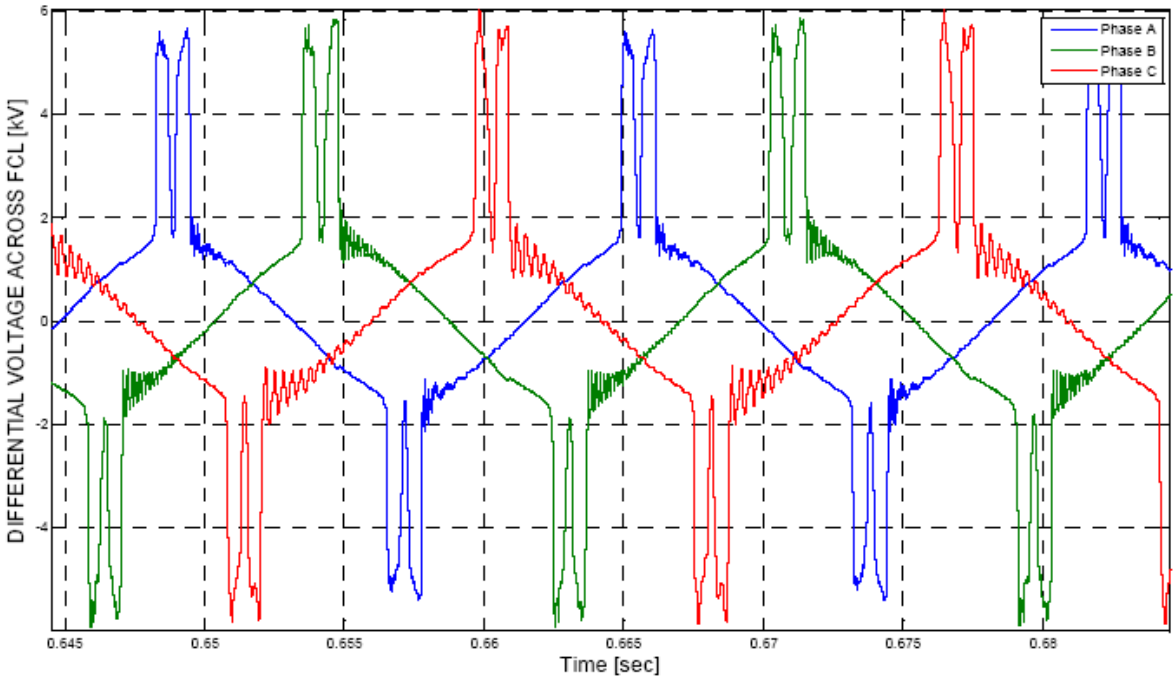

(b) Expanded View of Terminal Voltage

Source: Zenergy Power plc

The measured bus voltages under fault condition with the FCL bypassed and with the FCL active are shown in Figures 53(a) and (b), respectively. Comparison of the waveforms clearly shows that due to the FCL's protective clipping the upstream bus voltage sag was significantly limited.

Figure 52: Actual vs. Simulated Fault Current Clipping (%) as a Function of Prospective Fault Current Level

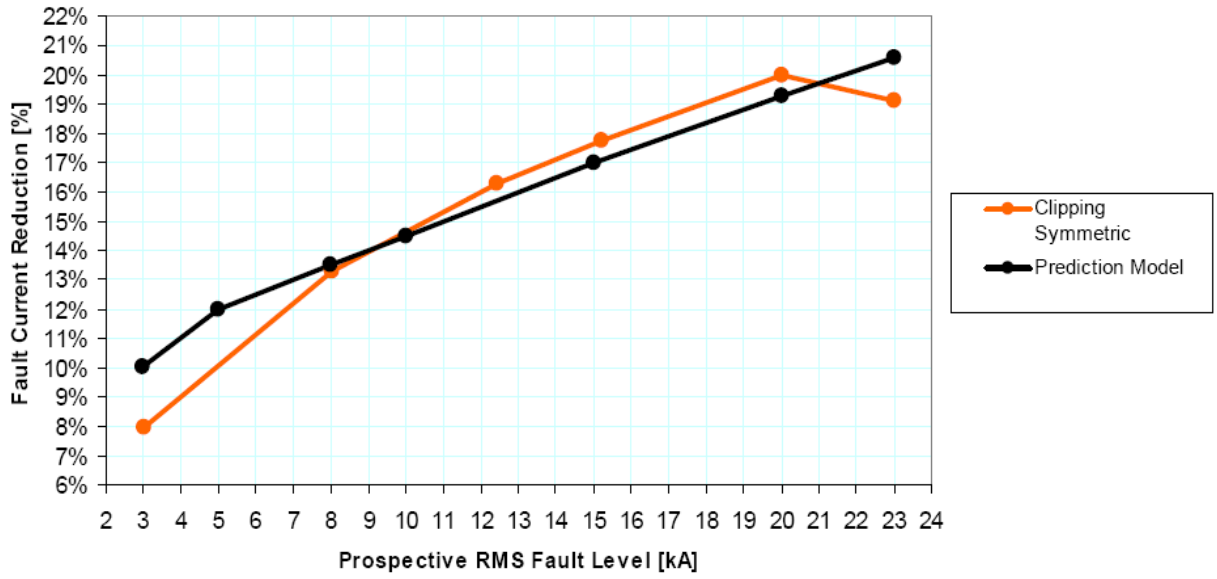

Source: Zenergy Power plc

5.4.2 Double-fault Sequence

The prototype FCL also withstood a 20 kA, double-fault sequence lasting for 20 cycles within a two-second time interval. The FCL succeeded in limiting both faults. Inspection of the experimental FCL current and voltage waveforms, shown in Figures 54(a) and (b) respectively, reveals that on clearance of the fault the prototype FCL had successfully recovered under load.

5.4.3 Endurance Test

The prototype FCL was also subjected to an endurance test and withstood a 20 kA extra-long duration fault for 1.25 seconds, which is 82 cycles long. The FCL successfully clipped the fault without damage to itself. The experimental waveforms of the fault current during the endurance test are shown in Figure 55 and show no signs of abnormal activity.

5.4.4 AC to DC Coil Coupling Test

One of the major concerns in implementing the Saturable Core FCL is the AC voltage that may be induced by the AC coil current in the DC coil. High voltage induced across the HTS DC coil may, potentially, destroy both the DC coil and the bias power supply and, therefore, should be controlled.

During normal operation the cores operate almost symmetrically, so that the AC flux in the center leg is mostly canceled out. As a result, the AC voltage induced in the DC coil is negligible. During the fault, however, the cores operate asymmetrically, with one of the cores at

times out of saturation. By proper geometry of the coils the coupling was minimized. Still, in a practical device some residual coupling, about 5 percent, between the AC and DC coils was observed as shown in Figure 56. As can be seen, higher DC bias results in lower coupling between the AC and DC coils. This reduces the risk of high-voltage shock to the DC coil and power supply.

Figure 53: Experimental Bus Voltage Sag Under a 20 kA Fault Condition

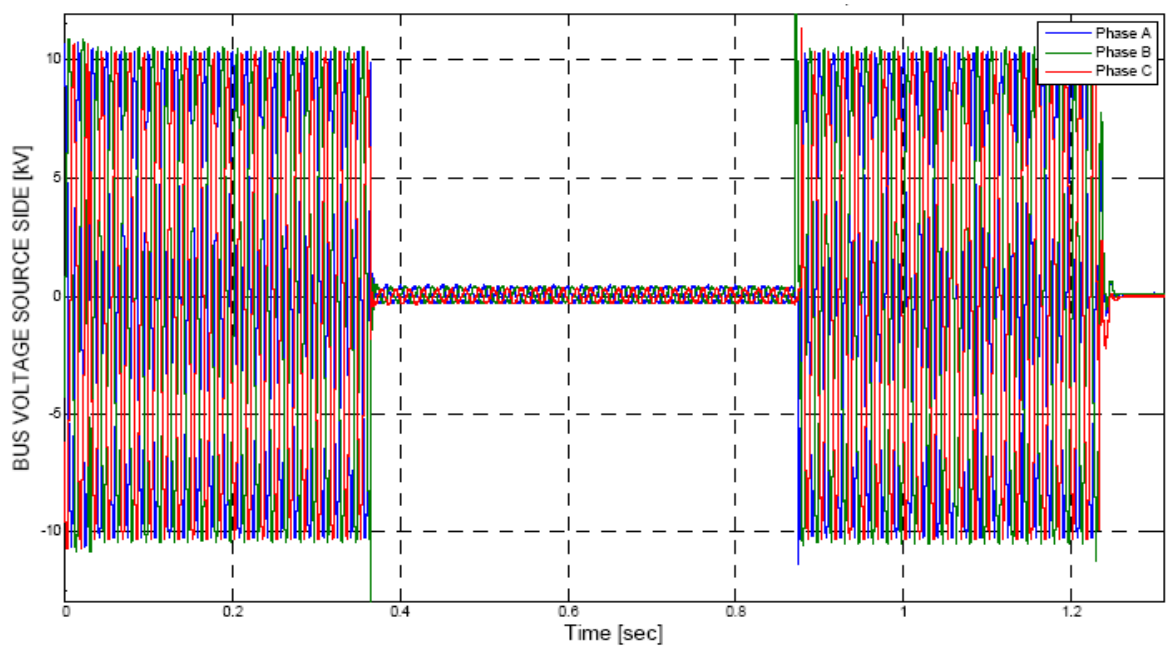

(a) FCL Bypassed

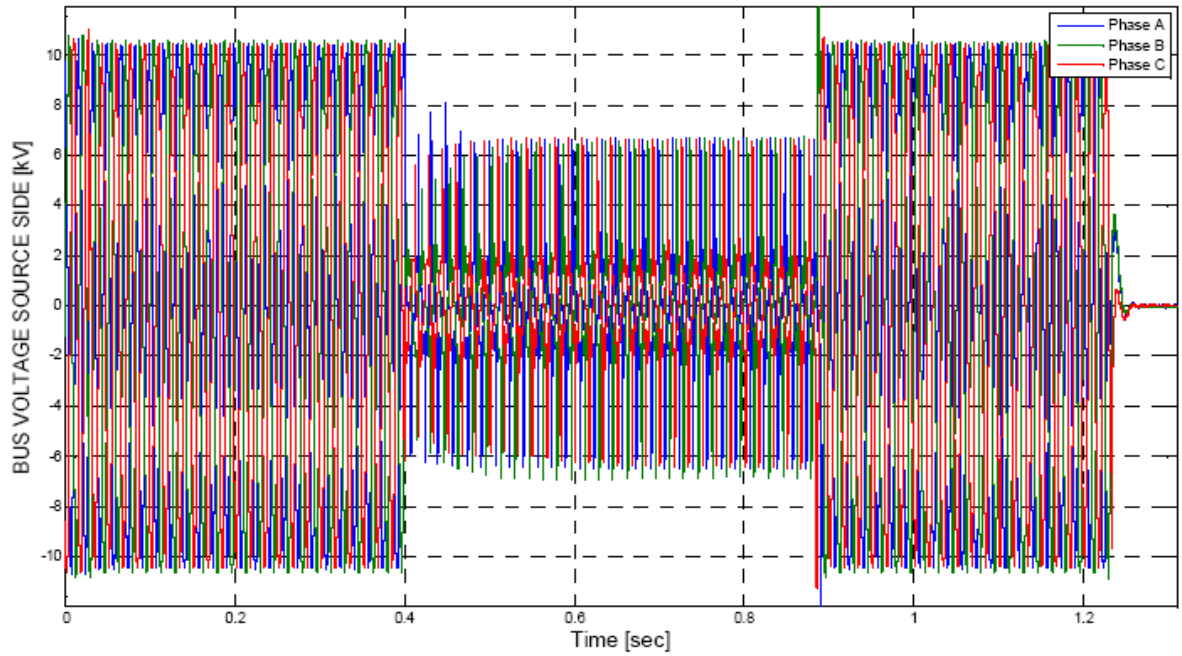

(b) FCL Active

Source: Zenergy Power plc

Figure 54: FCL Current and Voltage Waveforms for a 20 kA Symmetric Double Fault with 2 Seconds Spacing

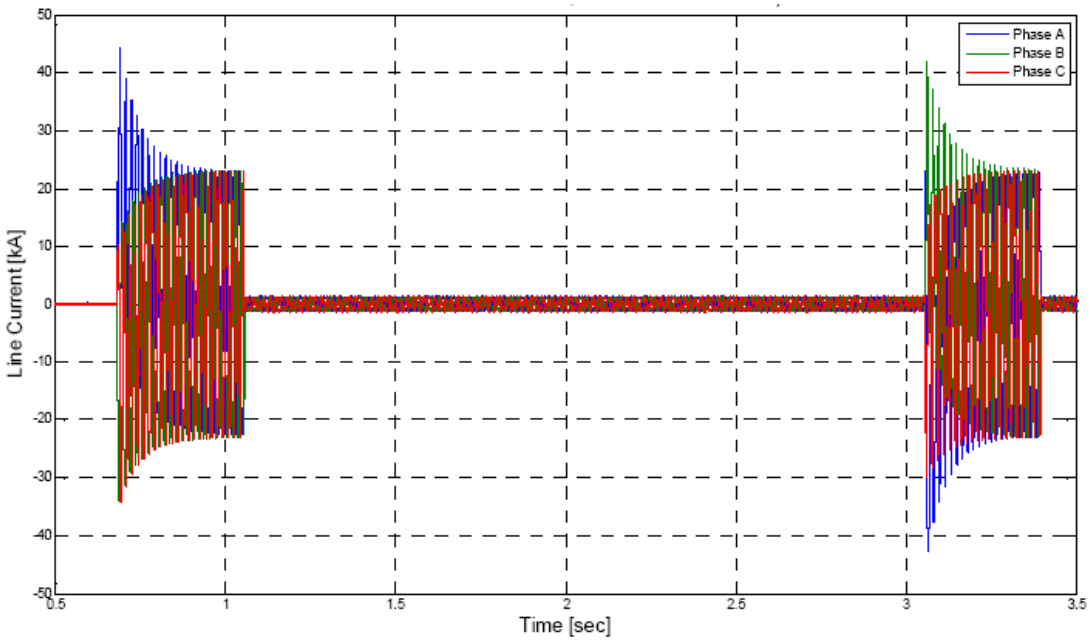

(a) Current

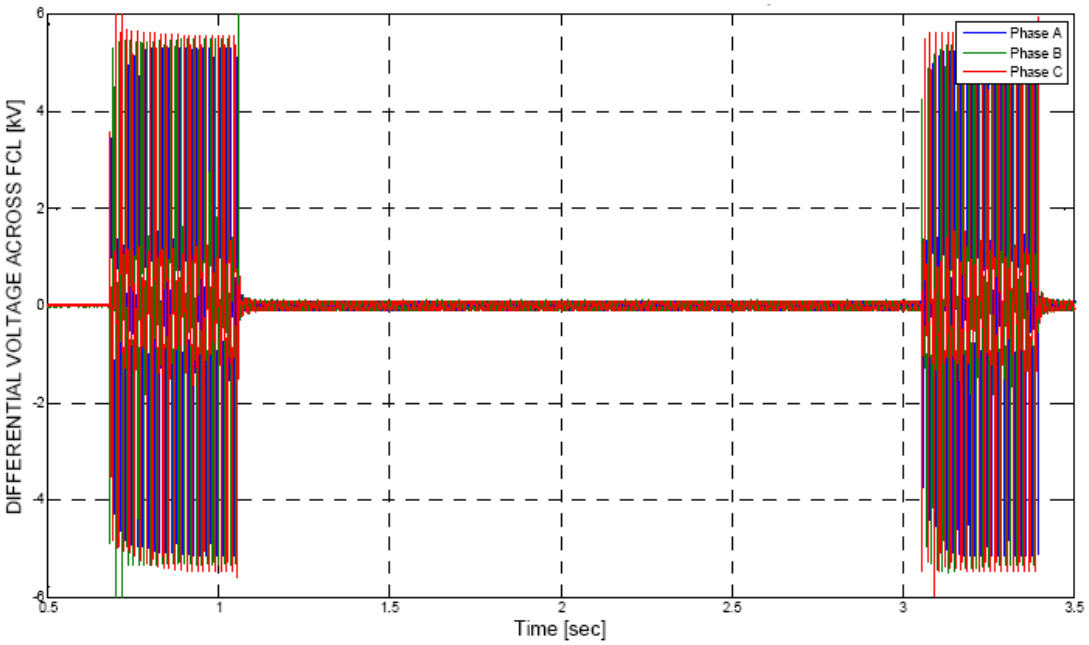

(b) Voltage

Source: Zenergy Power plc

Figure 55: Experimental FCL Current During the 20 kA, 1.25-second, Extra-long Fault

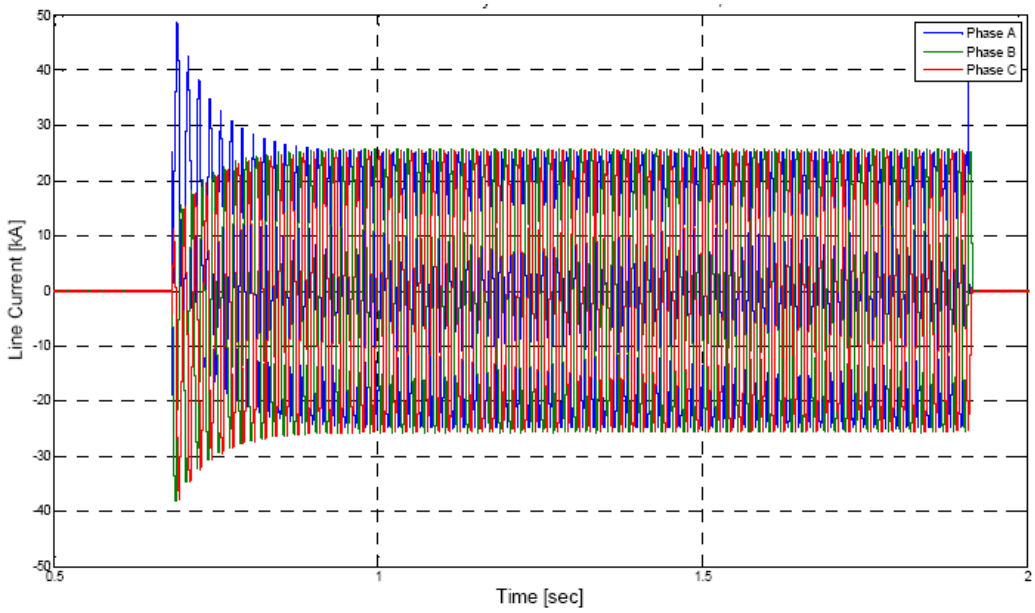

Source: Zenergy Power plc

Figure 56: Coupling of the AC-to-DC Coils in the Normal State and Under Fault Conditions

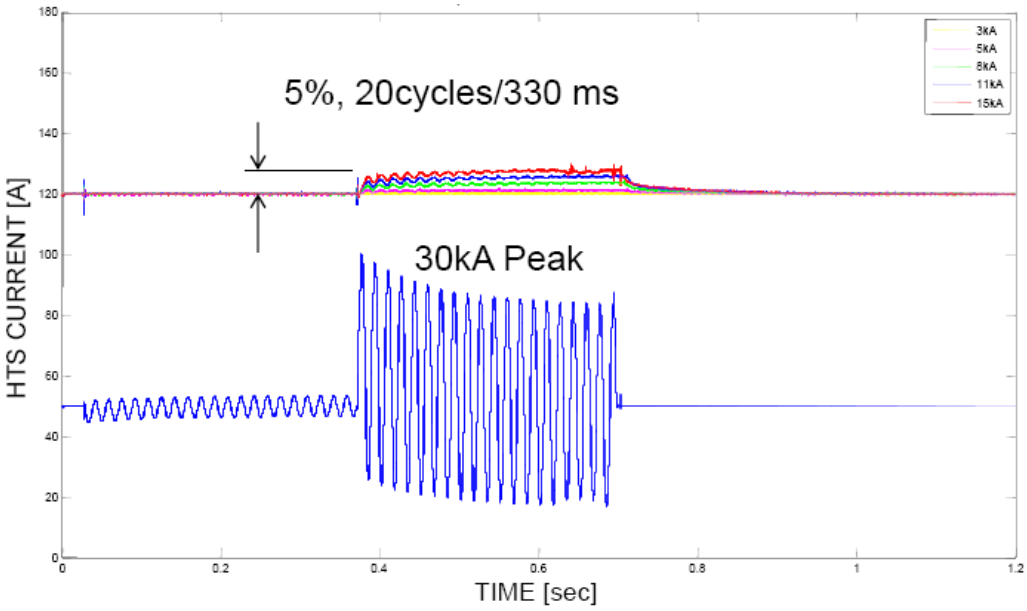

Source: Zenergy Power plc

5.5 Summary

The prototype HTS FCL went through a series of rigorous laboratory tests in BC Hydro's Powertech Laboratory in Surrey, BC, Canada. A total of 65 separate tests were performed, including 32 full-power fault tests with first-peak fault current levels up to 59 kA at the rated voltage. Fault tests included individual fault events of 20 to 30 cycles duration, as well as multiple fault events in rapid sequence (to simulate automatic re-closer operation) and extended fault events of up to 82 cycles duration, simulating primary protection failure scenarios.

The experimental FCL prototype passed all the pre-connection, normal state, and fault condition testing procedures. The prototype FCL proved to have low normal-state insertion impedance, was able to withstand real fault conditions, endured long duration faults, tolerated the resulting magneto-mechanical forces and thermal stresses with no damage, and demonstrated instantaneous recovery under load.

Successful laboratory testing of the prototype Zenergy Power FCL demonstrated, to the satisfaction of both Zenergy Power and the host utility SCE, that the unit was ready to be connected to a commercial electric utility circuit with commercial, industrial and residential loads in the subsequent field trials at SCE's Avanti Circuit of the Future.

CHAPTER 6:
Zenergy Power HTS FCL Field Testing

The experimental Zenergy Power HTS FCL prototype was installed by Southern California Edison Co. (SCE) in the Avanti "Circuit of the Future" in San Bernardino, CA, and was in operation from March 2009 until October 2010 for field testing and data collection. The Circuit of the Future (COF) is a key part of SCE's program for performance evaluation of new and emerging grid technologies and systems, as well as for gaining experience with novel "smart grid" equipment. As such, it was an ideal test bed for the field trial of FCC technology that was the primary objective of this research project, and SCE was an enthusiastic partner and host utility, as they were keenly interested in the evaluation and, hopefully, the commercial uses of FCCs. The prototype FCL was integrated into SCE's SCADA system and was operated in real time, providing protection to the distribution circuit by limiting any fault currents that might occur on the COF. This comprehensive field demonstration was the first-of-its-kind instance of an HTS FCL being used in commercial service in the US electric grid.

6.1 Setup and Metering

6.1.1 Avanti "Circuit of the Future"

The Avanti Circuit, shown in Figure 57, is a 12.47 kV feeder serving residential, commercial and light-industry customers in San Bernardino, California. The Avanti Circuit is specially commissioned and instrumented to assess new "smart grid" technologies. The main feeder is about 7 miles long and composed of about 20 percent overhead and 80 percent underground construction.

The experimental FCL prototype (Figure 58) was installed inside the Shandin substation fence line (Figure 59), immediately beyond the main feeder circuit breaker. The FCL was connected in series between the feeder loads and the 12 kV side of the substation's transformer bank. The FCL was also equipped with a bypass switch so that it could be taken off-line if needed.

The purpose of the installation was to demonstrate the FCL's functions and gain operational and maintenance experience under real-world conditions [66], [67]. The operating environment at the substation is a severe, southwest US desert environment with hot, dry, dusty, high-wind conditions. Summer daytime temperatures were frequently well in excess of 40° C (104° F). Additionally, a residential neighborhood located nearby imposed a very restrictive ambient noise requirement on the operation of the unit.

6.1.2 Metering

Figure 60 shows the schematics of the Shandin substation and installation of data recorders 1 and 2. Data recorder 1 is installed in the control room. Data recorder 2 is installed in the immediate proximity of the Zenergy Power FCL.

Dranetz™ Power Xplorer PX5 data recorders (http://dranetz.com/portable/powerxplorer-px5) were used, having the following basic characteristics:

- Data volume: 1 GB memory card (upgraded to 2 GB).
- Data rate: 256 samples per cycle (60 Hz line).
- Recording: Adjustable. Depends on setting; is triggered by current level.
- Available recording time: Adjustable. Depends on number and duration of recorded events.

These recorders have four independent channels. Three channels were monitoring the line currents and one channel was unused.

Figure 57: Diagram of the Avanti "Circuit of the Future"

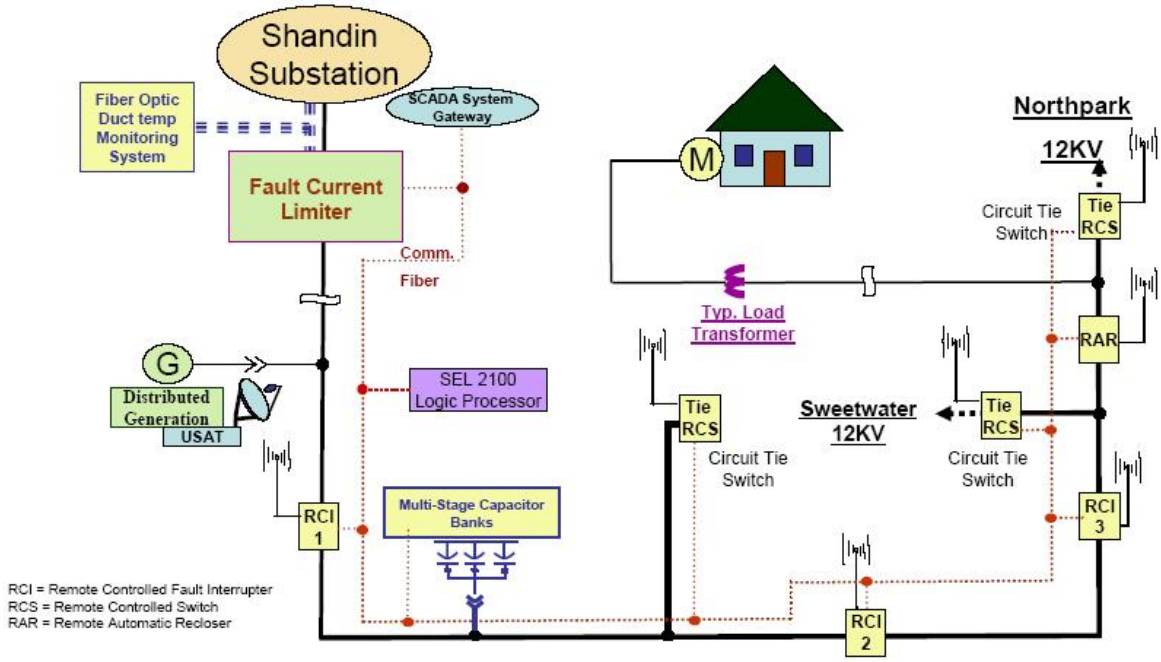

Source: Southern California Edison Co.

Figure 58: Zenergy Power HTS FCL Prototype in Operation at SCE's Avanti Circuit of the Future

Source: Zenergy Power plc

Figure 59: Aerial View of Zenergy Power HTS FCL Installation in SCE's Shandin Substation, San Bernardino, California, March 2009

Source: Zenergy Power plc

Figure 60: Location of the Data Recorders at Shandin Substation

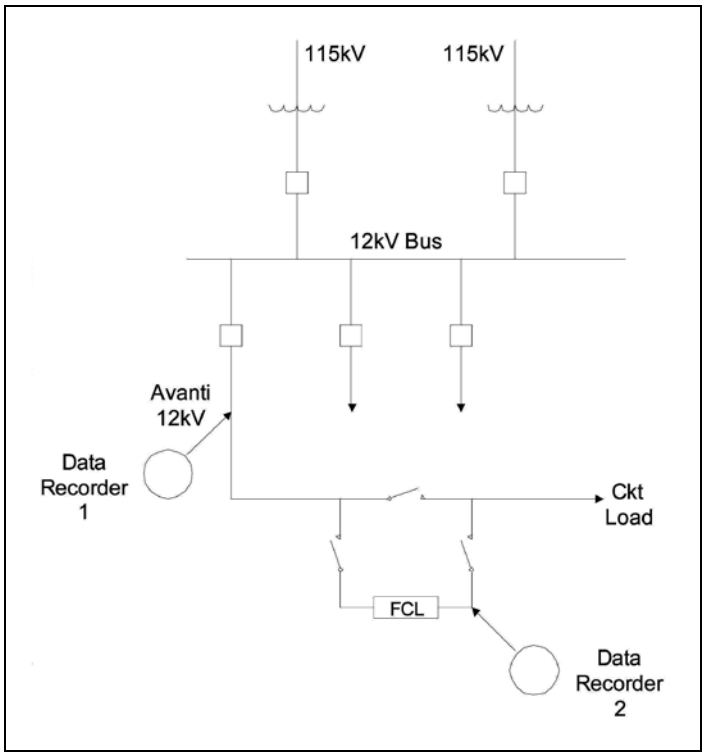

Source: Southern California Edison Co./University of California–Irvine

6.2 FCL Key Technical Events

6.2.1 Pre-Installation Events

6.2.1.1 Controller Assembly and Software Testing – May 2008

This development task performed by Zenergy in preparation for the field prototype's implementation was a critical milestone in the field trial. The basic monitoring and control software necessary to operate the FCL as designed was thoroughly tested and debugged in the lab prior to sending the FCL to the demonstration site. From this initial testing, the most important conclusions, derived in consultation with SCE's Advanced Engineering Group, were that redundant and fail-safe hardware and software designs as well as secure telecommunications were necessary in order to ensure reliable operation with a minimum of required maintenance interventions.

6.2.1.2 Seismic Analysis per IEEE Standard 693 – June 2008

Seismic modal analysis of the FCL unit was performed by Zenergy to determine any structural requirements to withstand a 0.5 g zero-period acceleration, and to provide the necessary information for SCE to design the anchorage system and the stress release for the electrical connection according to the reaction forces. Finite element modeling and spectrum analysis up to 40 Hz with 2 percent damping indicated that the iron core of the AC coils required extra supports to limit stresses and deflections to within the allowable values, per IEEE Standard 693 [78].

SCE's Civil Engineering Group was consulted to determine the best option for the physical installation of the FCL. One option considered for the foundation was to use railroad ties over the existing crushed gravel in the substation's yard. Another alternative was to build a traditional concrete foundation to ensure that the FCL would remain level in this seismically active area. The civil engineering team's recommendation was to set the FCL on compacted and leveled crushed gravel without any additional support because the FCL's enclosure was welded to steel I-beam skids, providing adequate seismic rigidity.

6.2.1.3 FCL Assembled and Continuity and Temperature Rise Tests Performed – September 2008.

As there were no industry-accepted standards for FCL testing, NEETRAC, in close collaboration with several of its member utilities, including SCE, cooperated with Zenergy Power to develop a detailed FCL test protocol (Attachment I) based on IEEE and CIGRE standards for transformers and reactors. The FCL was rated at 15 kV, 1,200 A, 110 kV BIL, and designed to limit a prospective 23 kA symmetric fault by at least 20 percent, with less than 1 percent voltage drop at maximum load current in the normal state. The FCL was first subjected to heat runs at a load current of 750 A and full DC bias current to verify the maximum temperature rise of the AC coils and the high voltage terminations. All measurements were within the limits specified in IEEE Standard C57.16-1996 [75].

6.2.1.4 High-power and High-voltage Testing Completed at BC Hydro – September 2008.

Prior to high-power testing, continuity and insulation resistance measurements were performed to verify that no movement of the device's components occurred during shipping. Source and load-side bushing terminations were measured separately. A comprehensive series of high-power tests was then conducted at BC Hydro's Powertech Laboratories. A total of 65 separate tests were performed, including 32 full-power fault tests with first-peak fault current levels up to 59 kA, all at rated voltage. Fault tests included: individual fault events of 20 to 30 cycles duration; multiple fault events in rapid sequence to simulate operation of automatic circuit reclosers; and extended fault events of up to 82 cycles duration to simulate primary protection failure scenarios. The FCL's measured performance agreed closely with the engineering calculations in all cases.

The FCL was then tested under full lightning impulse tests at Powertech's high voltage laboratory. During the first round of tests, flashovers occurred between the HV jumper cables connecting the AC coils. All jumpers were replaced and rearranged with more separation. Other HV insulation enhancements made in order to pass the more severe chopped impulse tests included: application of heat shrink insulation over the exposed terminations; larger lugs and wall openings; molding mastic rubber to cavities, sharp objects, and connectors; and solid connection of all ground leads to a common ground point.

6.2.1.5 High-voltage Testing Performed at SCE's Westminster HV Lab – December 2008

High-voltage acceptance testing was also conducted by SCE at its laboratories in Westminster, California, as follows:

- One reduced (1.2 x 50 μs) full wave – 50 percent or 55 kV peak wave

- One full (1.2 x 50 μs) wave – 100 percent or 110 kV peak wave
- One reduced chopped wave – 50 percent or 60 kV peak wave (chopped at 2 μs)
- Two full chopped waves – 100 percent or 120 kV peak waves
- Two full (1.2 x 50 μs) waves (within 10 minutes after the last chopped wave)

All the above tests, as well as the partial discharge tests, were successfully passed by the FCL per IEEE Standard C57-12.01-2005 [77].

6.2.1.6 Cold-head Replacement – February 2009

One of the two cold heads of the helium refrigeration sub-system was replaced as a routine preventive maintenance task that was due. From this experience it was learned that this hardware needs better accessibility when performing maintenance in the field.

6.2.2 Post-Installation Events

6.2.2.1 FCL Commissioned on the Avanti Circuit of the Future – March 9, 2009

On-site commissioning tests performed by SCE engineers were successfully passed. These tests consisted of coil resistance, power factor, and impedance measurements of all phases. These measurements were performed as a safety and reliability check every time work was conducted in the HV compartment to verify that the HV insulation had not been disturbed.

The change of the FCL's insertion inductance as a function of the DC bias current was also measured by SCE when the HTS DC magnet bias system was first energized and de-energized.

6.2.2.2 Damped Resonance Event Triggered by Controller Memory Overflow – March 16, 2009.

The FCL experienced a loss of DC bias current, caused by a reset of the Programmable Automation Controller that was triggered by a RAM overflow. This shutdown occurred at a time when the Avanti Circuit's load current was approximately 120 A. The FCL remained in the circuit for approximately 45-50 minutes, producing an initial 300 V line voltage rise, followed by a 400 V line voltage drop on the 12 kV circuit bus. During this period, two large automatic capacitor banks operated to regulate the voltage on the circuit according to their programmed limits. The combination of the FCL's high inductance due to the absence of DC bias current and the high shunt capacitance caused an intermittent damped resonance condition. The FCL was bypassed after 50 minutes and the circuit returned to normal operations. The FCL remained bypassed and was operating in the standby mode until December 9, 2009, when an automatic bypass was installed.

The event occurred as follows: At 10:10 am the DC bias current source shut off, initiating the feeder's voltage rise. At 10:13 am, three minutes into the event, the system voltage had risen above the upper dead-band limit (12.45 kV) of the 1.8 MVAR capacitor bank. After 60 seconds above the dead-band limit the 1.8 MVAR capacitor opened. Without a capacitor bank, the system voltage dropped to about 11.65 kV at 10:14 am. At approximately 10:17 am the 1.2 MVAR capacitor bank switched in, due to the system voltage being below the lower limit of the dead-band for three minutes. This action caused the feeder to re-enter a resonance condition. As a result the feeder voltage increased to 12.4 kV, remaining there until the FCL was manually

bypassed at approximately 11:35 am. After the FCL was bypassed, the feeder voltage dropped to approximately 12.2 kV, which was approximately the same voltage as before the event. There were no negative consequences, but as a result of this event, SCE installed an automatic bypass switch and set it in its automatic mode whenever the FCL was in service.

Due to delays in acquiring and installing the bypass switch, the FCL was maintained in a ready condition, but was off-line (not installed in the circuit in active service) until December, 2009.

6.2.2.3 HVAC Shutdown Due to High Ambient Temperature – June 2009

An ambient temperature of 108° F was reached at the site in June 2009. The refrigeration systems of the device had operated almost continuously since its installation. During a hot summer week, the FCL experienced venting of the cryogenics fluid and required replenishment of the liquid nitrogen due to a shutdown of the HVAC unit in the compressor compartment.

The solution was to upgrade the 3-ton HVAC to a 5-ton unit rated at 125° F ambient working temperature. An extension to the existing compressor enclosure was added to provide sufficient air flow to the three faces of the heat-exchanger coils. A shade structure for the 5-ton HVAC and the compressor enclosure was also built to protect the FCL from direct sun exposure. No changes were needed to the station's power and light supply and there were no more HVAC interruptions through the rest of the summer, which saw even hotter days than before.

6.2.2.4 Controller Upgraded, Including Watchdog Function – June 2009

During the outage taken to install the higher rated HVAC unit, the controller was also upgraded. A more robust industrial-grade controller was installed with software and communications to perform the monitoring and control functions being performed by the original controller but with higher reliability to withstand the harsh environment found at Shandin Substation.

At this time a watchdog function was also added at the request of SCE to bypass the FCL in the event of loss of any of the critical control functions or loss of auxiliary and/or backup power.

6.2.2.5 Helium Leak Detected and Fixed – June 2009

A slow helium leak was detected by observing the pressure and temperature trends of the cooling system. This did not cause any malfunction or shutdowns, but the leak was located and corrective action was taken.

6.2.2.6 Automatic Bypass Switch Installed and FCL Returned to Service – December 9, 2009.

Once the automatic bypass switch was installed, the FCL was returned to active service on the COF. Since the unit had been in off-line mode for 9 months, it was not possible to collect fault or performance data on the FCL. The FCL not entered its official field trial and data collection period.

6.2.2.7 Multiple-Fault Event – January 14, 2010

One month after being returned to active service, the FCL experienced its first in-service fault. Measured data by SCE and Zenergy Power confirmed that the event evolved from a phase-to-phase fault, to a three-phase fault, to a temporary recovery, to a phase-to-phase fault, to another three-phase fault, and ended with a line opening and fault clearing. This multi-fault event

occurred over a three-second period. The sequence initiated when phases A and B of the overhead section of the Avanti Circuit came together during high wind conditions. This phase-to-phase fault lasted about 250 milliseconds, when Phase C also faulted, thus evolving into a three-phase fault, lasting about half a second. The air recovered its dielectric strength and extinguished the fault arc for about one second, but then the conductors of phases A and B again flashed over to each other for about three quarters of a second. The arc was about to be extinguished at this time, but again Phase C also flashed, resulting in a three-phase fault. The event ended about a quarter of a second later when the Phase B conductor separated and dropped to the ground, and the circuit's protection cleared this solid ground fault.

The FCL limited the fault current throughout the various faults and sent the corresponding monitoring and control signals as designed.

6.2.2.8 Nitrogen Pressure Stability Problem – February 2010

The cause of this problem was that the cold-head heaters' power changed in steps that were too large, causing overshoot in the system's temperature control. As with the slow leak problem, this was detected through long-term observations.

An improvement with finer resolution of the power increments to the heater elements and a feedback loop stabilized the pressure and temperature and solved the problem.

This problem did not have any negative impact on the operation of the FCL, but the associated engineering and maintenance needed to fix the problem inspired Zenergy to pursue the option of using dry (i.e., non-superconducting) cooling systems in future FCL designs.

6.2.2.9 Shutdowns Due to Loss of Auxiliary Power from Transmission Fault Events – March 2010.

The FCL experienced three outages of substation auxiliary power due to faults on the high-voltage side of the substation or on the transmission lines. In one of these events, a fault on the 115 kV high-voltage side caused a voltage dip and a two-minute outage on the 12 kV side of the substation.

As required by SCE, the FCL's controller immediately issued a bypass command, sent out alerts to SCE and to Zenergy, and initiated an orderly shutdown of the DC bias current and cooling systems. It sent the correct alarms and bypass commands to SCE. Upon resuming AC power, the cooling system compressor was restarted and the cryogenic parameters returned to normal, with the HTS coil ready to be re-energized.

The FCL is now equipped with an uninterruptible DC power supply, which allows it to ride through these types of outages without downtime.

6.2.2.10 Shutdown Due to Shorted Terminal Block – August 2010

This event initiated tripping of the auxiliary power from the substation's light and power panel. The FCL's controller again safely bypassed the unit, alerted SCE of the event, and shut down the unit as designed.

The problem was caused by a loose connection at one of the supply cables on the terminal block where the auxiliary power to the FCL is received. A higher rated terminal was installed and the proper torque value to use when installing this terminal was included in the FCL installation manual.

6.2.2.11 Decommissioning of the Zenergy HTS FCL – December 2010.

The Zenergy FCL successfully completed its intended period of field testing by October 30, 2010. Per the agreement with SCE, the unit was subsequently decommissioned, and removed from service on December 16, 2010.

6.3 Analysis of Major Events

6.3.1 Loss of DC Bias Current, March 16, 2009

6.3.1.1 General Overview

A loss of DC bias event is a severe failure of the FCL. The event that occurred on March 16, 2009 was analyzed in detail in order to study the implication of such an event on the power system, and was described in a paper presented at the 2010 IEEE PES Transmission and Distribution Conference and Exposition, April 2010 [68].

The Avanti Circuit is a 12 kV distribution feeder. There are four shunt capacitor banks installed on the Avanti Circuit for voltage support. At the time of the event, two of the four capacitor banks were disabled. The capacitor banks remaining in service (see Figure 61) are rated at 1.2 MVAR and 1.8 MVAR. Both banks are connected in an ungrounded wye configuration and are capable of switching automatically. Prior to the event the 1.8 MVAR bank was closed, and the 1.2 MVAR bank was open.

Figure 61: Diagram of the Avanti Circuit Prior to the March 16, 2009 Loss of DC Bias Event

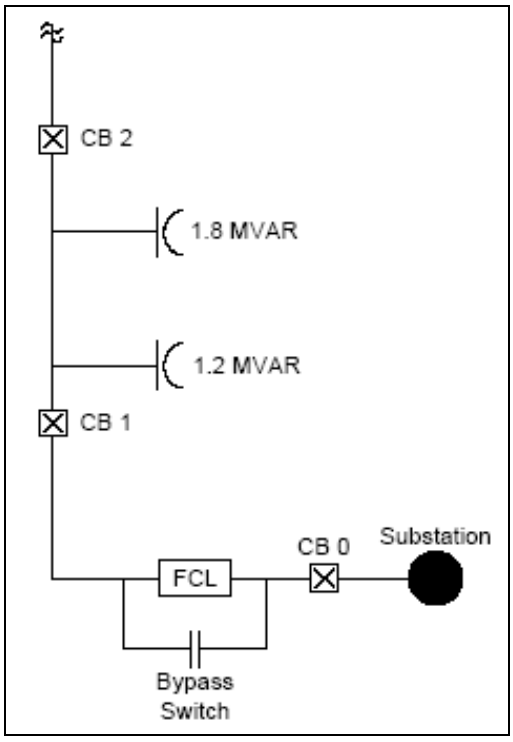

Source: Zenergy Power plc

The switchable capacitor banks operate on a time-biased voltage control. The switched capacitor banks open or close if the measured voltage is outside of a programmed dead-band for a set duration. The capacitor banks also were set to perform an emergency open or close if the voltage is measured at 130 V or 110 V (on a 120 V base), respectively, for five seconds. The 1.8 MVAR capacitor bank was programmed to open on 124.5 V and close on 120.0 V, and had a delay of 60 seconds. The 1.2 MVAR bank was programmed to open on 125.0 V and close at 121.0 V and had a delay of 180 seconds. It is important to note that the capacitor controls are set with a five-minute lockout delay before a capacitor bank can perform another open or close operation. Data was sampled at CB 1 and CB 2 where SEL-351 relays from the Avanti Circuit's advanced protection scheme were monitoring and reporting A-B phase voltage and current every 5 seconds.

6.3.1.2 Description of the Event

Prior to DC bias current loss on March 16, 2009, the FCL was operating normally. The FCL's inductance is not a constant number even during normal operating conditions, but is a function of instantaneous AC current.

As shown in Figure 62, at 10:09 am the DC bias current source shut off, initiating the feeder's voltage rise. Current in the DC coil took approximately 5 minutes to decay to trace levels. Figure 62 shows the HTS coil's DC current (blue) and its voltage (red) during the event. The coil voltage dropped from 0.12 V (with predominantly resistive coil impedance) to -2.0 V

(predominantly inductive coil impedance), and decayed to zero after several minutes as the HTS current also settled to zero.

Figure 62: HTS Coil Current and Coil Voltage for the March 16, 2009 Loss of DC Bias Event

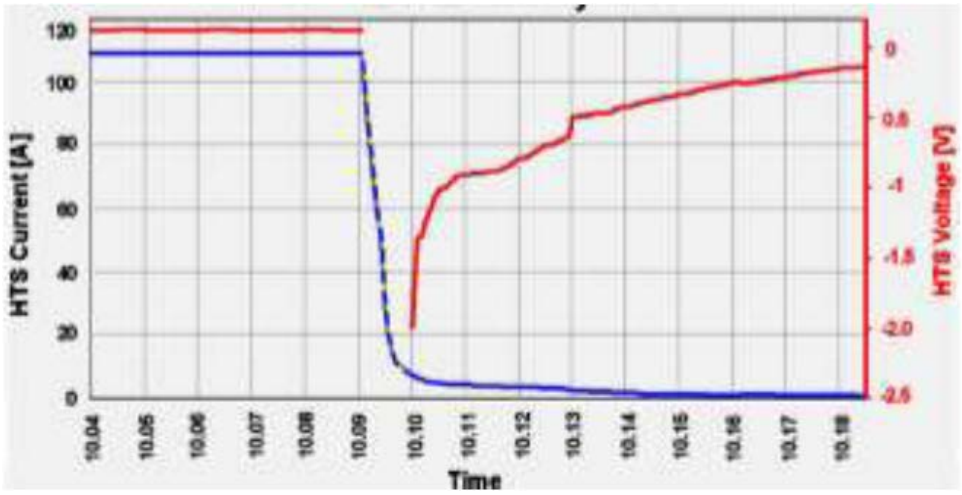

Source: Zenergy Power plc

At 10:13 am, four minutes into the event, the system voltage had risen above the 1.8 MVAR capacitor bank's upper dead-band limit (12.45 kV). After 60 seconds above the dead band limit, the 1.8 MVAR capacitor opened. Without a capacitor bank, the system voltage dropped to about 11.65 kV at 10:14 am (see Figure 63(a), with time scale of 10 minutes before the event to 25 minutes after event onset, and Figure 63(b), with expanded time scale of the first 18 minutes of the event). At approximately 10:17 am the 1.2 MVAR capacitor bank switched in due to the system voltage being below the dead-band lower limit for three minutes. This action caused the feeder to re-enter a resonance condition. As a result, the voltage increased to 12.4 kV, where it remained until the FCL was manually bypassed at approximately 11:31 am. A loud humming sound in the FCL was heard, due to the high magnetostriction (mechanical stresses and vibration due to large magnetic flux variations) of the iron cores. After the FCL was bypassed, the feeder voltage dropped to approximately 12.2 kV, which was approximately the same voltage as before the event.

Figure 63: Line-to-line Voltage between A and B Phases at CB #1 for the March 16, 2009 Loss of DC Bias Event

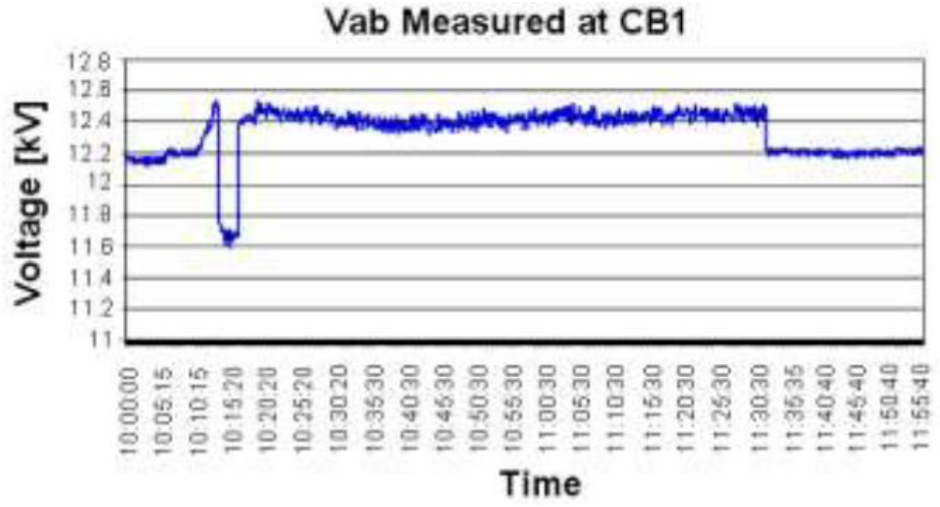

(a) 10 Minutes Before Event to 25 Minutes After

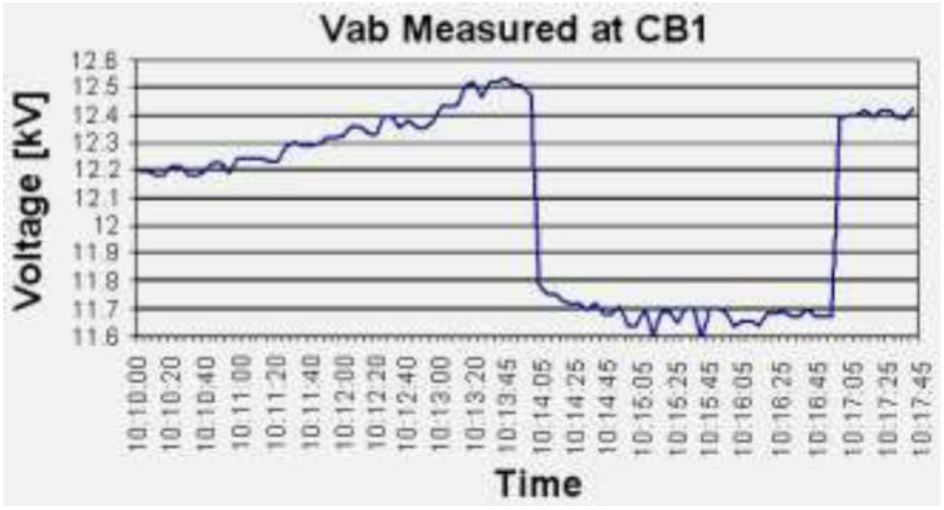

(b) Expanded Time View of Fault

Source: Southern California Edison Co.

Figure 64 shows the line-to-ground voltages, as measured by the three potential transformers installed at the load side of the FCL. The HTS current (black) also appears for reference. Both feeder voltage and feeder current as measured at the FCL agreed with SCE's field data.

6.3.1.3 Observations

The measured bus voltage tended to increase due to resonance between the 1.8 MVAR capacitor and the increasing FCL inductance of de-saturation due to loss of the DC bias in the FCL. Note that the 1.8 MVAR capacitor bank switched out before the DC coil's current decayed to trace amounts. If the DC coil had decayed to trace amounts before the 1.8 MVAR capacitor bank

opened, simulations show the line voltage would have risen to 12.65 kV. Simulations also showed that, under normal system conditions, the voltage rise due to the 1.8 MVAR and the 1.2 MVAR capacitor banks would be about 0.2 kV and 0.12 kV, respectively. When the 1.8 MVAR bank opened, the resonance condition ceased and the system voltage dropped to 11.87 kV. This voltage drop from the pre-event 12.2 kV was due to the FCL's voltage-drop under de-saturating conditions. This measurement allows comparison of the line voltage for the saturated FCL with that for the de-saturating FCL without a masking effect due to resonance. Furthermore, the DC current was still decreasing, causing the FCL's voltage drop to increase, resulting in a further decrease to 11.65 kV.

Figure 64: Line-to-ground Phase Voltages and HTS Coil Current for the March 16, 2009 Loss of DC Bias Event.

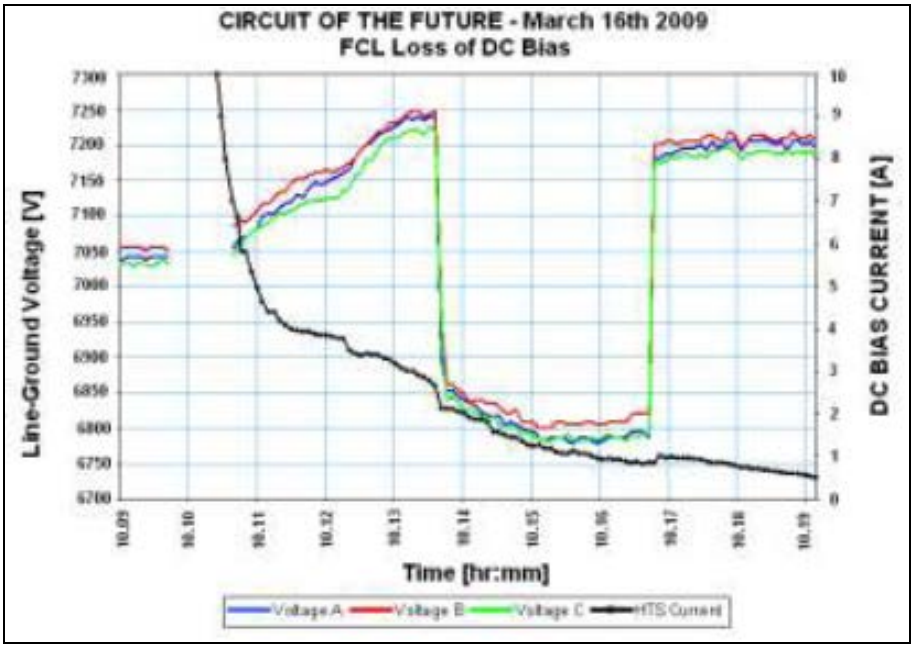

Source: Zenergy Power plc

6.3.1.4 Simulation Study of the Event

The PSCAD model shown in Figure 65 was adapted to simulate FCL interaction with the Avanti Circuit during the DC bias current loss and the resulting resonance phenomenon. The event was simulated by estimating the transient decay of the DC bias current and calculating the transient increase of the FCL inductance. As the FCL's DC bias current collapses, simulated FCL inductance shows increasing swings riding upon a quasi-exponential rise, as shown in Figure 66. The steady increase in inductance occurs as the operating point of the FCL's core swings over to steep slopes in the B-H magnetization curve due to the DC bias current loss. The increased FCL inductance creates a resonance condition with the 1.8 MVA capacitor bank resulting in a rise in bus voltage.

Comparison of the simulated and measured line to ground voltages during the event is shown in Figure 67. Good agreement of the simulated and measured results suggests that the Zenergy

Power FCL model is capable of closely reproducing the loss of DC bias current event and the resonance condition that followed.

Figure 65: Simplified PSCAD Model of the FCL Installed in the Avanti Circuit

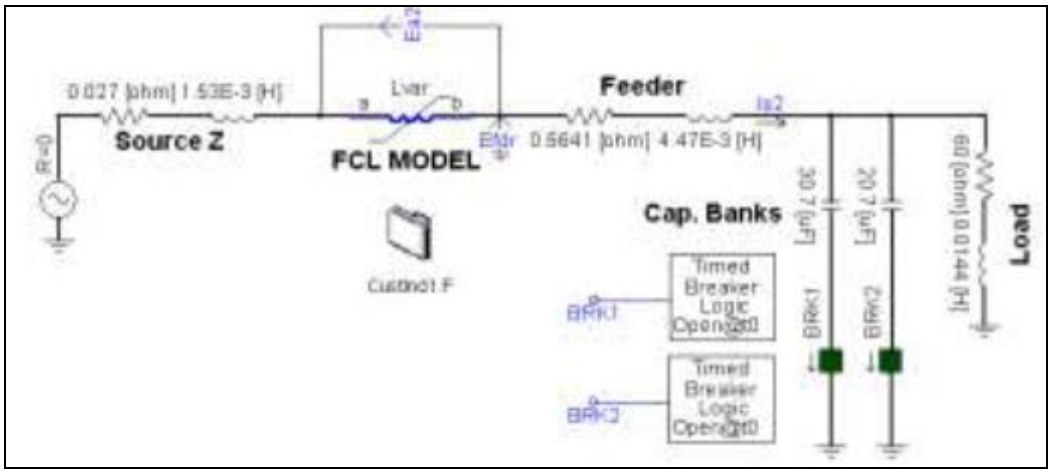

Source: Zenergy Power plc

Figure 66: Simulated FCL Inductance for the Loss of DC Bias Event

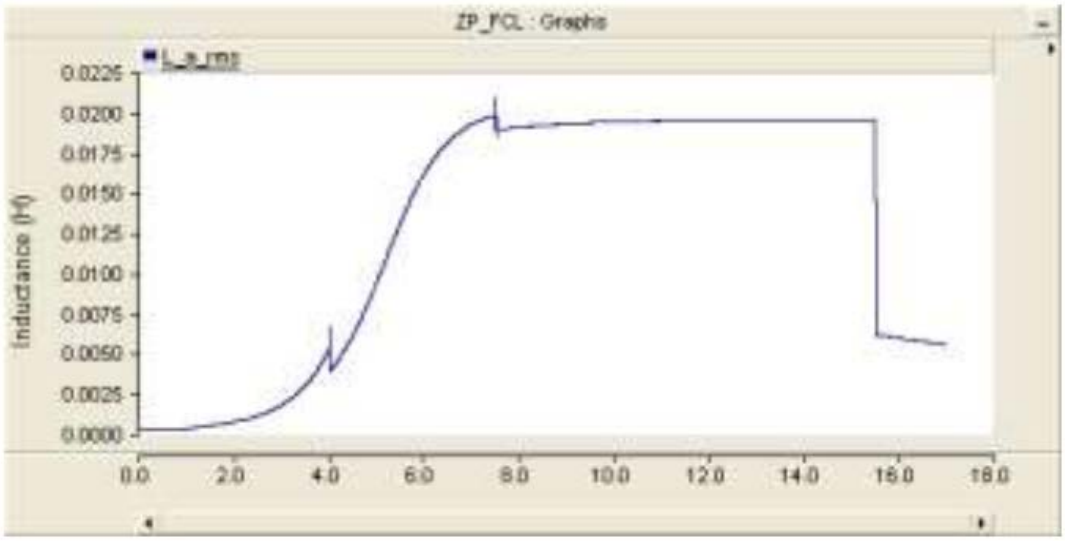

Source: Southern California Edison Co.

6.3.1.5 Recommendations for Resonance Suppression

i. Design

In the design process, simulation of the resonance should be conducted, including capacitor banks in the line where the FCL is to be installed at different loading conditions, to check for extraordinary events in the controller's logic. This entails an increased FCL inductance under de-saturation conditions.

Figure 67: Comparison of Simulated vs. Measured Line-to-ground Voltage for the Loss of DC Bias Event

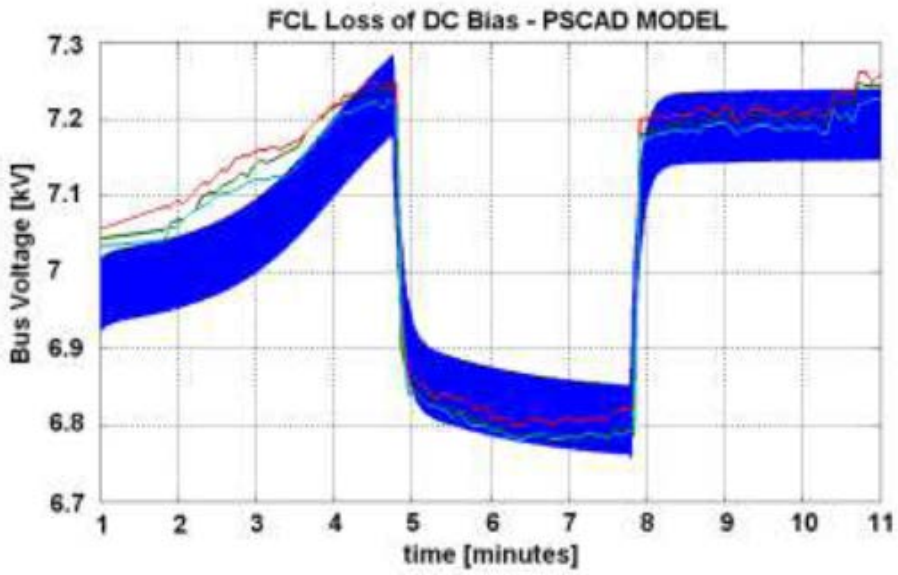

Source: Southern California Edison Co.

ii. Operational

The ideal protection against resonance in this case is to immediately bypass the FCL. Given that the event evolves relatively slowly, an automated switch that can operate on the order of seconds is adequate.

Fixed capacitor banks should be carefully evaluated, and if they are integral to the FCL installation, operational planning should account for their presence. This measure is recommended because if the automated bypass switch should fail to close, the capacitor banks could be disconnected automatically. A reactive compensation device, such as EPRI's solid-state STATCOM, should be a better alternative since it has the ability to regulate the circuit voltage within the design range. Lastly, base loading of the circuit should be increased, if operating conditions allow, because a more heavily loaded FCL is less likely to remain in a potential resonance condition.

6.3.2 Downstream Short Circuit Fault – Jan 14, 2010

6.3.2.1 Description of the Event

Prior to the fault event on January 14, 2010, the FCL was operating normally. The pre–event circuit load was approximately 100 A measured at the Avanti CB with system voltage approximately 12.1 kV near the fault. High winds were reported in the area of the overhead-line section of the Avanti Circuit, approximately 5.7 miles from Shandin Substation.

On January 14, 2010, at 9:58 am, a sequence of faults occurred on the Avanti feeder. The voltage data recorded at the load side of the FCL is shown in Figure 68. The data suggest the following scenario: The event evolved from a phase-to-phase fault, to a three-phase fault, to a temporary recovery, to a phase-to-phase fault, to another three-phase fault, ending with protection systems

clearing the line and fault. This very unusual, mostly symmetrical, multi-fault event occurred over a three-second period. Physically, the event was initiated by the overhead conductors of A and B phases slapping together during high wind conditions near the end of the Avanti Circuit. This phase-to-phase fault lasted about 250 milliseconds, when Phase C also faulted, thus evolving into a three-phase fault, lasting about half a second. The air insulation recovered its full dielectric strength for about one second, but then the conductors of phases A and B again arced to each other for about three quarters of a second. The arc was about to be extinguished at this time; however, Phase C also arced, becoming another three-phase fault. The event ended about a quarter of a second later when Phase B conductor separated and dropped to the ground, and the circuit was eventually cleared by system protection.

Figure 68: Voltages and Currents Measured Downstream of the FCL During the Multiphase Fault Event of Jan. 14, 2010

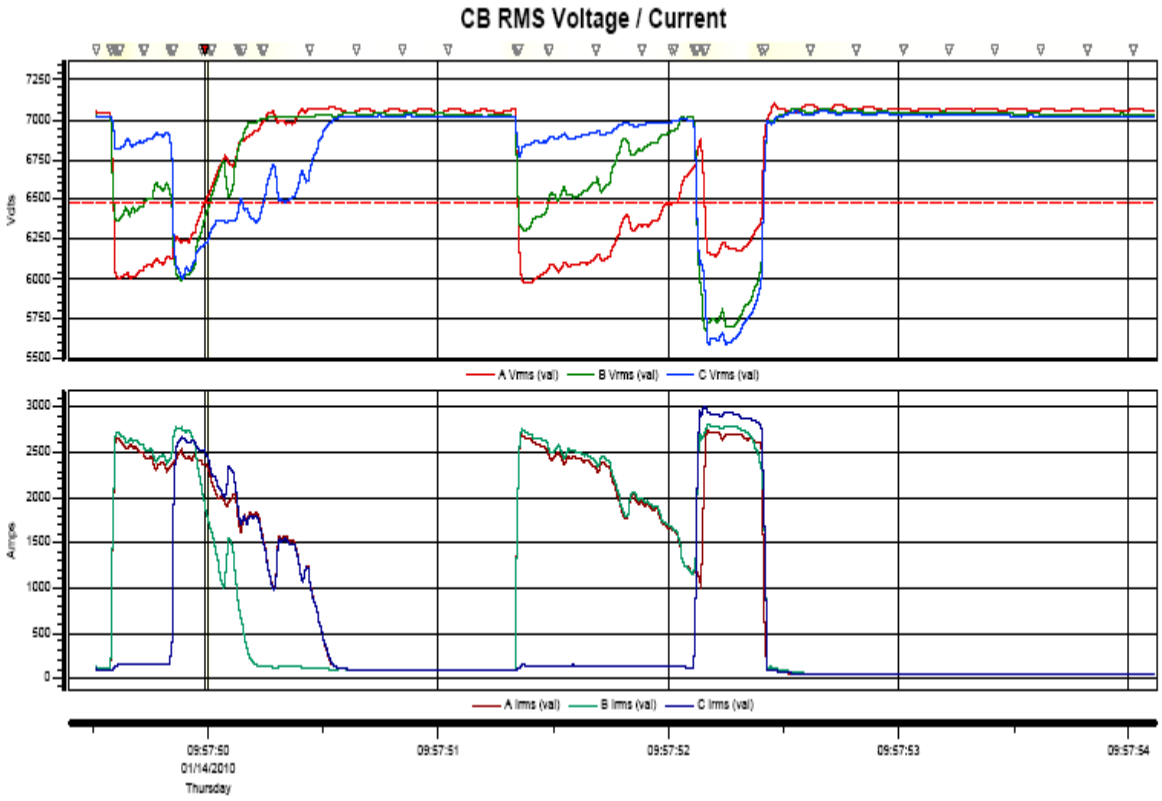

Source: Southern California Edison Co.

6.3.2.2 Simulation Study of the Event

The FCL performance during the fault event was evaluated using the Zenergy Power FCL PSCAD simulation model previously described. As a first step, the FCL model performance was verified by comparison with realistic test results obtained during the FCL's laboratory testing. The comparison of both simulated and real fault current clipping vs. the prospective fault current is shown in Figure 52. This comparison shows that the accuracy of the simulation model is satisfactory.

As the next step, the FCL model was embedded into a PSCAD model of the Avanti Circuit to perform a full-circuit simulation of the event. To resolve the difficulty of establishing the exact arcing impedances during the fault, the fault scenario was approximated by several linear segments of appropriate duration. Fault impedance for each segment was adjusted so as to generate the average fault current within the segment. PSCAD simulation results of the Avanti Circuit fault with the FCL bypassed are shown in Figure 69(a). Next, the FCL's bypass switch was opened and the FCL was introduced into the circuit, affecting the current flow. Since the FCL is a highly nonlinear device, during the normal state its impedance is very low; however, under fault conditions the FCL's inductance increases sharply. PSCAD simulation results of the fault event with the FCL in the circuit are shown in Figure 69(b).

Figure 69: PSCAD Simulation Results of the Multiphase Fault of Jan. 14, 2010

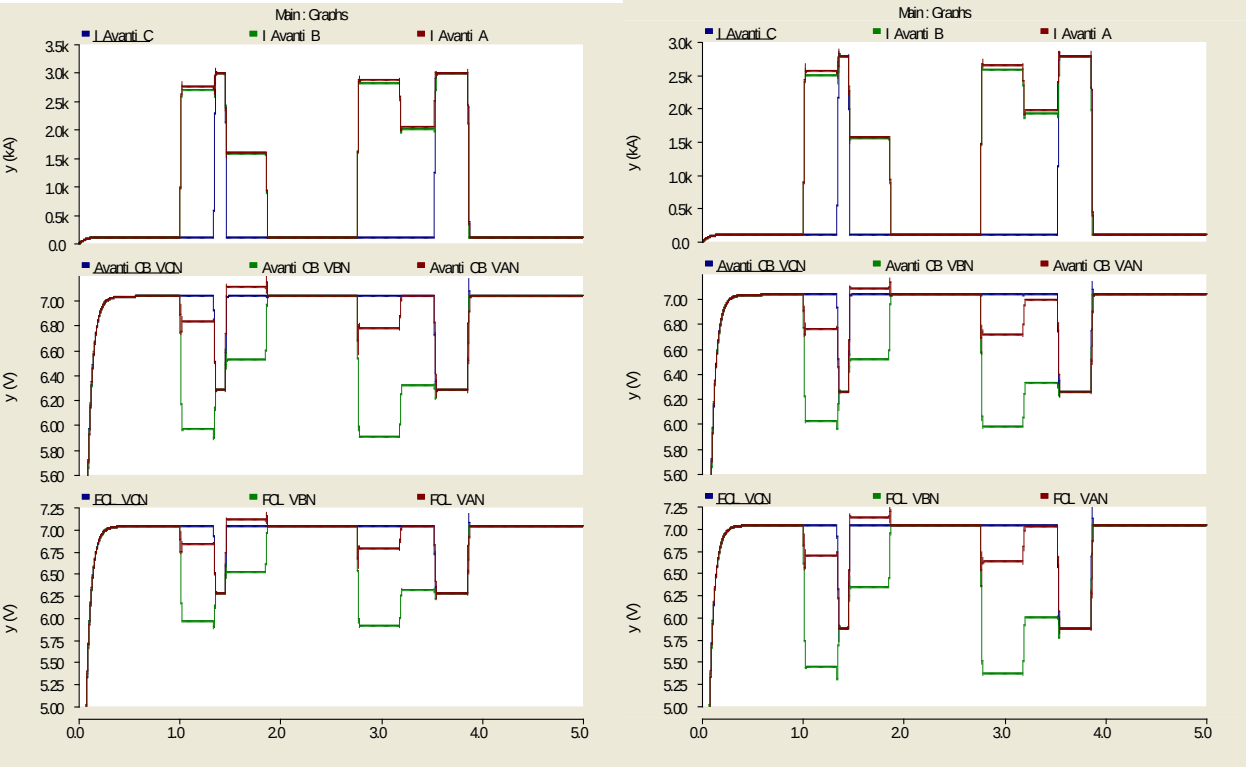

(a) FCL bypassed **(b) FCL active**

Source: Southern California Edison Co.

Comparison of the fault current levels for both cases, that is, with the FCL bypassed and with the FCL active, is summarized in Table 3. Clearly, during this sequence of events, the FCL operated as designed and limited the fault current. However, the prototype FCL was designed for clipping fault current up to 20 kA. Since the fault impedance was relatively high the fault current magnitude during the event was below 3 kA. For such current levels, the experimental FCL provided partial clipping as designed.

Another valuable observation was made regarding how the cryogenics and bias circuit responded during the fault. The measured performance is shown in Figure 70. The upper screen

shows HTS magnet current and voltage; the lower screen shows the line currents. The fault instant can be recognized by the sudden decrease in load current due to the CB clearing the affected branch. There was no noticeable change in the DC bias and it was not affected by the fault current, and no measurable effects on the cryogenics system, cold-head temperature or liquid nitrogen were observed.

Figure 70: Cryogenic System Behavior During the Jan. 14, 2010 Fault

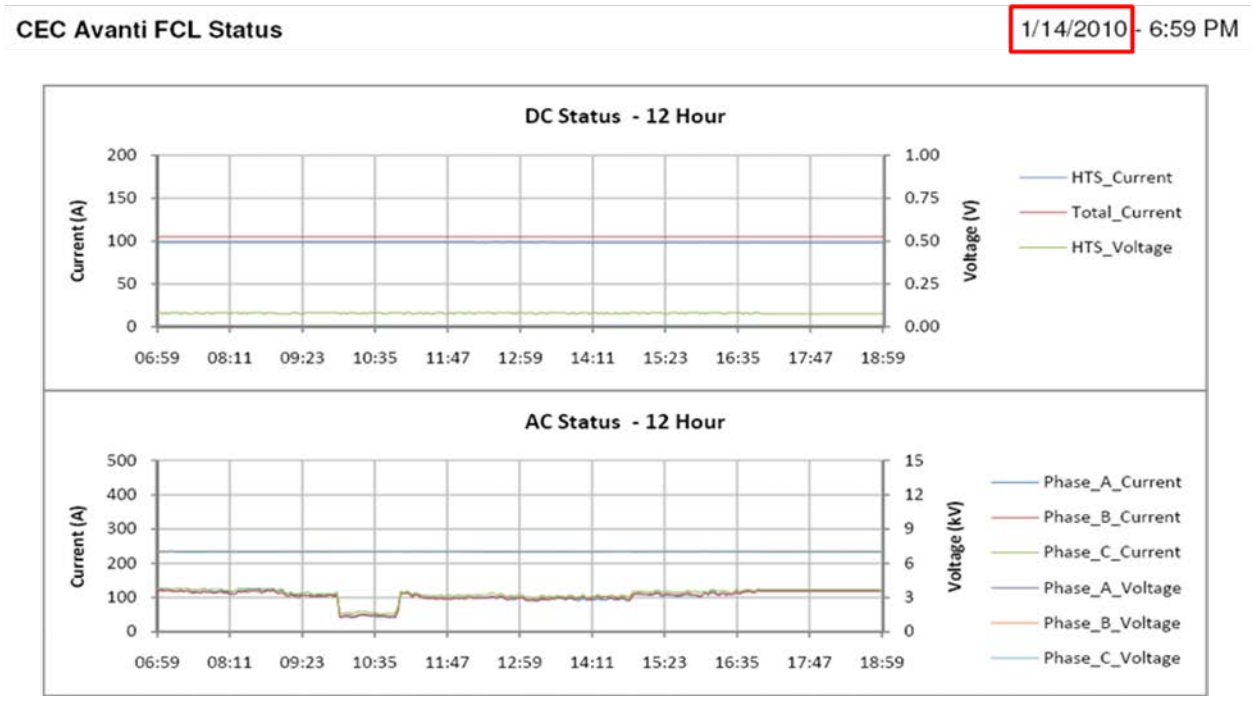

Source: Southern California Edison Co.

Table 3: Comparison of Fault Currents – FCL Active vs. FCL Bypassed

Segment	Active FCL	Bypassed FCL	% Clipping
F1	2554	2748	7.1%
F2	2782	2979	6.6%
F3	1568	1592	1.5%
F4	normal	normal	normal
F5	2643	2861	7.6%
F6	1968	2035	3.3%
F7	2782	2979	6.6%

Source: Zenergy Power plc

6.4 Summary

The prototype "Spider" saturable-core HTS FCL was installed by SCE on the Avanti "Circuit of the Future (COF)" in San Bernardino, California, for field testing in a "live," actual utility distribution feeder environment. The FCL was energized in March 2009, decommissioned in October 2010, and removed from Shandin Substation in December 2010. The Avanti COF is a dedicated 12.47 kV feeder serving actual residential, commercial and light-industrial customers of SCE. The objective of the demonstration was to obtain service experience with state-of-the-art fault current limiting equipment and operating procedures that could result in increased system reliability and lower costs. The FCL was integrated into the utility's SCADA system, and operated in real time to provide fault current protection to this distribution circuit of the California power grid.

The field demonstration provided a living laboratory to study the HTS FCL design, engineering, and operation. The experience gained from this demonstration has been invaluable to the evaluation and improvement of the FCL, contributing to a second-generation "compact" design, commercial sales, and migration to the development of a transmission-level HTS FCL.

CHAPTER 7:
Development of Zenergy Power Second-generation "Compact" HTS FCL

Despite the success of the "Spider" FCL design, the large size and weight of the air-dielectric, closed-core FCL architecture relative to its electrical power rating challenges the economic value proposition at distribution voltages. At the same time, the air-dielectric design complicates scaling-up the device to higher voltages. In light of these issues, Zenergy Power conceived an open-core FCL design that uses oil dielectric and conventional transformer design and manufacturing techniques to create a much smaller FCL with greater fault limiting performance and much higher voltage and power ratings. This new design is referred to as the "Compact" FCL.

7.1 "Compact" FCL Concept

The architecture of a single-phase Compact FCL is shown in Figure 71. The FCL is built around two I-shaped iron cores. The AC coils are wound in opposite polarity and are connected in series with the load. Two DC coils are wound on top of the AC coils around both iron cores. The DC coils are wound with first-generation HTS wire. The HTS coils form a strong magnetic field fed by a low-voltage, high-current DC power supply. Utilization of the HTS magnet allows reduction of the DC bias circuit resistance, which helps to achieve high bias current and high magnetic field intensity, and also to reduce the losses in the DC bias circuit.

Figure 71: The Architecture of a Single-phase Saturated-Core "Compact" FCL

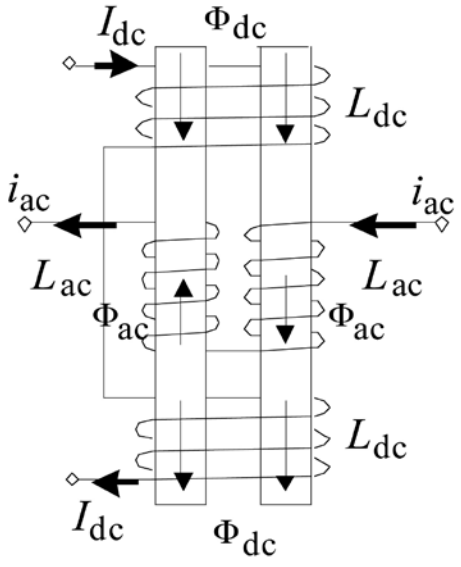

Source: Zenergy Power plc

The principle of operation of the device is as follows: The two HTS bias coils are axially aligned and constitute a Helmholtz coil, which generates an almost uniformly distributed magnetic

field in the cores with a higher magnetic field intensity than would be possible using only a single DC magnet with the same amount of ampere-turns. By regulating the DC coil current, the mmf-flux operating point of both cores is established in the vicinity of point B (see Figure 15), which is located in the saturation region of the core's B-H curve. As the AC line current flows through the AC coils, the core operating point is shifted. Due to the counter-directional winding of the AC coils, the AC induced mmf in one core reinforces the DC mmf, and weakens the DC mmf in the other core. Therefore, the operating point of one core shifts into a deeper saturation (Figure 15, point A), whereas the operating point of the other core moves towards a shallower saturation (Figure 15, point C), closer to the hysteresis knee point. In the normal state, the shift is designed to be small enough such that both cores remain in saturation; as a result their combined impedance is low, with less than 1 percent voltage drop across the AC coils.

When a fault occurs, the abnormal amplitude of the fault current is capable of driving the core with the counteracting mmf out of saturation and into the steep region C-D of the hysteresis curve. Here, the permeance of the desaturated core sharply increases, resulting in a considerable increase in coil inductance and, consequently, higher impedance, which helps to limit the fault current. Depending on the AC line current polarity, the coils alternate in and out of saturation to reduce the current in each half cycle.

The advantage of the proposed concept is that it has a rather wide potential operating range. There are several variables that can be adjusted, such as the iron core length, core cross-section area, number of AC coil turns, number of DC coil turns, and DC bias current. These parameters can be tuned to obtain the desired steady-state impedance Z_{min}, the percent of fault current reduction in the worst case, the faulted-state impedance Z_{max}, and the knee point current I_{knee} at which the limiting effect commences.

A unique feature of the compact FCL is that there is no physical interface between the AC side of the device (the line current and voltage in the circuit being protected) and the DC side of the device (the HTS DC bias coil and its associated power supply). The AC coils and buswork are located inside a dielectric tank, and the HTS DC bias magnets are placed in cryostats that surround the tank.

Another important design innovation is the use of "dry-type" cryogenics to conductively cool the HTS coil without the use of liquid nitrogen. Dry-type cooling allows the HTS coil to be cooled below the nitrogen freezing point, thereby improving the performance of the HTS wire and reducing the amount used in the magnets. The dry-type conduction cooling method also avoids the problem of having large volumes of liquid cryogens in confined spaces, creating potential pressure problems. Hence, maintenance is significantly simplified.

Section 7.3 below provides a more detailed description of the second-generation Zenergy Power HTS FCL This device has voltage, current and fault current limiting ratings similar to the "spider" HTS FCL, but is 75 percent smaller and only slightly heavier, representing a considerable saving in size, cost and maintenance requirements for the same or better electrical performance.

7.2 Comparison with Other Saturable Core FCL Designs

In the first generation spider-core FCL, each phase is constructed using dual CC iron cores as shown in Figure 72(a). A pair of ordinary AC coils is wound on the outer legs of the cores. The HTS DC bias coil is wound around the combined center limb. This has the advantage of requiring only a single HTS DC coil for the two cores. Another advantage is the closed magnetic path for both AC and DC coils, which facilitates relatively easy saturation of the core. A major disadvantage of this approach is the large volume and weight of the core. Another disadvantage is the large diameter of the HTS DC coil and, accordingly, the required length and cost of the HTS wire.

The structure of a saturated open-core FCL [56] is shown in Figure 72(b). This FCL uses a closed, strongly elongated "C" type magnetic core. This magnetic design provides a closed magnetic path for the DC bias flux, but an open magnetic path to the AC flux.

Figure 72: Saturated-core FCL Architectures: (a) "Spider" FCL; (b) Open-core

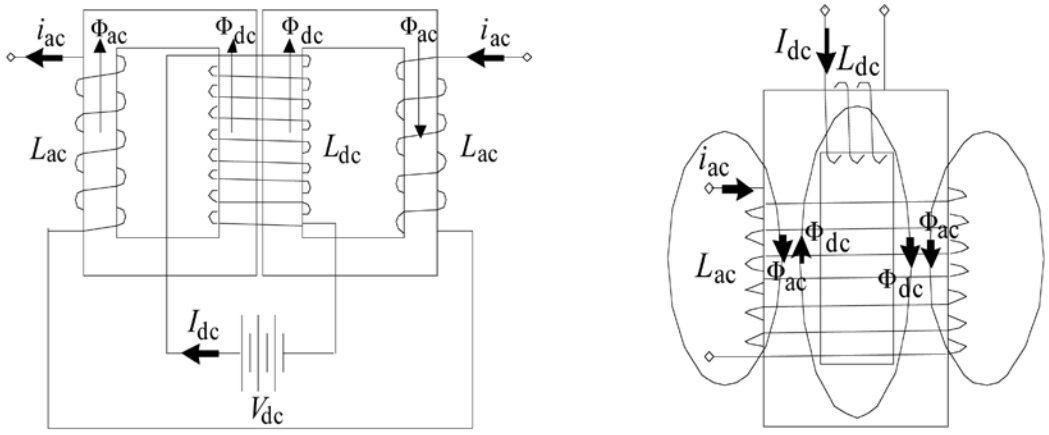

(a) **(b)**

Source: Zenergy Power plc (Rozenshtein et al. [56])

A clear advantage of this type of FCL is that the iron core has low volume and weight, owing to its narrow and compact shape. Moreover, the narrow diameter of the HTS DC coil results in shorter HTS wire length and, accordingly, lower cost. Furthermore, lower HTS magnet volume requires lower cooling power. Another important advantage of this FCL is the orthogonal arrangement of the DC and AC coils, which minimizes the AC-to-DC coupling.

The most significant advantage of the Compact FCL as shown in Figure 71 is that the I-cores have the lowest volume, weight and cost. Another major advantage is that the I-cores are well suited for oil-filled dielectric design. Thus, the Compact FCL can be adopted for high-voltage applications without over-sizing the device. The main disadvantage of the Compact FCL is the low-permeability magnetic path, which requires stronger DC bias mmf to saturate the core. Therefore, two HTS magnets of an appropriate diameter and two sizable cryostat units are needed. Comparison of these three devices is summarized in Table 4.

7.3 Distribution-Level "Compact" FCL Prototyping

A view of a three-phase Compact Saturable-core Reactor prototype FCL assembly is shown in Figure 73. A rectangular supporting frame design was used. The FCL is composed of six I-cores combined in a single bundle. An AC coil is wound on each core. A pair of AC coils is needed for each phase. In order to attain an electrostatic isolation sufficient for high-voltage applications, the cores are housed in an oil-filled tank. SF_6 gas may also be used as an insulating medium, just as it typically is used in circuit breakers and compact switchgear applications. The tank is placed inside the supporting frame to which the DC bias coils are also attached.

Table 4: Comparison of the "Spider," Open-core and Compact FCLs

	Spider FCL	**Open-core FCL**	**Compact FCL**
Core Volume	Large	Medium-Small	Small
HTS coil diameter	Large	Small	Large
Copper coil diameter	Small	Large	Small
Cryostat	Medium	Small	Large
Dielectric type	Air	Air	Oil

Source: Zenergy Power plc

Figure 73: Physical Structure of a Rectangular-frame, Three-Phase Compact FCL Prototype

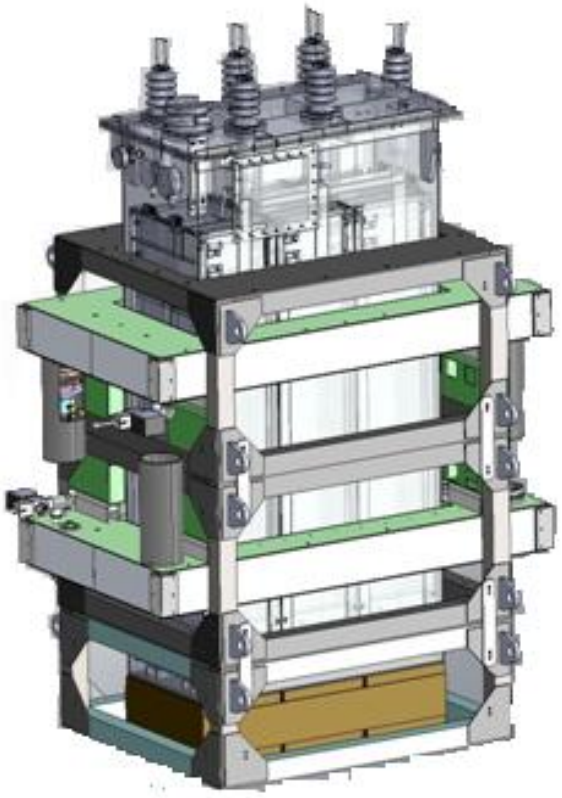

Source: Zenergy Power plc

The prototype Compact FCL's main specifications are as follows: line-to-line voltage 12.47 kV; line current 1.25 kA; prospective fault current 20 kA; line frequency 60 Hz; normal state voltage drop 1 percent; and fault current reduction 25 percent. The FCL uses an oil-filled dielectric design and cryogen-free, conduction-cooled HTS magnets, resulting in a reduced coil size.

A comparison of weight, size and cost between the first-generation Spider FCL and the second-generation Compact FCL designs with similar electrical characteristics is given in Table 5.

Table 5: Comparison of the Main Features of the "Spider" and Compact FCL Designs

	Spider FCL	Compact FCL
Iron Core Weight, lb.	52,000	67,000
Cost of Iron @ $3.00/lb.	$156,000	$201,000
FCL Size	19' x 19'	10' x 7'

Source: Zenergy Power plc

As a learning experience, several additional three-phase and single-phase full-scale prototypes for medium-voltage applications were built. The prototypes were constructed as modular units. The supporting frame was designed to hold the Helmholtz HTS coils aligned at their position. Together with the cryostat, the power supply and the control electronics, the structure formed a standard test bed. One of the advantages of the proposed FCL structure is that there are no physical interconnections between the AC coils and DC magnets. This allowed the tank with the AC coils to be lifted and removed from the frame and replaced with a differently designed AC coils module. By such an approach, the experimental FCL could be reconfigured as a single-phase or three-phase device with a different set of parameters. Four full-scale Compact FCL prototypes were designed, built and tested. The specifications of these FCLs are summarized in Table 6.

Table 6 shows all four of the compact HTS FCL prototypes that were built and tested. These prototypes have the same nominal 15 kV design voltage and 110 kV BIL rating, but differ in their steady-state AC current ratings, targeted steady-state AC current insertion impedance, and AC fault current limiting capability. The designed steady-state AC current levels ranged from 1,250 to 2,500 A (rms), and the targeted AC fault current reduction levels ranged from about 30 percent to more than 50 percent of a 25 kA potential steady-state fault current with an asymmetry factor yielding a first-peak fault current approaching 50 kA.

The compact FCL prototypes underwent full-power load and fault testing at Powertech Laboratories in July 2009 using essentially the same comprehensive test plan that was employed for the Spider FCL. All 118 separate tests were performed on the four compact FCL prototypes, including 55 calibration tests, 12 load current only tests, and 51 fault tests. In many cases, the measured performance exceeded expectations, and the test program fully validated both the performance potential of the compact FCL design and the efficacy of Zenergy Power's design protocol.

A particularly important result from the compact FCL testing program was the fact that the AC coils and the DC HTS coil exhibited very little electromagnetic coupling. The DC current in the HTS bias coil varied by only about 5 percent as the compact FCL was subjected to peak fault currents up to 30 kA. These results were typical for all of the compact FCL devices during fault current testing.

Table 6: Specifications of Prototype Compact FCLs

Parameter	Units	FCL #1	FCL #2	FCL #3	FCL #4
Line-to-Line Voltage	kV	12.47	12.47	12.47	13.8
Number of Phases	#	3	3	1	1
Line Frequency	Hz	60	60	60	60
Prospective Fault Current	kA	35	46	80	25
Limited Peak Fault	kA	27	30	40	18

Parameter	Units	FCL #1	FCL #2	FCL #3	FCL #4
Prospective Fault Current (symmetrical)	kA	20	20	40	11
Limited Symmetric Fault Current	kA	15	11.5	18	6.5
Load Current Steady-State	kA	1.25	1.25	1.25	2.5 – 4.0
Voltage Drop Steady-State Maximum	%	1	1	1	2
Line-to-Ground Voltage	kV	6.9	6.9	6.9	8.0
Asymmetry Factor	#	1.2	1.6	1.4	1.6
Source Fault Impedance	Ohms	0.346	0.346	0.173	0.724
Fault Reduction	%	25	43	55	41

Source: University of California – Irvine

Also, the steady-state voltage drop of the compact FCL typically remained low with increasing AC currents, and the AC power was very "clean" with total harmonic distortion (THD) levels well within the requirements of IEEE Std. 519-1992 [79].

The rectangular design of the experimental FCLs was adopted for the reason that rectangular shaped HTS magnets of an appropriate size as well as their cryostats were readily available and allowed rapid prototyping. The rectangular shape, however, is not the best choice for a practical device, because it requires more structural components. Considering the electromagnetic forces, a better structural form for a coil is a round shape. Hence, circular HTS coils, a circular supporting frame and a circular oil tank are more natural and easier to build. Therefore, a prospective compact FCL having a circular design was conceived.

The FCL evolution path to commercial product is shown in Figure 74. On the left is the first-generation Spider FCL that was tested, installed and operated in a commercially operating grid to verify performance and reliability. In the middle is the rectangular prototype Compact FCL, which was built and tested to validate a smaller and more efficient FCL. And on the right is the round Compact FCL for distribution-class applications that takes advantage of all lessons learned throughout the prototyping.

Figure 74: Path to Commercialization for FCL Prototypes

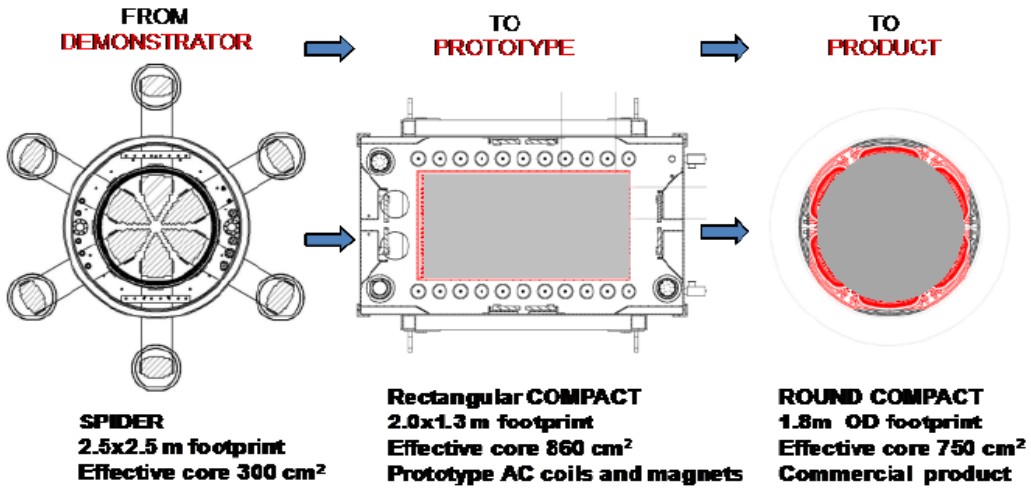

Source: Zenergy Power plc

A perspective view of a circular frame design three-phase compact FCL is shown in Figure 75. Such an FCL can be installed in a vault shielding it from the elements as well as from possible acts of vandalism. The auxiliary equipment such as the cryocoolers, chillers, power supplies and control electronics are installed in an adjacent control compartment having a safe access for maintenance personnel. Figure 76 shows the assembled three-phase distribution-level compact FCL.

Figure 75: Design and Layout of a Commercial 15kV-class Circular-frame Compact FCL Assembly

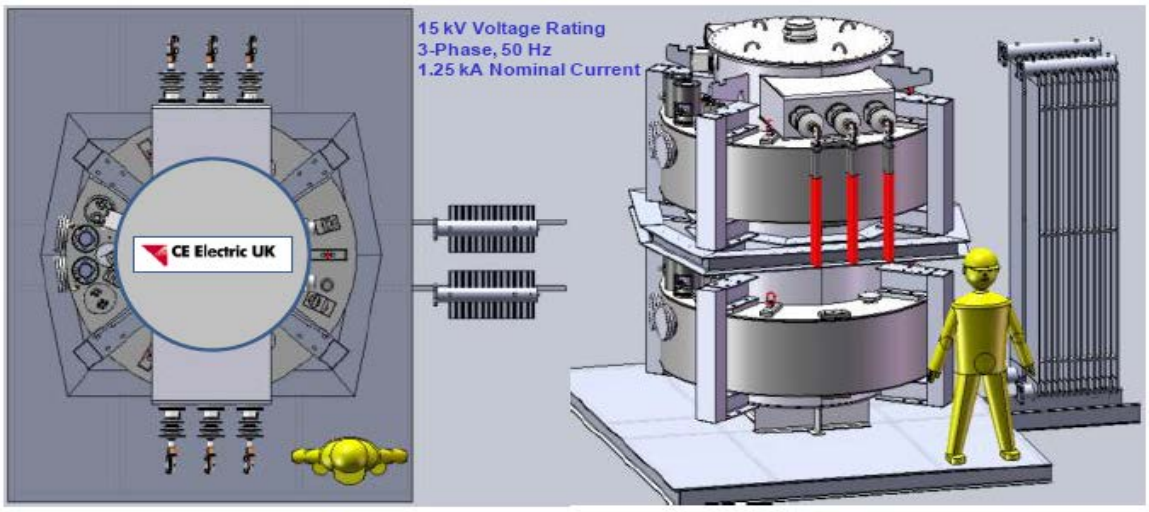

Source: Zenergy Power plc

Figure 76: Three-phase Distribution-level, 15kV-class, Compact FCL Prototype with "Dry-cooled" HTS Magnets Surrounding an Oil-filled Dielectric Tank with AC Coils

Source: Zenergy Power plc

7.4 Transmission-Level Compact FCL Development

A perspective view of a transmission-level single-phase compact FCL is shown in Figure 77. A high-voltage three-phase compact FCL can be built using a bank of three single-phase compact FCLs and installed in a substation as shown in Figure 78. Possible specifications of a prospective transmission-level compact FCL are summarized in Table 7. Such a device is feasible. Per a preliminary design, a single-phase FCL could require four HTS magnets. The estimated device dimensions are approximately 8.3 meters in length and 2.3 meters in diameter.

Zenergy Power has entered into an agreement with American Electric Power (AEP), Columbus, Ohio, to partner for the demonstration of a 138 kV three-phase FCL as a part of Zenergy Power's ongoing DOE-sponsored FCL development program. A single-phase 138 kV FCL prototype will be built and tested in 2011, and a three-phase FCL demonstration unit is slated to be built, tested and installed in AEP's Tidd substation located near Steubenville, Ohio in 2012. This device's specifications call for it to operate at 1.3 kA in the normal state, reduce an approximate 20 kA prospective fault by 43 percent, and recover instantaneously under load. The installation will be on the low side of the 138/345 kV transformer to protect the 138 kV feeder.

7.5 Summary

This chapter reported on the recent development of a second-generation "Compact" saturable-core FCL for medium-voltage distribution systems. This device is an evolution of the first-generation Spider FCL.

Figure 77: Perspective View of a Transmission-level Single-phase Compact FCL

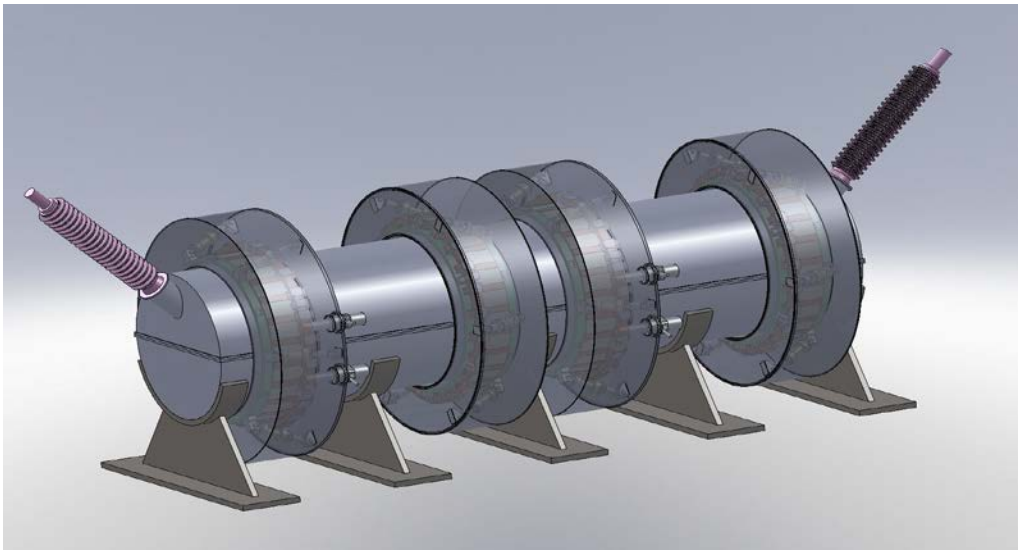

Source: Zenergy Power plc

Figure 78: Perspective View of a Compact FCL Substation Installation

Source: Zenergy Power plc

Table 7: Possible Characteristics of a Future Transmission-level Compact FCL

Parameter	Units	Value
Line-to-line Voltage	kV	230
Line Frequency	Hz	60
Rated Current (rms)	kA	2
Prospective Fault Current as Maximum Symmetric Fault Current (rms)	kA	63
Asymmetry Factor	#	2.75
Desired Limited Current (rms)	kA	52
Maximum Voltage Drop at Rated Current and Line Voltage	kV %	0.5 0.37
Prospective Peak Fault Current	kA	173
Percent Fault Limiting Capability	%	17.5
Line-to-ground Voltage	kV	132.8
Cryostat ID	m	1.34
Magnetic Core Volume	m^3	2.5
Magnetic Core Weight	kg	19,964

Source: University of California – Irvine

The compact FCL has several advantages, notably: reasonably small core size, completely passive design, the ability to limit first-peak fault current, sufficient fault current reduction, automatic recovery, and fail-safe operation. The decoupled high-voltage and cryogenic systems allow simplified oil-filled high-voltage design. This approach presents a relatively small heat load to the HTS magnet; therefore, cryogen-free, low-maintenance, and commercial off-the-shelf cryogenic equipment can be used.

The compact FCL prototype is the second superconducting FCL to be successfully tested for US utilities (the first-generation Spider FCL being the first). The compact FCL prototype is an advanced full-scale experimental model, which has helped to build confidence in the new technology. While the development and prototyping of distribution-level FCLs proved successful, the ultimate objective is to develop commercially feasible, full size transmission-level FCLs.

Research and development of FCLs has been conducted for many years. The compact FCL system described here is a promising, practical, efficient and economically feasible device that meets utility needs. The emerging compact FCL is a viable candidate to make a breakthrough into commercialization.

CHAPTER 8:
Lessons Learned

While the first-generation FCC demonstration program was a technical success, the objectives of the program, specifically with respect to the electrical performance of the FCC devices, were modest. The devices had a relatively low electrical rating, with maximum potential ratings on the order of 25 MVA, while the high duty-cycle ratings are significantly lower; and the overall costs, as might be expected for development prototypes, were high. The development and demonstration results clearly point out that the FCC technologies must be expanded to higher voltage and higher current capabilities in order to be commercially useful and cost-effective for high-power applications.

The cost effectiveness can be addressed in two directions. First, FCC technologies are being improved to reduce basic device manufacturing and maintenance costs. Second, the technologies are being improved to work reliably at higher voltages and currents. The latter consideration is arguably more important in terms of FCL technology cost-effectiveness and value proposition, especially in the short term, given the acute and growing needs of US utilities to mitigate the impacts of increasing fault currents on their systems, and the drawbacks of conventional solutions.

Higher voltage substations can often be more crowded and have fewer options for expansion, due to electrostatic clearance issues, and higher voltage components (switchgear, insulators, transformers, buswork, etc.) are exponentially more expensive than their low-voltage counterparts. Furthermore, it is becoming increasingly the case that large renewable power generators desire to connect to the electric grid via the high-voltage lines and substations, and high-voltage tie-lines have proliferated as more power is being wheeled from long distances and as grid interconnections become more necessary to improve system reliability and to better control power flows. Economic studies and performance models show that, at the current performance levels and price points, FCC technologies can be very cost-effective compared to major upgrade projects at high voltages.

The FCC demonstration project also clearly highlighted the shortcomings of the current Spider FCL with respect to reliability. While the Spider FCL performed satisfactorily while in active service in the grid, a large number of interventions were needed to keep the device completely operational. The demonstration suggested that cryogenics are a key shortcoming, and it is clear that cooling the HTS coil must be more reliable, less costly, and less intrusive. At a minimum, the cryogenics need to target “5-nines” reliability (0.99999 availability) with only a single, scheduled, short-duration annual maintenance outage. Even better would be extending the maintenance interval to two years or longer.

If an FCC is to be relied upon for protection (which is essential to the economic value proposition), it must be installed such that it can be bypassed and removed from service temporarily for maintenance, while fault currents will remain acceptable. This may be accomplished by splitting buses or otherwise configuring the electric grid in a manner that is

acceptable for short durations or at times of known reduced load, but which may not be optimal for long-term operation.

If such an alternate grid configuration is not acceptable or available, then the FCL must be designed, to the maximum extent possible, to allow essential routine maintenance, such as cryogenic maintenance, to be performed while the unit is energized, through measures such as locating the cryogenic coolers remote from the FCL itself. Also, the FCL must be designed to remain in the protected circuit indefinitely in the failed state, assuming the resulting higher voltage drop is tolerable, until replacement or repair can be arranged.

Ultimately, the FCC must be as reliable as a transformer of similar voltage class, and exhibit a similar maintenance profile. Then, even though major outages will occur, they will be infrequent and tolerable, as corresponding transformer failures are accommodated today. FCC developers and manufacturers are taking these reliability issues to heart and are aggressively modifying their FCC technologies for reduced maintenance requirements, and higher MTBF and lower MTTR metrics. They are also working with key industry partners and suppliers such as cryogenic cooler manufacturers to reduce the cost and improve the performance of enabling technologies.

One important weakness identified during the field test was that the nitrogen cooling system could be problematic for maintenance since it requires periodic maintenance of the cryostat, including drying the volume of, or replacing, the liquid nitrogen coolant. This may not be practical considering the fact that the unit is typically installed in a high-voltage area. However, this weakness was resolved in subsequent FCC designs by replacing the nitrogen cooling system with a liquid-cryogen-free, "dry-type" conductive cryogenic cooling system, which is commercially available off-the-shelf, resulting in a more reliable and robust system.

Overall, the Zenergy HTS FCL is considered as an important successful FCC development milestone, and it has already led to a scaled-up design for transmission-level applications at 138 kV. Further fast-paced and more advanced development of FCC technology to higher voltage levels is strongly recommended. This project has demonstrated the benefits of FCL technology, but has also shown that realizing those benefits will require accumulating significant operational experience in the field with beta hardware that is essentially the same as eventual series production items and extrapolating the FCC technology to considerably higher power levels.

While the private sector will probably achieve these objectives on its own, this trajectory will take too many years, most likely not until many US utilities have experienced considerable negative impacts from increased fault currents that they must manage with undesirable, conventional methods. Tremendous amounts of capital investment in general grid upgrades will have to be made on a fast-track basis in order to maintain required levels of reliability. Significant amounts of this investment are potentially avoidable and represent substantial value to ratepayers, if suitable FCC technologies are available to California utilities, and if California utilities are given reasonable incentives to deploy new technologies. The CEC and CPUC can perform a valuable service for California ratepayers and workers, and the economy in general,

if an accelerated program of high-voltage, high-power FCC technology is implemented under a consortium involving the CPUC, the CEC, California's electric utilities, and private industry.

CHAPTER 9:
Potential Applications of FCC Technology

This chapter suggests several possible high-value applications of FCL technology in the power transmission and distribution systems (see references [15] and [72]).

9.1 Fault Current Limiter in Substation Bus Tie

A substation bus tie ("coupling") is used to connect two previously separate substation buses, for the purpose of flexible and reliable operation. However, doing so can increase the available fault current, possibly beyond the capacity of the existing breakers and protection schemes. For this application, an FCL can be installed in the position as shown in Figure 79 [72]. In case of a fault, the FCL reduces the peak short-circuit current at the first current rise. The advantages of this application are: the parallel connection of the transformers (two systems) will result in an even distribution of the currents supplied; reduction of the required short circuit capability of the system; and reduction of the network impedance. No disconnection of the feeder transformers is required after tripping (bypass) of the FCL.

Figure 79: FCL Installation in Substation Bus Tie Application

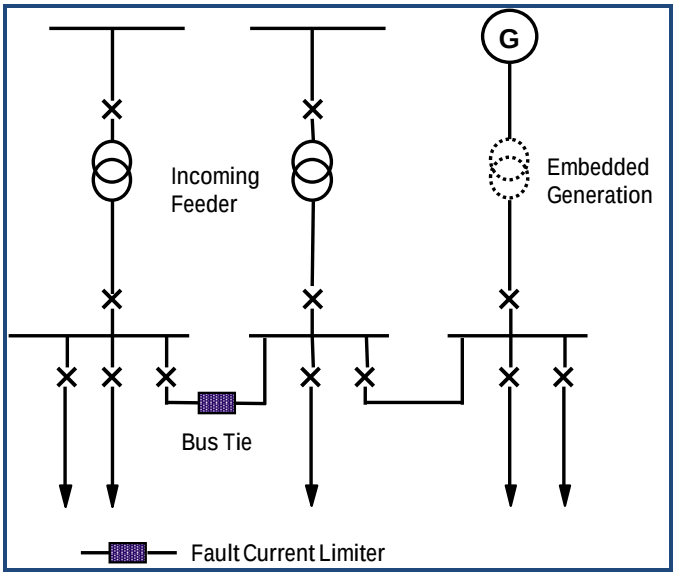

Source: CIGRE [72]

9.2 Fault Current Limiters in the Incoming Feeders

As an alternative to the previously described scheme, FCLs can be installed in each of the incoming feeders as shown in Figure 80 [72]. In case of a fault, the FCL reduces the peak short-circuit current at the first current rise. The advantages of this application are: the parallel connection of the transformers (two systems) will result in an even distribution of the currents supplied; reduction of the required short circuit capability of the system; reduction of the network impedance; and possibly smaller and less expensive FCLs than one large device.

Figure 80: FCL Installed in Incoming Feeders

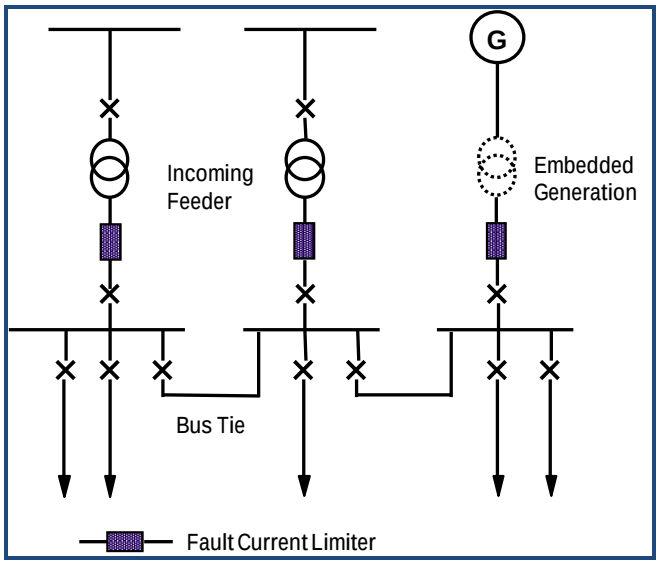

Source: CIGRE [72]

9.3 Fault Current Limiters in the Outgoing Feeders

Another approach is to install FCLs in the outgoing feeder positions as shown in Figure 81 [72]. In case of a fault, the FCL reduces the peak short-circuit current at the first current rise. The main bus must be capable of carrying the full fault current. The advantages of this application are: reduction of the required short circuit capability of the feeders on which the FCLs are installed; and reduction of the network impedance.

9.4 Grid Coupling

In the scheme shown in Figure 82 [72], two subgrids are fed via transformers from the 220 kV and 380 kV voltage level. The transformer capacity feeding into a 110 kV subgrid is approximately 1000 MVA taking into account the n −1 reliability criterion commonly used in utility applications. By connecting the grids with FCLs in this manner, the available surplus transformer capacity can be utilized without exceeding the admissible fault current level. This leads to the same technical benefits as in distribution levels, but with a considerable additional economic benefit by elimination of a 110/380 kV transformer and the associated switchgear components. In the specific case shown in Figure 82, this application removes the need for two transformers: the first one because of the introduction of the FCLs and the second one because a small increase in the loading capacity of the other transformers is permissible.

Figure 81: FCL Installation in Outgoing Feeders

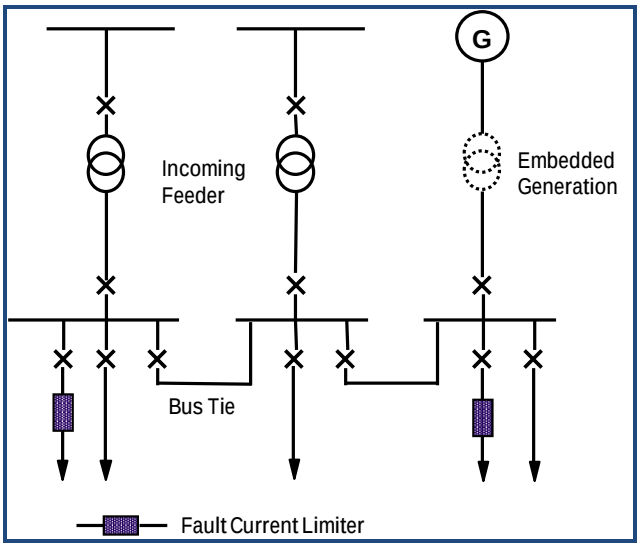

Source: CIGRE [72]

Figure 82: Two Sub-Grids Coupled by an FCL

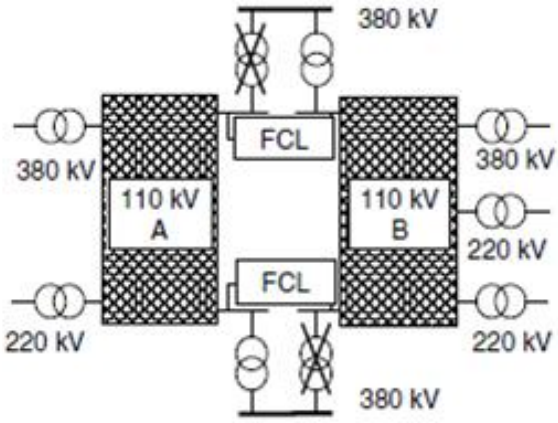

Source: Noe and Steurer [15]

9.5 Power Plant Auxiliary Power Feeder

Power plant auxiliary systems are usually connected to the power plant generator via a transformer. In general this will be a location with high short-circuit capacity because of the vicinity to the power plant generator. Hence, an FCL should be inserted at one or more of the points as shown in Figure 83 [15].

The main advantage of the FCL in this application is that the energy of the fault arc is reduced significantly, which means that additional measures to protect against arcing faults may no longer be needed. Savings can also be obtained from reduced stresses on switchgear

components, mainly at the medium-voltage level, and from the possibility of using cables or conductors with reduced cross section. Because of the fault current limitation it would no longer be necessary to use separate cables for each phase, resulting in much faster and cost-effective cable installations.

Figure 83: Location of FCLs in Power Plant Auxiliary Systems: (a), (b) Medium Voltage; (c) Low Voltage

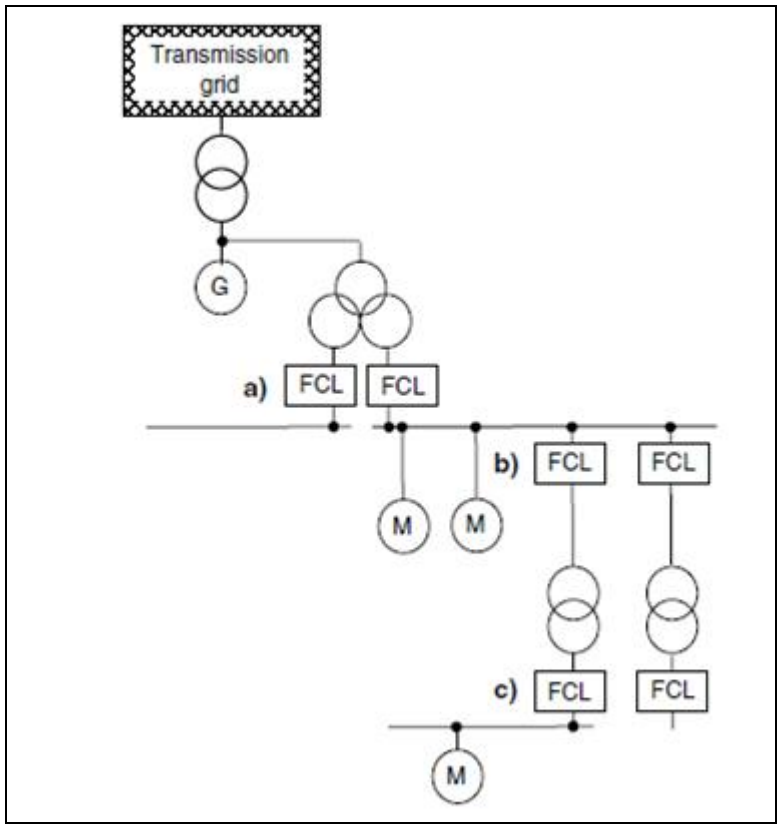

Source: Noe and Steurer [15]

CHAPTER 10:
Installation of the Zenergy Power HTS FCL

10.1 Site Preparation to Accommodate the FCL

As there were no industry-accepted standards for FCL testing, the National Electric Energy Testing Research and Applications Center (NEETRAC) in close collaboration with several of its member utilities, including SCE, developed a detailed FCL test program based on Institute of Electrical and Electronics Engineers (IEEE) and Conseil International des Grands Réseaux Électriques (CIGRE) standards for transformers and reactors.

The following measures were taken in order to test the FCL for acceptance by SCE and to prepare for the FCL's installation at the site.

10.1.1 Pre-installation High-Power and High-Voltage Testing

The FCL was first subjected to heat runs at full prospective normal load current and full DC bias current to verify the maximum temperature rise of the AC coils and the HV terminations. All measurements were within the limits specified in IEEE Standard C57.16-1996.

A total of 65 separate tests were performed at PowerTech Labs, Vancouver BC, including 32 full-power fault tests with first peak fault current levels up to 59 kA at rated voltage. Fault tests included individual fault events of 20-30 cycles duration, as well as multiple fault events in rapid sequence (to simulate automatic re-closer operation) and extended fault events of up to 82 cycles duration (to simulate primary protection failure scenarios).

The FCL was tested under full lightning impulse for:

- One reduced (1.2 x 50 μs) full wave – 50 percent or 55 kV peak wave
- One full (1.2 x 50 μs) wave – 100 percent or 110 kV peak wave
- One reduced chopped wave – 50 percent or 60 kV peak wave (chopped at 2 μs)
- Two full chopped waves – 100 percent or 120 kV peak waves
- Two full (1.2 x 50 μs) waves within 10 minutes after the last chopped wave

10.1.2 On-site Commissioning Test

Continuity and insulation resistance measurements were performed to verify that the device's internal components were not disrupted during shipping. Source-side and load-side bushing terminations were measured separately.

Commissioning tests at the site consisted of coil resistance, power factor, and megger measurements of all phases. These measurements were performed as a safety and reliability check every time work was conducted in the HV compartment to verify that the HV insulation had not been disrupted. The change of the FCL's insertion inductance as a function of the DC

bias current was also measured when the cryogenic system was first energized and de-energized.

10.1.3 Special Bypass Switch

To help assure service reliability, an innovative FCL bypass/isolation switch conceptualized by SCE and custom built by a leading circuit breaker supplier was installed. The design includes a three-phase pad-mount device with fixed input and output elbow connections for both line and load sides of the circuit. The device has two sets of elbow connections for insertion of any three-phase device (device input & device output). On the FCL itself there are three independent switches which can be operated either manually or remotely to open and close the vacuum bottles on the device-input and device-output connections, and a switch to control the bypass (or parallel the device-input and device-output) connections, as depicted in Figure 84.

The purpose of the bypass switch is to easily and quickly reconfigure the electrical arrangement consisting of the source transformer, the Avanti Circuit, and the FCL without the need to take a circuit outage.

The bypass switch has redundant controls and can be programmed to operate either in automatic mode, via remote control, or manually under local control (overriding the remote control for safety reasons). Physically the bypass switch is similar to a pad-mounted gas switch.

Figure 84: Bypass Switch for Zenergy Power FCL Installation

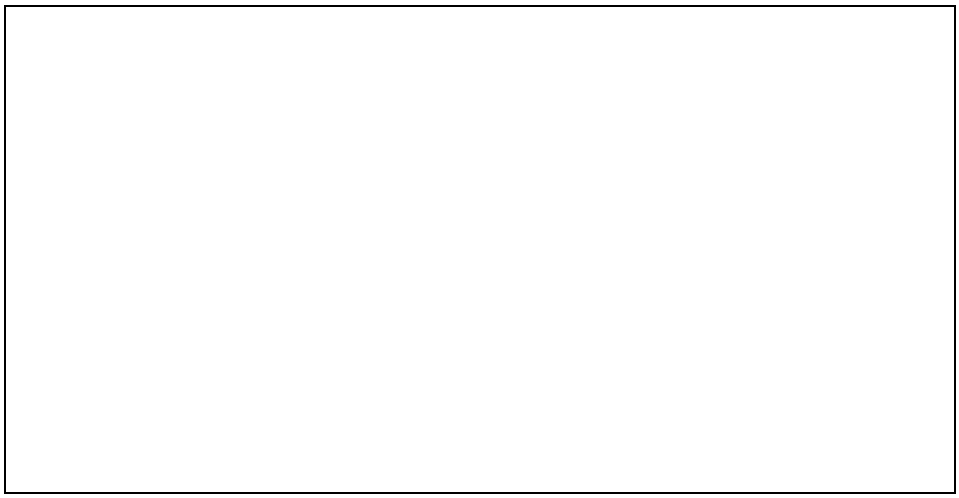

Source: Southern California Edison Co.

By means of the bypass/isolation switch the FCL can be connected in series with the source only, thus applying 12 kV to the FCL's AC coils, but without any load current flowing through the unit. A second arrangement connects the FCL in series with both the source and the load, which is the normal mode. The third arrangement completely isolates the FCL from the SCE system.

10.1.4 Civil Engineering

Seismic modal analysis of the FCL unit was performed by the manufacturer to determine any structural requirements necessary to withstand a 0.5 g, zero-period acceleration. Finite element

modeling and spectrum analysis up to 40 Hz with 2 percent damping were performed to verify that stresses and deflections were limited to within the allowable values, per IEEE Standard 693 [78].

SCE's civil engineering group was consulted to determine the best option for the physical installation of the FCL and to design the anchorage and stress release for the electrical connection according to the estimated reaction forces.

One alternative considered for the foundation was to use railroad ties over the existing crushed gravel in the substation's yard. Another option was to build a traditional concrete foundation to ensure that the FCL would remain level in seismically active area. The civil engineering team's recommendation was to set the FCL on compacted and leveled crushed gravel without any additional support because the FCL's enclosure is welded to steel I-beam skids.

10.1.5 High Voltage Connections and Grounding

The next element in the site preparation was to interface the high-voltage (HV) power terminations allowing the FCL to be easily connected to the circuit via the bypass switch. Elbow terminations were selected. The advantage here is that elbow connection at 12 KV would reduce cost and allow dead-front installation as opposed to live-front installation, which would entail costly civil engineering work to enable overhead installation.

Dead-break pre-molded cable connectors penetrating the FCL's enclosure three feet above ground level were installed for the 12 kV cable connections from the FCL to the bypass switch. This facilitated the physical connection and disconnection of the FCL and also eliminated cable splicing. The connector ratings are 25 kV class, 125 kV BIL, 900 A continuous, and 25 kA momentary. Stainless steel flanges were specified for these connectors to reduce induced eddy currents. The flanges and cable shields were grounded to the FCL's common grounding circuit, which in turn was connected to the substations ground mat.

10.1.6 Auxiliary Power

The SCE and Zenergy team worked together closely to define the auxiliary power needed to supply the FCL's electrical load. First, the most practical voltage to use was determined. Then the total power requirement for the FCL's peak load scenario was calculated. This reduced the cost and additional time requirements should the device control voltage need to be at a non-standard voltage value that is not typically supported at SCE substations.

The available voltage at the site was 120/240 volts, three-phase delta, and the FCL's low-voltage components were designed accordingly. To meet the FCL's 100 kVA requirement, the site's station light and power were upgraded, allowing the FCL to operate without affecting the substation's normal load. A 100A, three-phase circuit breaker was installed as a dedicated source for the FCL power. Six hundred feet of 2/0 copper conductor were pulled from the AC panel to a connection box next to the FCL.

10.1.7 Noise Ordinance Compliance

A local city ordinance allows no more than 55 db total sound energy emitted during the daytime and 45 db at night, as measured at the perimeter of the substation. Sound

measurements with the unit both on and off were performed. To comply with the stated limits, the FCL was sound insulated to better contain the sound emission of the compressors and cold heads. The FCL enclosure was also oriented so as to reduce the noise projected to the closest neighbors.

10.1.8 Connection to High Voltage Side

The design of the HV connection, dependent on the voltage class of the FCL, should be carefully discussed before the test unit is built for field demonstration. Initially Zenergy Power had planned to have overhead potheads installed for the HV interconnection, but SCE provided timely input to change to a better concept. SCE suggested that the input and output be equipped with 15 kV-class elbow connections. The resulting advantage was that elbow connection at 12 KV reduced the cost of installation and provided quicker and safer dead-front connection and disconnection, which was done more frequently because of the development nature of this project. In contrast, pothead/live-front installation would have necessitated additional costly civil engineering work to enable a safe overhead installation and more time to make the actual connections.

For future demonstration units the interconnection means should be carefully discussed with the host site to determine the optimal connection method.

10.1.9 Metering and Interconnection Cabinet

This interconnection cabinet was not part of the original installation, but was added later for monitoring purposes. The location where terminal blocks were added to provide 3-phase output voltage was limited to the side bypass alarm cabinet.

It is highly desirable to have relay-class PTs and CTs installed on both the input and the output of the FCL device, as illustrated in Figure 85. This makes possible the installation of digital fault recorders and power quality (PQ) instrumentation on the input and the output of the device, operating at the required bandwidths to monitor the expected transient events and to provide stand-alone high-speed PQ monitoring. This arrangement would allow the utility to capture fault profiles before and after the device operates, producing more accurate data retrieval for analysis and validation of the unit's operation.

The secondary of the monitoring voltage and current transformers will need to be in a weather-resistant enclosure mounted on the outside of the FCL unit, giving unrestricted safe access to utility personnel. An auxiliary 120 V AC outlet should also be made available in this cabinet.

Figure 85: Installation of Voltage and Current Monitors for the Zenergy Power HTS FCL

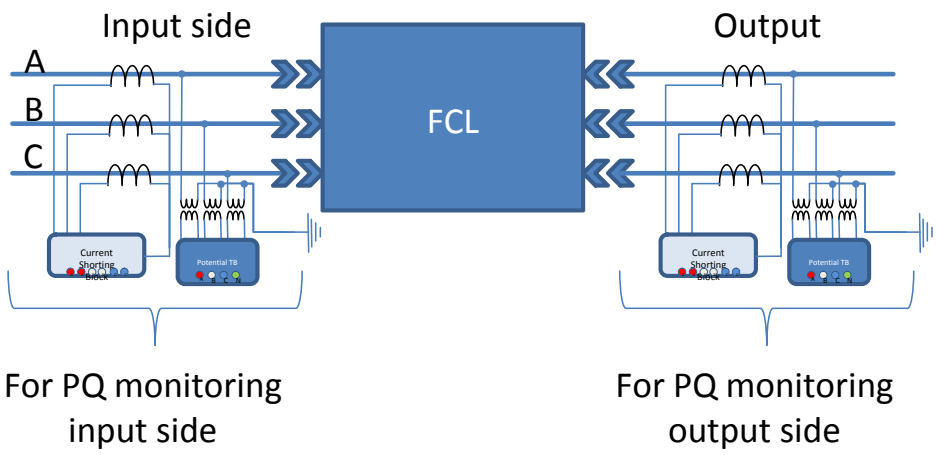

Source: Southern California Edison Co.

10.1.10 Communication Interconnection Point

For alarms and possible remote control (not used by SCE in this project), there should be some communication means to provide a secure and accessible point from which the utility can receive alarms and data acquisition system signals, if needed by operations personnel. During the FCL field test, one single alarm point to the control screen at the control center was necessary. It was set up to provide an alarm to the operator in case of an FCL abnormal condition.

10.1.11 Bypass Relay and Alarm Cabinet

As part of the operations requirements, the host utility at minimum should receive a single bypass condition alarm to safely isolate the FCL device from service and generate other appropriate alarms accordingly. This alarm should be in the form of a latching relay to maintain the condition until an operator can investigate the event. The bypass switch can also be automated to expedite isolation of the device during abnormal conditions.

CHAPTER 11:
Summary and Recommendations

11.1 Summary

The objective of this research project was to evaluate Fault Current Controller (FCC) technologies, also called Fault Current Limiter (FCL) technologies, through targeted development efforts and field trials at a California utility. Two different types of FCCs, one solid-state type and one saturable-core type, were selected for the development and field demonstration. After three years and 9 months of teamwork, the project is complete, from conceptual designs, to prototyping, to laboratory tests, to field trials and data evaluation.

From the earliest stage of the FCC development work, an important guideline was to "design for the test": given that the primary project objective was to be able to perform a comprehensive field test at a utility site, every aspect of prototype design was examined to ensure the ability to monitor and collect the necessary data in the field installation. Equally as important, significant efforts were dedicated to the development of the test plans that would be acceptable to SCE and workable for both the developer and utility teams. Zenergy worked closely with NEETRAC and several of its member utilities, including SCE, and developed a detailed FCC test program based on IEEE and CIGRE standards for transformers and reactors (the most applicable standards extant). EPRI/Silicon Power created their plan based on ANSI C39.09-1999 and ANSI C37.06-2000 standards, covering the entire spectrum of possible tests that need to be carried out on solid-state equipment, including component-level factory tests, system-level factory tests, acceptance tests, and system field tests. Many technical issues related to laboratory test and field test interface were resolved during a series of meetings with knowledgeable SCE engineers who provided valuable design and test guidelines. Both Zenergy and EPRI teams developed comprehensive test plans, which provided invaluable design and test guidelines and protocols for the field trials.

11.2 Development of a Solid-State Current Limiter

The Solid-State Current Limiter (SSCL) was developed by EPRI/SiliconPower Corp. The SSCL employs a modular and scalable design intended for 12 kV-class applications, but potentially applicable to a range of voltage classes and fault current ratings. The advantages of the emerging SSCL approach are: immediate recovery after a fault, no voltage or current distortion, no cryogenics, low losses and reduced size and weight. However, voltage sharing to maintain all the SBBs under the rated blocking voltage under dynamic conditions will likely be the key technical challenge for transmission level applications where the voltage level is above 100 kV.

The major technical issues with the SSCL design have been resolved and the detailed specifications of the system have been completed. One of the lessons learned from the first-generation SSCL was that the auxiliary circuit was the cause of many timing problems and control complications, requiring a multi-channel, high-voltage, isolated charging power supply for acceptable operation. This increased the SSCL cost and did not provide the desired level of

operational reliability. Therefore, in designing the second-generation SSCL, EPRI/Silicon Power opted to remove the auxiliary thyristors and resonant current-shaping inductor. Instead, a simple capacitive snubber was fitted to soften the main SGTO hard turn-off.

According to design predictions, the system size is estimated to be about 6.5'x12'x12' and weight about 62,000 lb. with oil cooling. These specifications are considered to be acceptable for a unit with the stated performance parameters.

The second-generation, single-phase SSCL was constructed under the scope of a subsequent research effort, separate from this Energy Commission-funded project. As of this writing, the results of the SSCL hardware design and elemental testing are encouraging, and the prototype underwent testing at KEMA Powertest Laboratories, Chalfont, PA, in May 2011. The SSCL had successfully passed the normal state testing at 15 kV and 1200 A, and successfully reduced a 23 kA prospective fault current to 9 kA. In the near future, construction of the full-size three-phase 15 kV, 1.2 kA SSCL for a 23 kA fault current rating will be initiated. This will include an extension of the existing design by duplication of the already tested power stack. Some additional tasks to be performed are to extend the control from a single-phase to a three-phase system; include additional diagnostics; design a full-size three-phase thermal management system; and build a full-size enclosure. Then the complete SSCL will be field tested by a host utility.

The EPRI/Silicon Power development team identified some thermal management issues during the simulation tests on their initial design. An improved system design was completed, and the major technical design challenges, particularly an improved thermal management system and more robust control architecture, have been resolved. However, the resulting increase in projected costs to build the prototype exceeded the available project budget; thus this FCC technology did not advance to the laboratory test and field demonstration stages under this program. EPRI continued with their development efforts at a later date, with additional funding from internal and other sources.

Notwithstanding the initial development setbacks, the EPRI/Silicon Power SSCL represents a potential cost-effective solution to the rapidly rising available fault currents seen in utility systems. One advantage of this type of FCC is the flexibility to be interrupting (i.e., act as a solid-state circuit breaker in addition to limiting fault current levels) or non-interrupting (fault current limiting only, coordinated with existing breakers and protection schemes). Furthermore, the SSCL may be used to limit the current of high-temperature superconducting cables, enabling the use of smaller cable sizes. It also has the unique capability of limiting inrush currents, even for capacitive loads.

11.3 Development of a Saturable-core High Temperature Superconducting Fault Current Limiter

The first-in-its-class 15 kV saturable-core type High Temperature Superconducting Fault Current Limiter (HTS FCL) prototype was designed and built by Zenergy Power Inc. It underwent successful laboratory testing, and was connected in the Southern California Edison Co. (SCE) Avanti Circuit of the Future for field demonstration. The HTS FCL was energized on

March 9, 2009 and decommissioned October 2010 after successfully completing its field testing period. This superconducting FCL was the first to be placed in commercial service in the United States [81].

This report presents the design, testing, and application issues as well as a systematic approach to modeling the electrical behavior of this type of fault current limiter. The derived computer model provided an excellent tool for predicting the overall fault current reduction of a saturated-core HTS fault current limiter. The model was useful in designing and operating an innovative distribution-class 15 kV saturated-core FCL.

The important results of this project were the development of the simulation model, design tools, operations and maintenance experience gained, and valuable protocols for the design, installation, control, monitoring, and employment of FCLs in an electric power system.

Also Zenergy Power and SCE have gained valuable experience in:

- Designing, building, installing and operating a fault current limiter in the electrical grid including integration with the SCADA system.
- Operating an HTS FCL in real-world conditions through all four seasons.
- Learning to address unplanned events, such as loss of station power and loss of FCL bias current.
- Observing the performance of the FCL as it responded to real fault events.
- Understanding the requirements of preventive maintenance, improving maintenance procedures and reducing their costs.
- Turning lessons learned into design improvements for future FCL devices.

The FCL performed well throughout the field demonstration, but several significant modifications were made in collaboration with SCE. Significant observations from the demonstration project include:

- The FCL's enclosure environmental conditions must be maintained within a narrow band to maintain the reliability of the control and monitoring instrumentation, cryogenic refrigeration, and DC power supply equipment. Additional air conditioning was installed in the FCL enclosure to meet hot-day cooling requirements.
- Air-cooled cryogenic refrigerators were satisfactorily employed (with sufficient enclosure air conditioning), but water-cooled cryogenic refrigerators may be more robust in the field.
- A sub-cooled liquid nitrogen re-condensing cryogenic system was successfully employed. Zenergy Power's current FCLs will use a "dry-type" conduction-cooling cryogenic system free of liquid cryogens, which is more reliable and easier to maintain.
- The FCL control system was able to shut itself down in an orderly and safe sequence under loss of station power events. Several substation blackouts were experienced

during the field trial period. The FCL is capable of automatically restarting when station power is restored, including the restoration and stabilization of cryogenic refrigeration, but this feature was disabled for safety purposes.

- A UPS was installed to provide control, instrumentation and DC bias current for up to two hours during station outages.
- While multiple channels for monitoring the FCL's systems and overall condition were provided, SCE desired a "watch-dog" monitoring system that provided a "Go" (all systems normal) or a "No-Go" (some system off-specification) with an automatic bypass switch to remove the FCL from service in the event of a "No-Go" condition.
- The FCL control system was successfully integrated through a secure Ethernet connection into the SCE SCADA system; a secure physically separated and independent MODBUS control scheme enabled secure, real-time monitoring and operation from the SCE Control Room.
- If the FCL is being relied upon for system protection, the system must be configurable (through temporary buss-splitting, for example) to control fault duty levels in the event the FCL must be removed for maintenance or repair.
- Saturated-core FCLs, seen as almost transparent inductors during steady-state conditions and large inductors during fault conditions, must be evaluated for compatibility with existing circuit resistance and capacitance values to ensure voltage stability on the protected circuit (see Zenergy's 2010 IEEE PES T&D paper [68]).
- The effects of saturated-core FCLs on circuit breaker transient recovery voltage must be considered to assure adequate rating of circuit breakers and determination of maximum allowable interruption currents (see Zenergy's paper presented at the 21st International Conference on Electricity Distribution (CIRED) [66]).

The research in this period has led to the successful field demonstration of the Zenergy Power HTS FCL, marking a milestone event in the history of FCL development in the United States. The experience gained from the research led to a more reliable controller, a dramatic reduction of the FCL's size and weight, and the replacement of liquid nitrogen cryogenic refrigeration by a low-maintenance dry cooling system.

The Zenergy Power HTS FCL was first laboratory tested successfully against FCL specifications and test criteria developed by US utilities, including the host utility Southern California Edison. The HTS FCL was then successfully demonstrated in actual field operation. The HTS FCL unit is rated at 15 kV, 1200 A, 110 kV (BIL), steady-state insertion impedance < 1 percent, and a fault current reduction capability of 20 percent of 23 kA prospective fault current.

The first-generation Spider-core HTS FCL had a dry-type transformer (air dielectric) structure, total overall dimensions of about 19'x19'x7', and weighed approximately 50,000 lb. The second-generation "Compact" HTS FCL that followed from this research employed innovative core architecture and oil dielectric transformer construction techniques that led to a much more

compact size of approximately 8'x10'x11' (including electric bushings for AC circuit connection, which protrude from the side in a customer-required air-filled cable box) and a weight of approximately 67,000 lb. The Compact FCL had a similar power rating but much higher fault current limiting performance, compared to the Spider-core FCL. The new Compact FCL design is an attractive option where real estate requirements are tight.

Regarding cost-effectiveness, since the first generation device has a relatively low electrical rating, with maximum potential ratings on the order of 25 MVA and high duty-cycle ratings significantly lower, the present manufacturing cost may not represent a high-value proposition. This issue has been addressed, in two directions: FCL technology is being improved to reduce basic device manufacturing cost, and FCL technology is being scaled up for higher voltages and currents. The latter may be more important in terms of cost-effectiveness and value proposition, considering the fact that higher-voltage substations can often be more crowded and have fewer options for expansion, due to electrostatic clearance issues, and higher voltage components (switchgear, insulators, transformers, buswork, etc.) are exponentially more expensive than their low-voltage counterparts. Further, as more and more large renewable power generators desire to connect to the electric grid, high-voltage tie-lines are becoming increasingly strained as more power is wheeled from long distances and as grid interconnections increase. All of these factors are projected to continue to increase energy levels within the grid, leading to potentially unsafe fault current levels. In some cases, higher-rated components cannot be retrofitted in the available space, leading to lengthy and costly major upgrades of grid infrastructure. Economic studies and performance models show that at current performance levels and price points, FCL technologies can be very cost-effective compared to major upgrade projects at high voltages.

The FCL demonstration project also brought to light an issue with respect to the device's reliability and maintenance requirements. While the FCL device was kept operable and performed satisfactorily while actively operating in the SCE grid, a number of interventions were needed to keep the FCL completely operational. For a research prototype, this was acceptable, but as a commercial product, it will need to be, and is being, substantially improved. A desirable FCL needs to target "5-nines" reliability with only a single, scheduled, short-duration annual maintenance outage to fit within today's utility maintenance requirements. Even better would be extending the maintenance interval to two years or longer, but an annual outage of a day or less would be acceptable if the FCL were reliable and required no other maintenance.

If the FCL is to be relied upon for protection, then bypassing it from service temporarily for maintenance can be a risk for the circuit. Perhaps a scheduled bypass can be accomplished by splitting buses or otherwise reconfiguring the electric grid in ways acceptable for short durations, but it may not be optimal for long-term operation, or not acceptable at all in some cases. Thus the FCL should be designed, to the maximum extent possible, to allow essential routine maintenance, such as cryogenic maintenance, to be performed while the unit is energized. Zenergy Power is aggressively modifying their FCL technologies for reduced maintenance requirements, higher MTBF, and lower MTTR, and these considerations are also an integral part of the EPRI/Silicon Power team's development efforts.

One important issue identified during the field test was that the nitrogen cooling system could be problematical for maintenance since it requires periodic maintenance of the cryostat, including drying and/or replacing the volume of liquid nitrogen. This may not be feasible in practice, considering the fact that the unit is typically installed in a high-voltage zone. However, this issue was addressed in the second-generation HTS FCL design by replacing the liquid nitrogen cooling system with a cryogen-free, "dry-type" conductive cryogenic cooling system, available as a commercial off-the-shelf unit, resulting in a more reliable and robust system with significantly reduce cryogenic maintenance requirements.

Overall, the Zenergy Power HTS FCL project is considered as an important success, which has already led to a scaled up design for a transmission level (138kV) commercial application.

11.4 Recommendations

Electricity is a vital force in our national and state economies. It is an important goal of the California Energy Commission to support the technologies required satisfying a reliable, safe and environmentally responsible electrical energy supply. As such, FCC technology is a potentially cost-effective alternative to the capital-intensive upgrades to the power system that would ordinarily be required to meet growth in electrical demand while maintaining the requisite level of electric service reliability. The development and demonstration efforts in this research project have already resulted in two FCC test plans, two full FCC designs, valuable information for developing the needed industry standards for FCCs, and have contributed to one commercial sale and one migration to a transmission-level FCC application. Further RD&D efforts building upon these results will promote additional progress toward achieving commercial application of FCCs.

The research team has accumulated extensive experience in the development of FCC technology, and in the operation and support of FCC field demonstration at Southern California Edison's Avanti Circuit. Further fast-paced and more advanced development of FCC technology is strongly recommended. As the demand for electrical energy rapidly increases, particularly in response to renewable power and "green technology" initiatives, substantial investment in capital-intensive system upgrades will have to made on a fast-track basis in order to maintain the required levels of system availability and reliability in the absence of advanced and cost-effective new technologies such as FCCs. Significant amounts of these investments are potentially avoidable, if suitable FCC technologies are available to California utilities, and if California utilities are given reasonable incentives to deploy the new technologies. An accelerated program of FCC technology focused on reducing the cost, improving the reliability, and increasing the voltage and current ratings of FCC technology is needed in order for California utilities and ratepayers to reap the benefits. California utilities have stepped up to the challenge by sponsoring an ambitious attempt to provide a real-world test bed and testing protocol for proving these technologies and showing how they can be implemented in the utility grid. Additional development efforts and demonstration projects on newer FCC technologies can play an important role in accelerating the acceptance of these technologies in the California and US utility systems.

GLOSSARY

A	Ampere, Amp (unit of current)
AC	Alternating Current
ANSI	American National Standards Institute
BIL	Basic Insulation Level
C	Celsius (temperature)
CB	Circuit Breaker
CAD	Computer-Aided Design
CEC	California Energy Commission
CES	China Electrotechnical Society
CIGRE	Conseil International des Grands Réseaux Electriques (International Council on Research for Large Electric Systems)
CLR	Current-Limiting Reactor
CT	Current Transformer
DC	Direct Current
EPRI	Electric Power Research Institute
ETO	Ethylene Oxide
FCC	Fault Current Controller
FCL	Fault Current Limiter
FEM	Finite Element Model
FPGA	Field-Programmable Gate Array
g	Gravitational Constant
GB	Gigabyte
GTO	Gate Turn-Off [Thyristor]
H	Henry (unit of inductance)
HMI	Human-Machine Interface
HTS	High-Temperature Superconducting
HV	High-Voltage
HVAC	Heating, Ventilating and Air Conditioning

I	Current (Amperes)
IGBT	Insulated Gate Bipolar Thyristor
IGCT	Integrated Gate-Commutated Thyristor
IEE	Institution of Electrical Engineers (UK)
IEEE	Institute of Electrical and Electronics Engineers (USA)
IET	Institution of Engineering and Technology
IPEC	International Power Engineering Conference
j	Square Root of -1 (represents 90^{o} phasor displacement)
kA	Kiloamp (Amp x 10^{3})
kV	Kilovolt (Volt x 10^{3})
kW	Kilowatt (Watt x 10^{3})
lb.	Pound
mH	MilliHenry (H x 10^{-3})
mmf	Magnetomotive Force
MOV	Metal-Oxide Varistor
MTBF	Mean Time Between Failures
MTTR	Mean Time to Repair
MVA	MegaVolt-Amperes
MVAR	MegaVolt-Amperes, Reactive
MW	MegaWatt (Watt x 10^{6})
NC	Normally Closed
NEETRAC	National Electric Energy Testing, Research and Applications Center
NO	Normally Open
Ω	Ohm (unit of resistance, reactance or impedance)
pC	picoCoulomb (Coulomb x 10^{-12}: unit of electrical charge)
PAG	Project Advisory Group
PG&E	Pacific Gas & Electric Co.
PLC	Programmable Logic Controller
PM	Permanent Magnet
PQ	Power Quality

PSCAD	Power System Computer-Aided Design
PT	Potential Transformer
PWM	Pulse-Width Modulation
R	Resistance
RAM	Random-Access Memory
RD&D	Research, Development and Demonstration
rms	Root Mean Square
ROM	Read-Only Memory
SBB	Standard Building Block
SC	Superconducting
SCADA	Supervisory Control and Data Acquisition
SCE	Southern California Edison Co.
SCR	Silicon-Controlled Rectifier
SEL	Schweitzer Engineering Laboratories
SGTO	Super GTO
SiC	Silicon Carbide
SMES	Superconducting Magnetic Energy Storage
SPS	Standard Power Stack
SRL	Saturable Reactor Limiter
SSFCL	Solid-State Fault Current Limiter
THD	Total Harmonic Distortion
UCB	University of California – Berkeley
UCI	University of California – Irvine
UPS	Uninterruptible Power Supply
V	Volt
VLC	Visual Logic Controller
W	Watt
X	Reactive Impedance (Ohms)
Z	Complex Impedance (R + jX) (Ohms)
ZnO	Zinc Oxide

REFERENCES

[1] "Anatomy of a Short Circuit," Siemens Tech Topic no. 44, rev1, December 12, 2003.

[2] L. A. Kojovic, S. P. Hassler, K. L. Leix, C. W. Williams, E. E. Baker. "Comparative Analysis of Expulsion and Current-limiting Fuse Operation in Distribution Systems for Improved Power Quality and Protection," *IEEE Transactions on Power Delivery*, vol. 13, no. 3, pp. 863-869, July 1998.

[3] "Using Current-limiting Fuses to Increase Short Circuit Current Ratings of Industrial Control Panels," Littelfuse Application Note, 2007.

[4] F. Pinnekamp. "The Circuit Breaker," ABB Review, Jan. 2007. Available at: http://library.abb.com/global/scot/scot271.nsf/veritydisplay/737de0b7f522f9b2c125728b00474780/$File/75-78%201M720_ENG72dpi.pdf

[5] T. Taylor, A. Hanson, D. Lubkeman, M. Mousavi. "Fault Current Review Study," ABB Report No. 2005-11222-1-R.04, pp. 41-45, December 22, 2005.

[6] P. G. Slade, R. E. Voshall, J. L. Wu, J. J. Bonk, E. J. Stacey, W. F. Stubler, J. Porter, L. Hong. "The Utility Requirements for a Distribution Fault Current Limiter," *IEEE Transactions on Power Delivery*, vol. 7, no. 2, pp. 507-515, April 1992.

[7] M. Noe, B. R. Oswald. "Technical and Economical Benefits of Superconducting Fault Current Limiters in Power Systems," *IEEE Transactions on Applied Superconductivity*, vol. 9, no. 2, June 1999, pp. 1347-1350.

[8] A. Neumann. "Application of Fault Current Limiters," Department for Business, Enterprise and Regulatory Reform (BERR) report, pp. 3-14, 2007. Available at: http://www.ensg.gov.uk/assets/dgcg00099rep.pdf

[9] S. Eckroad. "Utility Needs Survey for Fault Current Limiters," *International Workshop on Coated Conductors for Applications (CCA08),* Electric Power Research Institute, p. 7, December 4-6, 2008.

[10] D. Haught. "Fault Current Limiters," DOE newsletter, Nov. 6, 2009. Available at: www.oe.energy.gov/DocumentsandMedia/hts_fcl_110609.pdf.

[11] J. C. Krause. "Short-Circuit Current Limiters – Literature Survey 1973-1979," TH-Report 80-E-109, ISBN 90-6J44-109-9, Eindhoven University of Technology, July 1980.

[12] A. J. Power. "A Look at Tomorrow," *IEE Colloquium on Fault Current Limiters,* pp. 1-5, Jun. 8 1995.

[13] E. M. Leung. "Superconducting Fault Current Limiters," *IEEE Power Engineering Review,* vol. 20, pp. 15-18, 30, 2000.

[14] C. Meyer, S. Schröder, R. W. De Doncker. "Solid-State Circuit Breakers and Current Limiters for Medium-Voltage Systems Having Distributed Power Systems," *IEEE Transactions on Power Electronics,* vol. 19, no. 5, pp. 1333-1340, Sep. 2004.

[15] M. Noe, M. Steurer. "High-temperature Superconductor Fault Current Limiters: Concepts, Applications, and Development Status," *Superconductor Science & Technology,* vol. 20, pp. R15-29, January 15, 2007.

[16] D. Larbalestier, R. D. Blaugher, R. E. Schwall, R. S. Sokolowski, M. Suenaga, J. O. Willis. "Power Applications of Superconductivity in Japan and Germany," World Technology Evaluation Commission (WTEC) Report, pp. 45-48, 1997. Available at: http://www.wtec.org/loyola/scpa/toc.htm.

[17] M. M. Lanes, H. A. C. Braga, P. G. Barbosa. "Limitador de Corrente de Curto-Circuito Baseado em Circuito Ressonante Controlado por Dispositivos Semicondutores de Potência," *IEEE Latin America Transactions,* vol. 5, no. 5, pp. 311-320, September 2007.

[18] C. Meyer, P. Köllensperger, R. W. De Doncker. "Design of a Novel Low Loss Fault Current Limiter for Medium-Voltage Systems," *Nineteenth Annual IEEE Applied Power Electronics Conference and Exposition (APEC04),* pp. 1825-1831, 2004.

[19] B. Chen, A. Q. Huang, M. Baran, C. Han, W. Song. "Operation Characteristics of Emitter Turn-Off Thyristor (ETO) for Solid-State Circuit Breaker and Fault Current Limiter," *Twenty-First Annual IEEE Applied Power Electronics Conference and Exposition (APEC06),* pp. 174-178, 2006.

[20] T. Genji, O. Nakamura, M. Isozaki, M. Yamada, T. Morita, M. Kaneda. "400V-class High Speed Current Limiting Circuit Breaker for Electric Power System," *IEEE Transactions on Power Delivery*, vol. 9, issue 3, pp. 1428-1435, July 1994.

[21] M. M. R. Ahmed, G. Putrus, Li Ran, R. Penlington. "Development of a Prototype Solid-State Fault-Current Limiting and Interrupting Device for Low-Voltage Distribution Networks," *IEEE Transactions on Power Delivery,* vol. 21, no. 4, pp. 1997-2005, Oct. 2006.

[22] M. M. R. Ahmed, G. A. Putrus, L. Ran, L. Xiao. "Harmonic Analysis and Improvement of a New Solid-State Fault Current Limiter," *IEEE Transactions on Industry Applications,* vol. 40, no. 4, pp. 1012-1019, July/August 2004.

[23] H. J. Boenig and D. A. Paice. "Fault Current Limiter Using a Superconducting Coil," *IEEE Transactions on Magnetics,* vol. 19, no.3, pp. 1051-1053, May 1983.

[24] M. T. Hagh, M. Abapour. "DC Reactor Type Transformer Inrush Current Limiter," *IET Electric Power Applications,* vol. 1, issue 5, pp. 808-814, 2007.

[25] T. Nomura, M. Yamaguchi, S. Fukui, K. Yokoyama, T. Satoh, K. Usui. "Single DC Reactor Type Fault Current Limiter for 6.6 kV Power System," *IEEE Transactions on Applied Superconductivity*, vol. 11, no. 1, pp. 2090-2093, March 2001.

[26] Z. Lu, D. Jiang and Z. Wu. "A New Topology of Fault-Current Limiter and Its Parameters Optimization," *34th Annual IEEE Power Electronics Specialists Conference (PESC03),* pp. 462-465, 2003.

[27] W. Fei and Y. Zhang, "A Novel IGCT-based Half-controlled Bridge Type Fault Current Limiter," *CES/IEEE 5th International Power Electronics and Motion Control Conference (IPEMC 2006),* pp. 1-5, 2006.

[28] W. Fei, Y. Zhang and Z. Meng. "A Novel Solid-State Bridge Type FCL for Three-Phase Three-Wire Power Systems," *Twenty-Second Annual IEEE Applied Electronics Conference and Exposition (APEC07),* vol. 2, pp. 1369-1372, 2007.

[29] W. Fei, Y. Zhang and Q. Wang, "A Novel Bridge Type FCL Based on Single Controllable Switch," *Seventh International Conference on Power Electronics and Drive Systems (PEDS '07),* pp. 113-116, 2007.

[30] W. Fei, Y. Zhang, Z. Lu. "Novel Bridge-Type FCL Based on Self-Turnoff Devices for Three-Phase Power Systems," *IEEE Transactions on Power Delivery,* vol. 23, issue 4, pp. 2068-2078, October 2008.

[31] V. K. Sood, S. Alam. "Three-Phase Fault Current Limiter for Distribution Systems," *Sixth International Conference on Power Electronics and Drive Systems (PEDS '06)*, pp. 1-6, 2006.

[32] T. Hoshino, K. M. Salim, A. Kawasaki, I. Muta, T. Nakamura, M. Yamada. "Design of 6.6 kV, 100 A Saturated DC Reactor Type Superconducting Fault Current Limiter," *IEEE Transactions on Applied Superconductivity*, vol. 13, no. 2, pp. 2012-2015, 2003.

[33] E. Yokoyama, T. Sato, T. Nomura, S. Fukui and M. Yamaguchi. "Application of Single DC Reactor Type Fault Current Limiter As a Power Source," *IEEE Transactions on Applied Superconductivity*, vol. 11, no. 1, March 2001.

[34] Z. Caihong, W. Zikai, Z. Dong, Z. Jingye, D. Xiaoji, G. Wengyong, X. Liye, L. Liangzhen. "Development and Test of a Superconducting Fault Current Limiter-Magnetic Energy Storage (SFCL-MES) System," *IEEE Transactions on Applied Superconductivity,* vol. 17, issue 2, pp. 2014-2017, 2007.

[35] T. Hoshino, K. M. Salim, M. Nishikawa, I. Nuta, and T. Nakamura, "DC Reactor Effect on Bridge Type Superconducting Fault Current Limiter During Load Increasing," *IEEE Transactions on Applied Superconductivity,* vol. 11, no. 1, pp. 1944-1947, March 2001.

[36] T. Nomura, M. Yamaguchi, S. Fukui, K. Yokoyama. "Study of a Single DC Device Type FCL for Three Phase Power System," *Cryogenics,* vol. 41, pp. 125-130, 2001.

[37] M. T. Hagh, M. Abapour. "Nonsuperconducting Fault Current Limiter with Controlling the Magnitudes of Fault Currents," *IEEE Transactions on Power Electronics*, vol. 24, no. 3, pp. 613-619, March 2009.

[38] M. M. Lanes, H. A. C. Braga, P. G. Barbosa. "Limitador de Corrente de Curto-Circuito Baseado em Circuito Ressonante Controlado por Dispositivos Semicondutores de Potência," *IEEE Latin America Transactions,* vol. 5, no. 5, pp. 311-320, September 2007.

[39] G. G. Karady. "Principles of Fault Current Limitation by a Resonant LC Circuit," *IEE Proceedings on Generation, Transmission and Distribution,* vol. 139, pp. 1-6, 1992.

[40] S. Sugimoto, J. Kida, H. Arita, C. Fukui, T. Yamagiwa. "Principle and Characteristics of a Fault Current Limiter with Series Compensation," *IEEE Transactions on Power Delivery*, vol.11, no. 2, pp. 842-847, 1996.

[41] C. S. Chang, P. C. Loh. "Designs Synthesis of Resonant Fault Current Limiter for Voltage Sag Mitigation and Current Limitation," *Proceedings of IEEE Power Engineering Society Winter Meeting*, vol. 4, pp. 2482 – 2487, January 2000.

[42] M. Hojo, Y. Fujimura, T. Ohnishi, T. Funabashi. "Experimental Studies on Fault Current Limiter by Voltage Source Inverter with Line Voltage Harmonics Compensation," *European Conference on Power Electronics and Applications 2007,* pp. 1-8.

[43] S. S. Choi, T. X. Wang, D. M. Vilathgamuwa. "A Series Compensator with Fault Current Limiting Function," *IEEE Transactions on Power Delivery,* vol. 20, pp. 2248-2256, 2005.

[44] M. Hojo, N. Kuroe, T. Ohnishi. "Fault Current Limiter by Series Connected Voltage Source Inverter," *IEEE Transactions on Industry Applications,* Special Issue on IPEC-Niigata, vol. 126, no. 4, pp. 438-443, 2006.

[45] B. P. Raju, K. C. Parton, T. C. Bartram. "A Current Limiting Device Using Superconducting DC Bias, Applications and Prospects," *IEEE Transactions on Power Apparatus and Systems,* vol. 101, pp. 3173–3177, 1982.

[46] G. A. Oberbeck, W. E. Stanton, A. W. Stewart. "Saturable Reactor Limiter for Current," US Patent 4152637, May 1979.

[47] Y. Pan, J. Jiang. "Experimental Study on the Magnetic-controlled Switcher Type Fault Current Limiter," *Third International Conference on Electric Utility Deregulation Restructuring and Power Technologies 2008,* DRPT 2008, pp. 1987-1991.

[48] D. Cvoric, S. W.H. de Haan, J.A. Ferreira. "Improved Configuration of the Inductive Core-Saturation Fault Current Limiter with the Magnetic Decoupling," *IEEE Industry Applications Society Annual Meeting 2008 (IAS '08),* pp. 1-7, 2008.

[49] D. Cvoric, S. W.H. de Haan, J.A. Ferreira. "New Saturable-Core Fault Current Limiter Topology with Reduced Core Size," *IEEE 6th International Power Electronics and Motion Control Conference (IPEMC '09),* pp. 920-926, 2009.

[50] M. Iwdiara, S. C. Mukl, S. Yaniada, et al. "Development of Passive Fault Current Limiter in Parallel Biasing Mode," *IEEE Transactions on Magnetics,* vol. 35, no. 3, pp. 3523-3525, 1999.

[51] H. Liu, Q. Li, L. Zou, Y. Ma, W. H. Siew. "An Equivalent Magnetic Circuit Coupled Model of PMFCL for Transient Simulation," *Proceedings of the 4th International Universities Power Engineering Conference (UPEC),* pp. 1-5, 2009.

[52] S. Young, F. P. Dawson, A. Konrad. "An Extended Magnet in a Passive dI/dt Limiter," *Journal of Applied Physics,* vol. 76, no. 10, pp. 6874-6876, November 1994.

[53] J-L. Rasolonjanahary, J. P. Sturgess, E. F. H. Chong, A. E. Baker, C. L. Sasse. "Design and Construction of a Magnetic Fault Current Limiter," *The 3rd International Conference on Power Electronics, Machines and Drives,* pp. 681-685, 2006.

[54] S. Young, F. P. Dawson, A. Konrad. "A Three-material Passive dI/dt Limiter," *Journal of Applied Physics,* vol. 76, no. 10, pp. 6871-6873, November 1994.

[55] S. Young, F. P. Dawson, M. Iwahara, S. Yamada. "A Comparison Between a Two-material and Three-material Magnetic Current Limiter," *Journal of Applied Physics,* vol. 83, no. 11, pp. 7103-7105, June 1998.

[56] V. Rozenshtein, A. Friedman, Y. Wolfus, F. Kopansky, E. Perel, Y. Yeshurun, Z. Bar-Haim, Z. Ron, E. Harel, N. Pundak. "Saturated Cores FCL—A New Approach," *IEEE Transactions on Applied Superconductivity*, vol. 17, no. 2, pp. 1756-1759, June 2007.

[57] H. Hong, Z. Cao, J. Zhang, X. Hu, J. Wang, X. Niu, B. Tian, Y. Wang, W. Gong, Y. Xin. "DC Magnetization System for a 35 kV/90 MVA Superconducting Saturated Iron-Core Fault Current Limiter," *IEEE Transactions on Applied Superconductivity*, vol. 19, no. 3, pp. 1851-1854, June 2009.

[58] Y. F. He, J. H. Li, X. H. Zong, J. Sun, Y. N. Wang, C. L. Wu, J. X. Wang. "The High Voltage Problem in the Saturated Core HTS Fault Current Limiter," *Physica C (www.sciencedirect.com),* vol. 386, pp. 527-530, 2003. Available at: http://www.sciencedirect.com/science/article/pii/S0921453402021536

[59] Y. Xin, J. Zhang, W. Gong. "Voltage Surge Protection Circuit for Superconducting Bias Coil," *IEEE Transactions on Applied Superconductivity,* vol. 20, no. 3, pp. 1118 - 1121, 2010.

[60] V. Temple. "Super GTO's Push the Limits of Thyristor Physics," *35th Annual IEEE Power Electronics Specialists Conference (PESC04),* vol. 1, pp. 604-610, 2004.

[61] V. Temple. "GTO's Fight Back," *Power Electronic Europe,* Issue 6, pp. 32-34, 2004.

[62] V. Keilin, I. Kovalev, S. Kruglov, V. Stepanov, I. Shugaev, V. Shcherbakov. "Model of HTS Three-Phase Saturated Core Fault Current Limiter," *IEEE Transactions on Applied Superconductivity,* vol. 10, No. 1, pp. 836-839, 2000.

[63] Y. Xin. "Development of Saturated Iron Core HTS Fault Current Limiters," *IEEE Transactions on Applied Superconductivity,* vol. 17, no. 2, pp. 1760-1763, 2007.

[64] F. Moriconi, N. Koshnick, F. De La Rosa, A. Singh, "Modeling and Test Validation of a 15kV 24MVA Superconducting Fault Current Limiter," *2010 IEEE PES Transmission and Distribution Conference and Exposition,* pp. 1-6, April 19-22, 2010.

[65] S. B. Abbott, D. A. Robinson, S. Perera, F. A. Darmann, C. J. Hawley, T. P. Beales. "Simulation of HTS Saturable Core-Type FCLs for MV Distribution Systems," *IEEE Transactions on Power Delivery*, vol. 21, no. 2, April 2006.

[66] A. Nelson, L. Masur, F. Moriconi, F. De La Rosa, D. Kirsten. "Saturated-Core Fault Current Limiter Experience at a Distribution Substation," *21st International Conference on Electricity Distribution,* June 6-9, 2011.

[67] F. Moriconi, F. De La Rosa, F. Darmann, A. Nelson, L. Masur. "Development and Deployment of Saturated-Core Fault Current Limiters in Distribution and Transmission Substations," *IEEE Transactions on Applied Superconductivity*, vol. 21, no. 3, pp. 1288-1293, June 2011.

[68] C. R. Clarke, F. Moriconi, A. Singh, A. Kamiab, R. Neal, A. Rodriguez, F. De La Rosa, N. Koshnick. "Resonance of a Distribution Feeder with a Saturable Core Fault Current Limiter," *2010 IEEE PES Transmission and Distribution Conference and Exposition,* pp. 1-8, April 19-22, 2010.

[69] A. Abramovitz, K. Smedley. "Review of the Saturable Core Fault Current Limiter Technology," submitted to *IEEE Transactions on Power Delivery*, Nov. 2010.

[70] A. Abramovitz, K. Smedley, et al. "Prototyping and Testing of a 15kV/1.2kA Saturable Core Reactor High Temperature Superconductive Fault Current Limiter," submitted to *IEEE Transactions on Power Delivery,* April, 2011.

[71] A. Abramovitz, K. Smedley. "Survey of Solid State Fault Current Limiters," accepted for publication in the *IEEE Transactions on Power Electronics*.

[72] "Fault Current Limiters: Report on the Activities of CIGRE WG A3.10," *ELECTRA*, no. 194, pp. 23-29, February 2001.

[73] Available at: http://www.siliconpower.com/documents/comp_data/spt315.pdf

[74] Available at: http://www.siliconpower.com/_documents/sscl-datasheet.pdf

[75] IEEE Standard C57.16-1996: Requirements, Terminology, and Test Code for Dry-Type Air-Core Series-Connected Reactors, IEEE 1996.

[76] IEEE Standard C57.12.00-2010: IEEE Standard for General Requirements for Liquid-Immersed Distribution, Power, and Regulating Transformers, IEEE 2010.

[77] IEEE Standard C57.12.01-2005: General Requirements for Dry-Type Distribution and Power Transformers Including Those with Solid-Cast and/or Resin-Encapsulated Windings, Rev. 2005, IEEE 2005.

[78] IEEE Standard 693-2005: IEEE Recommended Practice for Seismic Design of Substations, Rev. 2005, IEEE 2005.

[79] IEEE Standard 519-1992: IEEE Recommended Practices and Requirements for Harmonic Control in Power Systems, Rev. 1992, IEEE 1992.

[80] S. Weckmann, "Dynamic Electrothermal Model of a Sputtered Thermopile Thermal Radiation Detector for Earth Radiation Budget Applications," Master's Thesis, Mechanical Engineering, Virginia Polytechnic University, August 2008.

[81] L. Sanford. "First HTS FCL Goes into a US Grid," *Modern Power Systems,* May 2009.

APPENDIX A:
List of Attachments

Attachment I: Zenergy Power HTS FCL Test Plan

Attachment II: Zenergy Power HTS FCL Laboratory Test Report

Attachment III: Zenergy Power HTS FCL Dielectric and HV Test

Attachment IV: Zenergy Power HTS FCL Normal State Temperature Rise Test

Attachment V: Zenergy Power HTS FCL Short Circuit Test

Attachment VI: Zenergy Power HTS FCL High Voltage Field Test

Attachment VII: Zenergy Power HTS FCL Operation Manual

Attachment VIII: Zenergy Power HTS FCL Cryostat Evacuation and Moisture Removal Procedure

Attachment IX: Zenergy Power HTS FCL Liquid Nitrogen Fill Procedure

Attachment X: Silicon Power SSCL Test Plan